Sediment-hosted base metal deposits

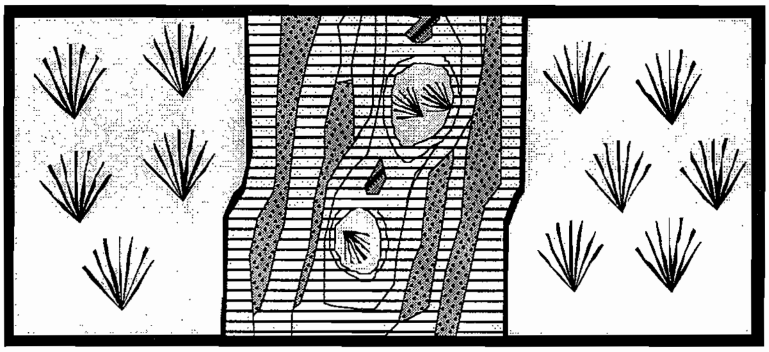

AMIRA/ARC project P384A

Report 3
April 1997

Centre for Ore Deposit Studies
University of Tasmania

CODES Special Research Centre
Geology Department
University of Tasmania
GPO Box 252-79
Hobart Tasmania
Australia 7001

another Pongratz Production 1997

Contents

Introduction

Project Objectives

- To determine the primary geological, geochemical and structural controls on the location and timing of base metal mineral deposits in sedimentary basins, and to develop and refine ore deposit models applicable to exploration.

- To investigate the chemical processes controlling brine compositions and metal sulfide accumulation during fluid movements in sedimentary basins, including the relationships between copper and lead-zinc deposition

- To investigate the physical and hydrological processes involved in the evolution and movement of metalliferous fluids in sedimentary basins

- To develop geological and geochemical vectors to a variety of styles of sedimentary base metal mineralisation that may be used in the exploration for large tonnage deposits.

For convenience, the programme for these projects has been run as three separate, but related modules (see figure). Several studies overlap more than one module, and several integrated reports were presented in P384 and are planned for P384A (see below). The final report in P384A, due in May 1998, will present a new integrated exploration model for Australian Proterozoic stratiform sediment-hosted Zn-Pb-Ag deposits.

This introduction includes three colour coded diagrams:

- A idealised Australian Proterozoic basin cross-section illustrating the location of research reported in this progress report.
- A geologic plan of the Mount Isa and McArthur Basins with locations of all the work carried out to date in P384 and P384A, and areas covered in this report high lighted in red.
- A stratigraphic column annotated to show the stratigraphic location of all work to date in P384 and P384A.

These latter two diagrams are cross-referenced with a list of all relevant reports from P384 (in blue), and all reports and proposed studies for P384A (in pink).

Research Modules for P384/P384A

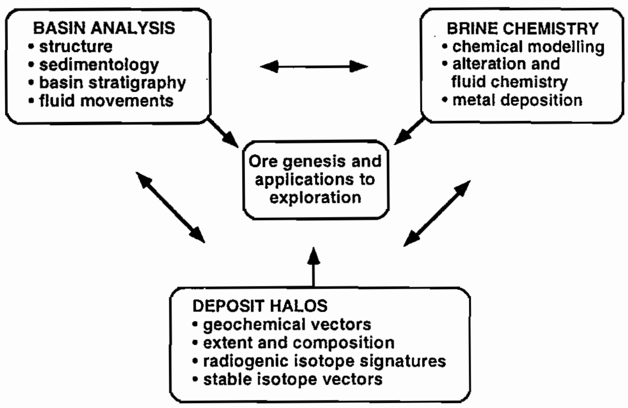

Basin Analysis

Aims

- to develop sedimentologic and basin stratigraphic criteria to enable the identification of favourable horizons for Zn-Pb deposits
- to better understand the basement architecture of the McArthur and Mt Isa Basins
- to document the detailed structural evolution, and the interplay between structure and sedimentation, in key areas of the McArthur and Mt Isa Basins
- to integrate sediment facies studies with sediment chemistry and alteration indices from the other two modules

Methods

- geophysical modelling of public domain gravity and magnetic data sets
- sedimentary facies mapping & core logging
- diagenetic studies
- detailed structural mapping of key areas

Deposit Halos

Aims

- to document primary geochemical, mineralogical and isotopic dispersion halos associated with sedimentary base metal deposits
- to use indices defined for known deposits to define 'favourable horizons' for mineralisation

Methods

- major and trace element geochemical studies and C/O/S isotopic analysis of (barren) host sediments to known mineralisation
- regional studies to help define 'background' variations. and detailed geochemistry and isotopic analysis in conjunction with diagenetic studies
- radiogenic isotope studies to discriminate source rocks for base metals

Brine Chemistry

Aims

- to model base metal and ore associated elements solubility in a variety of possible ore fluids
- to test metal sulphide preciptation processes
- to account for the geochemical halos documented in the Deposit Halos module
- to test novel potential ore-forming ('trap') scenarios in sedimentary basins

Methods

- the thermodynamic modelling packages developed by Mark Read (CHILLER and SOLVEQ) will be used for computer modelling studies
- (where possible) fluid inclusion and stable isotope studies will be used to constrain fluid character for this modelling

This Report

This is the third progress report for AMIRA Project P384A and covers work during the six months November 1996 to April 1997.

The work reported here covers several aspects of middle McArthur group sedimentology and diagenesis, and possible links to tectonic processes operating during middle McArthur times. The report by Winefield re-examines enigmatic 'Coxco needles' from the Teena Dolomite and concludes they are pseudomorphs after chemically precipitated aragonite. Elevated HCO3– in the basin waters (needed to stabilise primary aragonite) may be yet another manifestation of regional tectonism preceding the main HYC ore-forming event.

A description of a condensed Teena Dolomite – Barney Creek Formation – Reward Dolomite section from the Berjaya area to the west of HYC is presented in the report by Bull, Cooke and Winefield. Their observations, including algal features suggestive of photic zone deposition, are consistent with a half-graben model for the area with the Berjaya section accumulating on the uplifted footwall block.

The report by Winefield et al describes sediment- and fibrous cement-infilled fractures (Neptunian dykes) in the Teena and Emmerugga Dolomites from the southern McArthur Basin. The fibrous dolomite cements are similar to marine calcite cements from Phanerozoic sequences, and there is no evidence for emergence prior to Barney Creek Formation times. Furthermore, the consistent orientation of the dykes and sills suggest slumping of lithified sediments during tilt block formation and/or deformation directly linked to syn-sedimentary faulting. In the area of the Gorge Prospect this tilting pre-dates deposition of the Barney creek Formation.

Reports by Cooke and co-workers continue the systematic geochemical modelling of important constituents of sedimentary Zn-Pb deposit, and extends the base metal modelling to very high salinities (25wt% NaCl equivalent).

The final report is a preliminary geological interpretation of gravity and magnetic data from parts of the Camooweal and Dobbyn 1:250,000map areas. Much of the data from Camooweal are consistent with interpretations from previous reports for map areas to the west and north. To the east the rocks display evidence for east facing overthrusting, and there may be (younger) west facing thrusts where the western and eastern domains abut.

Also to be presented at the meeting, but not reported here, are descriptions of the Grevillea prospect mineralisation and associated primary geochemical dispersion halos, a written report will be presented to sponsors at a subsequent meeting. John Dunster will present an overview of his PhD work on the Lady Loretta Formation. Logs from a 'distal' hole at Lady Loretta (DDH LA64) will be on display comparing lithological, geochemical and radiometric ('gamma-log') data for this hole.

A short review paper describing an exploration model for sediment-hosted base metal deposits is included as an appendix to the report.

Peter McGoldrick
Project Manager

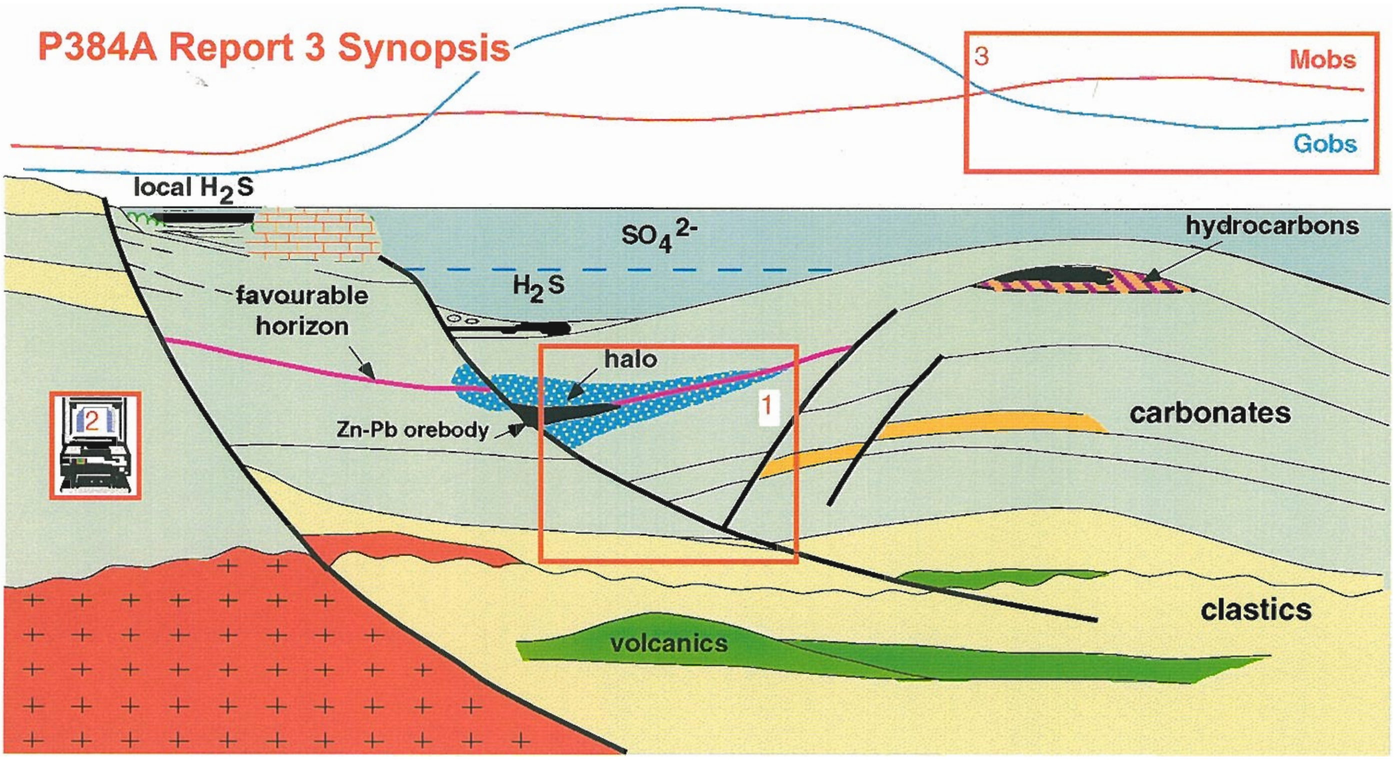

1 Basin Analysis Module: Coxco needles: are they necessarily gypsum pseudomorphs? p.1; Progress report: sedimentology and mineralisation at the Berjaya Prospect. p. 21; Progress report: neptunian dykes and associated features within pre-Barney Creek Formation sediments, southern McArthur Basin. p. 31.

2. Brine Chemistry Module: Iron transport in sedimentary brines: implications for SEDEX deposits. p. 71; Salinity controls on mineral stabilities and metal solubilities in 150°C sedimentary brines. p. 77; Europium transport in sedimentary brines: physicochemical controls in the ore-forming environment of McArthur- and Broken Hill-type sediment-hosted Pb-Zn deposits. p. 85; The solubility of gold in 150°C saline brines: implications for the gold tenor of SEDEX ores. p. 91.

3 Basin Analysis Module: Regional geophysics: preliminary study and comments, Camooweal and Dobbyn. p. 97.

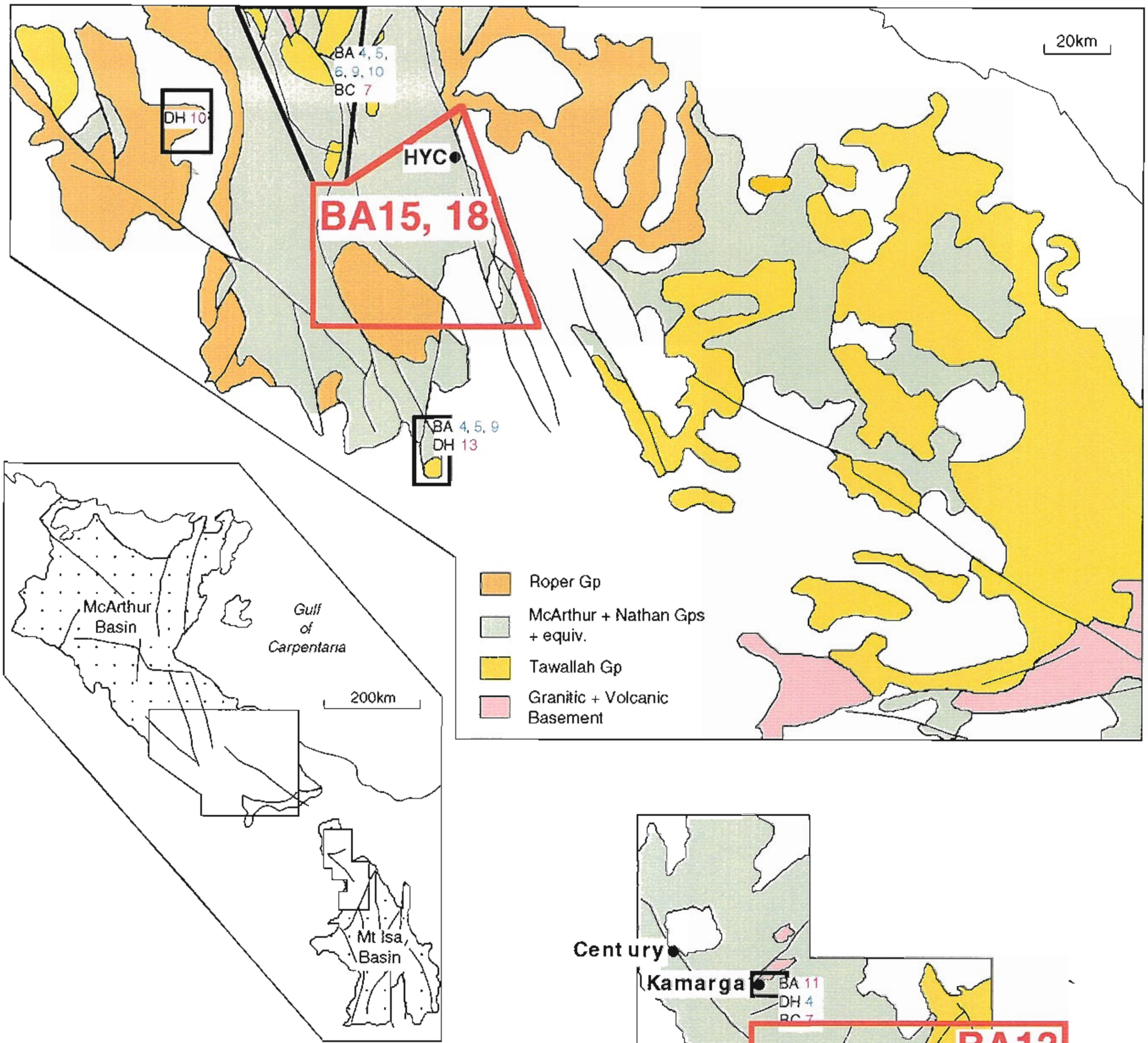
20km
BA 4, 5, 6, 9, 10
BC 7
DH 10
HYC
BA15, 18
BA 4, 5, 9
DH 13
McArthur Basin
Gulf of Carpentaria
200km
Mt Isa Basin
Roper Gp
McArthur + Nathan Gps + equiv.
Tawallah Gp
Granitic + Volcanic Basement

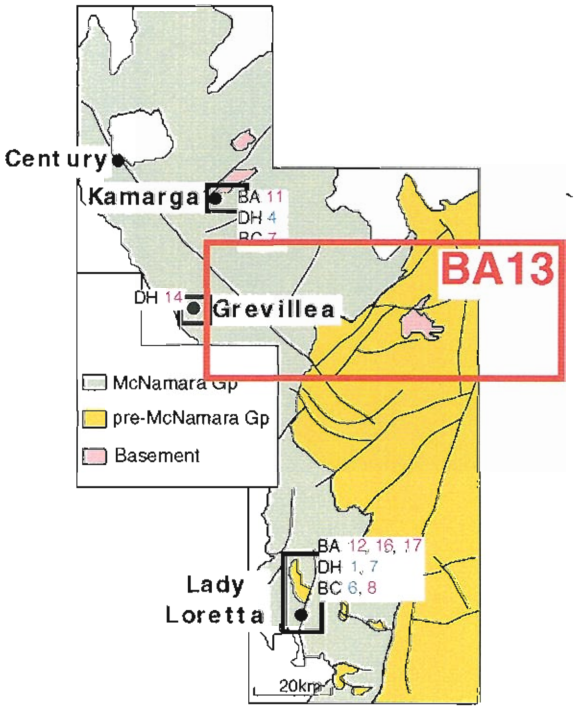
Century
Kamarga
BA 11
DH 4
BA13
DH 14
Grevillea
McNamara Gp
pre-McNamara Gp
Basement
BA 12, 16, 17
DH 1, 7
BC 6, 8
Lady Loretta
20km

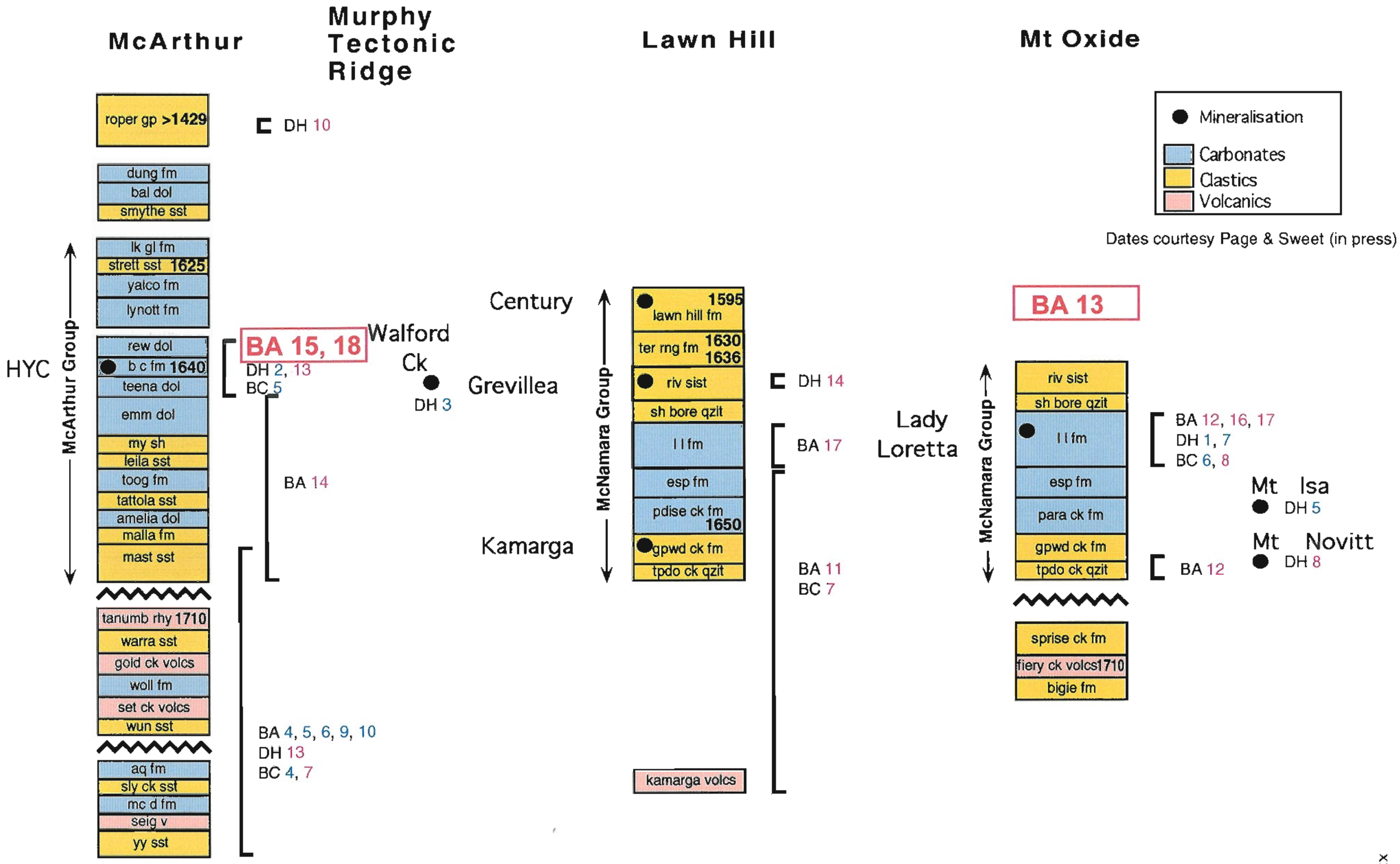

McArthur
Murphy Tectonic Ridge
Lawn Hill
Mt Oxide
Mineralisation
Carbonates
Clastics
Volcanics
Dates courtesy Page & Sweet (in press)
roper gp >1429
DH 10
dung fm
bal dol
smythe sst
lk gl fm
strett sst 1625
yalco fm
lynott fm
McArthur Group
HYC
rew dol
b c fm 1640
teena dol
emm dol
my sh
leila sst
toog fm
tattola sst
amelia dol
malla fm
mast sst
BA 15, 18
DH 2, 13
BC 5
BA 14
Walford Ck
DH 3
tanumb rhy 1710
warra sst
gold ck volcs
woll fm
set ck volcs
wun sst
aq fm
sly ck sst
mc d fm
seig v
yy sst
BA 4, 5, 6, 9, 10
DH 13
BC 4, 7
Century
Grevillea
Kamarga
McNamara Group
1595
lawn hill fm
ter rng fm 1630
1636
riv sist
sh bore qzit
l l fm
esp fm
pdise ck fm
1650
gpwd ck fm
tpdo ck qzit
kamarga volcs
DH 14
BA 17
BA 11
BC 7
Lady Loretta
BA 13
McNamara Group
riv sist
sh bore qzit
l l fm
esp fm
para ck fm
gpwd ck fm
tpdo ck qzit
sprise ck fm
fiery ck volcs1710
bigie fm
BA 12, 16, 17
DH 1, 7
BC 6, 8
BA 12
Mt Isa
DH 5
Mt Novitt
DH 8

Key to locality plan and stratigraphic column

Basin Analysis P384

BA1 Architecture of the McArthur Basin, northern Australia — Leaman, P384 Final Report, p.1

BA2 Considerations on the regional setting of mineralised sites in northern Australia — Leaman, P384 Final Report, p.25

BA3 Evolution and tectonics of the North Australian Zinc Belt — the Southern McArthur Basin and Lawn Hill Platform — Leaman & Keele, P384 Final Report, p.113

BA4 Structures in the Northwest Batten Fault Zone, southern McArthur Basin, Northern Territory: with reference to tectonic uplift during Tawallah times — Keele, P384 Final Report, p.37

BA5 Analysis of some fault striae in the Proterozoic southern McArthur Basin, Northern Territory: with reference to the Mallapunyah Dome and Four Archers Fault — Keele & Wright, P384 Final Report p.61

BA6 Brittle deformation events in the western McArthur River region, southern McArthur Basin, Northern Territory — Rogers, P384 Final Report p.79

BA7 Towards a regional depositional model for the Palaeoproterozoic Barney Creek Formation, southern McArthur Basin, Northern Territory — Bull, P384 Final Report p.133

BA8 (DH2) Sedimentology, geochemistry, alteration patterns and C/O isotope chemostratigraphy, DDH BMR McArthur 2, McArthur Basin, NT — Bull & Large, P384 Final Report, p.159

BA9 Sedimentology and volcanology of the southern McArthur Basin — Bull, P384 Report 4 p.33

BA10 Geology and tectonic setting of the Tawallah Group, southern McArthur Basin, Northern Territory — Rogers, PhD thesis 1996

Basin Analysis P384A

BA11 (DH9) Sedimentology and structure of the southern flank of the Kamarga Dome, Bloodwood Bore area, NW Queensland — Bull, McGoldrick & two Honours students

BA12 Surprise Creek Fm / Torpedo Creek Quartzite transition in the Lady Loretta area —Keele & Bull

BA13 Regional scale geophysical modelling of Camooweal, Mount Isa, and parts of Dobbyn and Cloncurry 1:250,000 sheets — Leaman & Duffett

BA14 The interplay between sedimentology and structure during deposition of the lower McArthur Group —Selley & Bull

BA15 (DH9) Sedimentology and diagenesis of the middle McArthur Group — Winefield PhD

BA16 Structure and mineralisation in the Lady Annie area — Keele, McGoldrick, Cooke

BA17 (DH9) Sedimentology of the Lady Loretta Formation — Dunster, PhD

Deposit Halos P384

DH1 Lady Loretta area— McGoldrick, Large, Dunster, Duhig, Aheimer, P384 Rpts 3, 5, 7 & Final Report

DH2 HYC area — Large, Bull, Duhig, McGoldrick, Cooke, P384 Rpts 3, 5, 7 & Final Report

DH3 Geochemical vectors to stratiform sediment-hosted base metal deposits at the Walford Creek prospect, northwestern Queensland — McGoldrick, P384 Final Report, p.303

DH4 The Alteration Index and MnO_D at Kamarga (re-visited): new geochemical data Queensland — McGoldrick, P384 Final Report, p.319

DH5 Application of the Alteration Index and MnO_D to the Mount Isa and Hilton zinc-lead-silver deposits Queensland — McGoldrick, P384 Report 7, p.115

DH6 XPLOR® — a set of Excel macros to aid processing large geochemical databases — Duhig & Le Maitre, June 1995 Report; & The geochemical database and 'background' data for late Palaeoproterozoic sediments from the McNamara and McArthur Groups & the Explor program Queensland — McGoldrick, P384 Report7, p.141

DH7 Stratigraphic variations in sulfur isotopes in late Palaeoproterozoic sediments from the McNamara Group, northwestern Queensland Queensland — McGoldrick, P384 Final Report, p.333

Deposit Halos P384A

DH8 Halos to the Mt Novit Zn-Pb-Ag mineralisation — McGoldrick

DH9 Carbonate geochemistry and isotope signatures of stratabound and stratiform sediment-hosted base metal mineralisation — McGoldrick et al.

DH10 Velkerri Formation geochemistry — McGoldrick & Bull

DH11 Geochemical and isotopic chemostratigraphy of selected parts of the McNamara and Fickling Groups — McGoldrick et al.

DH12 A geochemical atlas of northern Australian Palaeoproterozoic sedimentary rocks — McGoldrick et al.

DH13 Fluid flow pathways and base metal source rock studies in the southern McArthur Basin — Leaman et al.

DH14 Halos at the Grevillea prospect, NW Qld — McGoldrick & Bull

DH15 Belt Basin pilot studies: Sullivan and Sheep Creek — McGoldrick & Bull

Brine Chemistry P384

BC1 Transport and deposition of base metals at 250°C — Cooke, P384 Report 4, p.111

BC2 Transport and deposition of base metals at 150°C — Cooke, P384 Report 4, p.131

BC3 Conditions of formation for siderite and barite from sedimentary brines: implications for the formation of sediment-hosted base metal deposits — Cooke, P384 Report 7, p.149

BC4 Potassic alteration in the Settlement Creek and Gold Creek Volcanics, McArthur Basin, Northern Territory — implications for base-metal mineralisation — Cooke, P384 Final Report, p.183

BC5 Alkali metasomatism of volcaniclastic and clastic rocks in the McArthur Group, with emphasis on the HYC Zn–Pb deposit — Davidson, P384 Final Report, p.227

BC6 (DH1) Variation of carbon and oxygen isotopes in the alteration halo to the Lady Loretta deposit — implications for exploration and ore genesis — Large et al., P384 Final Report, p.289

Brine Chemistry P384A

BC7 Sandstone diagenesis: Masterton Sandstone and Torpedoe Creek Quartzite — Cooke & Bull

BC8 Fluid inclusions at Lady Loretta — McGoldrick & Dunster

BC9 Chemical modelling of Fe and Cu solubility — Cooke

Integrated Studies P384

IS1 The Lady Loretta zinc–lead–silver deposit: primary dispersion halos, sedimentology, ore textures, stable isotopes, and metal distributions — towards a genetic model — McGoldrick et al., P384 Final Report, p.409

IS2 Review of genetic models at HYC: constraints from new sedimentology, alteration halo studies and fluid chemical modelling — Large et al., P384 Final Report, p.371

IS3 Two classes of stratiform sediment hosted Pb–Zn deposits — Cooke et al., P384 Final Report, p.345

Integrated Studies P384A

IS4 Carbonaceous and pyritic facies in the McArthur and McNamara Groups — Bull et al.

IS5 Sandstone aquifers and controls on basinal fluid composition in northern Australian late Palaeoproterozoic rocks — Cooke & Bull

IS6 A new exploration model for Australian Proterozoic stratiform sediment-hosted Zn-Pb-Ag deposits — everybody

Summaries

Coxco needles: are they necessarily gypsum pseudomorphs?

Peter R. Winefield

Radiating, acicular 'Coxco needles' are the characteristic feature of the Coxco Dolomite Member of the Teena Dolomite. They have been variously interpreted as pseudomorphs after aragonite, gypsum and trona. The interpretation that they were originally gypsum has been used as evidence for an evaporative, emergent depositional setting (Jackson et al., 1987), however results from a new study of the Teena Dolomite are inconsistent with this interpretation. Crystal morphology, petrographical and sedimentological relationships are more consistent with an aragonite precursor for 'Coxco needle' crystal fans. The widespread occurrence of 'Coxco needles' at a discrete stratigraphic interval is thought to be a function of a subtle change in the $[HCO_3^-]$ concentration of the southern McArthur Basin, possibly related to a major tectonic event during the deposition of the Teena Dolomite.

Progress report: sedimentology and mineralisation at the Berjaya Prospect

Stuart Bull, David Cooke and Peter Winefield

The Berjaya Prospect is an occurrence of Pb-Zn mineralisation hosted in the middle McArthur Group approximately 17 km west of HYC Deposit. Unpublished company reports suggested that the in the prospect area the Barney Creek Formation thins to the north across a prominent east-west lineament. This feature extends to the west from the area of the HYC Deposit and is the site of several base metal prospects. It has been implicated as a reflecting a growth fault that acted as a conduit for the metalliferous fluids that formed the HYC Deposit. The Berjaya Prospect area was chosen for study during AMIRA/ARC Project P384 in the 1995 field season because of its potential to provide the opportunity to document both syn-sedimentary structural activity at or around Barney Creek Formation time, and the plumbing system for the HYC Deposit.

Sedimentological analysis of selected drill cores from the Berjaya area indicates that the stratigraphy is constrained by the recognition of the Coxco Member of the Teena Dolomite in the base of the drill core intersections, and the Caranbirini Member of the Lynott Formation in the top. Correlation of these formation boundaries confirm that the intervening package, representing Barney Creek Formation/Reward Dolomite time, thins to the north from > 500 m to < 30 m over a distance of only 2.7 km. Although more detailed lithostratigraphic correlations within this package are difficult due to lateral facies changes, the most likely mechanism for the thinning of section appears to be onlap of the lower part of the Barney Creek Formation (W-Fold and lower HYC Pyritic Shale Members) to the northwest. This configuration would be consistent with tectonostratigraphic models for HYC Deposit time that invoke accumulation of the host sediments in half grabens. In areas where the Barney Creek Formation/Reward Dolomite section is thin/condensed, distinctive sedimentary features occur that suggest accumulation of in situ algal mat. This must represent deposition above the photic zone under conditions of relatively low sediment input. In the half graben model these areas would represent deposition above the uplifted footwall block.

Progress report: Neptunian dykes and associated features within pre-Barney Creek Formation sediments, southern McArthur Basin

Peter R. Winefield, Stuart W. Bull, David Selley & Malcolm Wallace

Sediment- and fibrous cement-infilled fractures (or neptunian dykes) have been identified in the Teena and Emmerugga Dolomites within the southern McArthur Basin. They are commonly infilled by successive generations of radial-axial fibrous dolomite cement and internal sediment, and intraclasts rimmed with fibrous dolomite cement are occasionally observed as part of the infilling sequence. The fibrous dolomite cements display very similar characteristics to radial-axial fibrous calcite cements commonly inferred to be of a marine origin in Phanerozoic carbonate sequences.

At each locality, the structural orientation of neptunian dykes and sills is remarkably consistent and there is strong evidence for surfical extension, sliding and slumping of lithified carbonate sediments creating open spaces within the displaced mass. Individual neptunian dykes display fitted and regular features with little evidence of dissolution associated with subaerial exposure. This is supported by the lack of sedimentological evidence for emergence. Two possibilities are suggested for neptunian dyke formation; slumping of lithified sediment as a function of 'tilt-block' formation or deformation directly related to syn-sedimentary fault development.

Sedimentological relationships between the Teena Dolomite and Barney Creek Formation in the 'Gorge Prospect' area would support the 'tilting' of the Coxco Dolomite Member and older units and subsequent deposition of Barney Creek Formation sediments into the resultant sub-basin. Further structural work is needed to better constrain neptunian dyke formation and its relationship to Barney Creek Formation deposition.

The Grevillea Prospect, Riversleigh area, north west Queensland: ore texture and primary lithogeochemical characteristics

Peter McGoldrick

The Grevillea prospect comprises stratiform base metal mineralisation in pyritic black shales and siltstones of the lower Riversleigh Siltstone. The surface expression of the mineralisation is a prominent baritic gossan located 8 km south east of Riversleigh Homestead. Drilling in the immediate vicinity of the gossan revealed several intersections of between 15 an 25 m true thickness with Zn grades of 4-5%, up to 1% Pb, and about 35 g/t Ag in primary mineralisation. Although not outcropping, the pyritic horizon has a recognisable geophysical signature for at least 1.5 km north of the gossan. The pyritic sequence has been sampled by percussion drilling 250 m and 450 m to the north of the gossan, however, only low levels of base metals were encountered.

For this study quarter core was collected from cored holes near the gossan, and assay pulps from percussion holes to the north. Core samples were used to document the lithogeochemistry of barren siltstones and shales interbedded with pyritic and base metal sulphide-rich horizons, and for petrographic study of sulphide textures. The percussion hole samples provided examples of low-grade equivalents of the mineralisation to test the persistence of mineralisation-related geochemical signatures.

All the base metal mineralisation is associated with highly pyritic lithologies. Barite is locally abundant and associated with pyrite. Much of the pyrite is 'reactive' and has a 'spongy' appearance in hand specimen. Siltstones often display brown discolouration very similar in appearance to sideritic siltstones from the Lady Loretta deposit. Gypsum mush textures indicate the former presence of sulphate evaporites in the mineralised sequence. Macroscopic and microscopic textures of spongy pyrite are consistent with pyrite formation by replacement of prone microbial mat. Base metal sulphides occur as infilling within the spongy pyrite.

Twenty three samples of core and thirty two percussion pulps were analysed for major elements and selected trace elements. As in all previous case studies, sulphide-rich samples were avoided where possible. The analyses were used to calculate modal mineralogies, carbonate compositions, and alteration index parameters for all the samples. Five of the core samples contain siderite as the major carbonate phase, and in many of the remaining samples the carbonate is ankerite, not dolomite. Alteration indices (AI3 and SedexAI) and MnOd/s are often elevated in both core and pulp samples. Thallium levels are strongly anomalous in all the core samples, and many of the pulps. The best combined response comes from samples spanning the most strongly mineralised fifty metres of the core. None-the-less, the response from the pulps is still very encouraging, and would warrant follow-up drilling within a radius of 500 m.

A comparison of sedimentological, lithogeochemical and gamma log features in DDH LA 64, Lady Loretta area, north west Queensland

Peter McGoldrick and John Dunster

Drill hole LA 64 is collared approximately 4 km NNE of the Lady Loretta mine site, and provides a cored interval of about 600 m of Lady Loretta Formation from beneath thin Cambrian and Meszoic cover east of the Western Border Fault. Pyritic interbeds from this hole and several others in the area are the stratigraphic equivalents of the mineralised sequence at the mine. The area has been considered favourable for Lady Loretta style mineralisation and has undergone several base emtal exploration phases without any significant discoveries.

This report presents results form fifty four new whole rock major and trace element analyses from siltstone and shale samples from LA 64, and compares theses results with the sedimentological and gamma logs for the hole. Geochemical vectors developed from the Lady Loretta deposit have been calculated for these samples. For virtually all samples these indices (AI3, SedexAI, MnOd, Ankerite Ratio, and Tl) are low and consistent with LA 64 being in a distal position with respect to Zn-Pb mineralisation. Graphical comparisons of K_20 and Al_2O_3 with gamma logs will be made at the meeting.

Iron transport in sedimentary brines — Implications for SEDEX deposits

David R Cooke

Calculations presented in this report illustrate that iron is soluble in acidic hydrothermal solutions at 150°C, and is insoluble in neutral to alkaline solutions. Redox processes are mostly unimportant for Fe deposition over the common range of f_{O2} values in hydrothermal systems, with Fe soluble in acid, oxidised and acid, reduced waters.

Based on fluid chemistry, Cooke et al. (1995) proposed two subdivisions for stratiform sediment-hosted ("SEDEX") Pb-Zn deposits — *McArthur-type,* which form from oxidised fluids, and *Selwyn-type,* which form from reduced, acid fluids. Based on calculated solubilities, Selwyn-type fluids can carry the requisite Fe, Mn, Ba, Pb and Zn required to form a Selwyn-type deposit. However, acid Selwyn-type fluids cannot form a McArthur-type deposit during early diagenesis, because interaction with the host dolomitic siltstones would cause carbonate dissolution and generation of secondary porosity, and the development of metasomatic fronts. In contrast, if McArthur-type SEDEX deposits form from relatively oxidised, near-neutral to alkaline fluids that are in equilibrium with thick packages of carbonates and oxidised clastic sediments, then only Pb and Zn can be introduced by the mineralising solution. As proposed by Large et al. (1995), a second, low-T reduced fluid is required to introduce the necessary Fe and Mn into the HYC system prior to each pulse of mineralised brine, thus accounting for the textural evidence for pyrite predating galena and sphalerite in each ore horizon

Salinity controls on mineral stabilities and metal solubilities in 150°C sedimentary brines

David R Cooke

This report compares calculations of metal solubilities and mineral stabilities for 10 and 25 eq. wt. % NaCl sedimentary brines at 150°C. At constant temperatures, higher salinity brines are (not surprisingly) concluded to be more effective at transporting Pb and Zn as chloride complexes. However, higher salinities have little effect on Fe solubilities, because even at high salinities, a significant component of Fe is transported as the bare ion (Fe^{+2}). Compared to 10 eq. wt. % brines, oxidised brines with salinities around 25 eq. wt. % NaCl and in equilibrium with siderite are capable of transporting sufficient Pb and Zn (1-100 ppm) to form a McArthur-style SEDEX deposit. They are not, however, capable of transporting enough Fe to account for the large pyrite accumulations in the Paleoproterozoic SEDEX deposits.

Europium transport in sedimentary brines — Physicochemical controls in the ore-forming environment of McArthur- and Broken Hill-type sediment-hosted Pb-Zn deposits

Stephen B. Bodon and David R. Cooke

Positive europium anomalies on chondrite normalised rare earth element (REE) plots, are characteristic of hydrothermal precipitates in modern day sea-floor sulphide deposits. They are also characteristic in Broken Hill-type and VHMS deposits. As a result of this feature, positive europium anomalies have been used in the exploration industry to characterise potential ore-forming fluids, as well as some physicochemical conditions of the fluid (c.f. Sverjensky, 1984). To appreciate the potential of Eu for exploration and ore genesis applications, it necessary to understand the behaviour of Eu in hydrothermal solutions.

For 25 eq. wt% NaCl brines that contain $\sum C=0.256$ molal and $\sum S=0.001$ molal, europium is predominantly transported as $EuCl_4^{-2}$ (Eu^{+2} species) under most ore-forming conditions. Hydrothermal precipitates in the "SEDEX" (both McArthur and Selwyn-types) and BHT environments should therefore, display positive Eu anomalies. Eu speciation is not sensitive to fluctuations in fO_2 over the common range of hydrothermal ore-forming conditions, and therefore, the presence of positive Eu anomalies in hydrothermal precipitates is not a good indicator of oxidation state. Further work is required to assess the effects of changes in $\sum S$, $\sum C$, temperature and salinity on Eu speciation in both the source region for Eu and the ore-forming environment.

The solubility of gold in 150°C saline brines – implications for the gold tenor of SEDEX ores

David R. Cooke and Peter McGoldrick

Gold does not occur in anomalous concentrations in McArthur-type SEDEX deposits (e.g. Mount Isa, HYC; McGoldrick et al., 1996). Our calculations show that Au will only be transported in insignificant amounts (<< 0.1 ppb) within 150°C, saline, oxidised (siderite–hematite–carbonate–stable), near-neutral pH brines. In contrast, Selwyn-type SEDEX deposits that precipitate from reduced, acid, H_2S-bearing brines (pyrite–sericite-stable) should contain anomalous gold, because > 0.1 ppb can be transported in these brines as AuHS. There is potential for ore-grade gold in Selwyn-type deposits, provided that the fluids contained sufficient H_2S for Au transport, and that an effective Au depositional mechanism (H_2S loss, oxidation or reduction) operated at the trap site.

Regional geophysics — Preliminary study and comments, Camooweal and Dobbyn

David Leaman

Regional interpretation of geophysical data has been largely restricted to the Dobbyn region pending completion of thesis studies in the Camooweal-Lady Loretta region. Sufficient analysis has now been completed, however, to show that structures and sequences within the Camooweal sheet are generally consistent with those previously described for the Mt Drummond and Lawn Hill areas. These structures and sequences are distinctive and unlike those exposed in the Dobbyn and Cloncurry regions.

This report presents a summary of preliminary findings only.

Previous work had suggested that the major mafic sequence interpreted across the region may be a correlate or extension of the Eastern Creek Volcanics and this appears to be confirmed. Felsic sequences were tied to exposure in the Scrutton Ranges or the Murphy Inlier and were generally assumed to be equivalent elsewhere. This work suggests that many parts of these may be extensions of the Leichhardt Metamorphics or Argylla Formation. The disposition of sequences, and their implied repetition on a regional scale, suggests gross east-facing over-thrusting has occurred within the eastern succession and that some younger west-facing thrusts may be present where the eastern and western sequences abut. The western sequence appears to have experienced less deformation on the basis of implied structural style and gross relationships.

Insufficient analysis has been completed to enable proper association of mineralisation to primary structures but it seems likely that most mineralisation in the eastern sequence may be linked to complex alteration zones which disrupt thick sequences and, in the western sequence, to significant distortions or breaks in structural continuity. Lady Loretta may be correlated with such a feature which has been concealed by the younger cover sequences.

Coxco needles: are they necessarily gypsum pseudomorphs?

Peter R. Winefield
CODES Special Research Centre, Geology Department, University of Tasmania

Abstract

Radiating, acicular 'Coxco needles' are the characteristic feature of the Coxco Dolomite Member of the Teena Dolomite. They have been variously interpreted as pseudomorphs after aragonite, gypsum and trona. The interpretation that they were originally gypsum has been used as evidence for an evaporative, emergent depositional setting (Jackson et al., 1987), however results from a new study of the Teena Dolomite are inconsistent with this interpretation. Crystal morphology, petrographical and sedimentological relationships are more consistent with an aragonite precursor for 'Coxco needle' crystal fans. The widespread occurrence of 'Coxco needles' at a discrete stratigraphic interval is thought to be a function of a subtle change in the [HCO_3^-] concentration of the southern McArthur Basin, possibly related to a major tectonic event during the deposition of the Teena Dolomite.

Introduction

The McArthur Basin is located along the southern and western margins of the Gulf of Carpenteria in Northern Australia (Fig. 1). The McArthur Group is best exposed in the southern McArthur Basin in two elongate N–S trending belts, separated by the Tawallah Fault. The eastern band is bounded by the Emu Fault Zone to the east and the western band by the Roper Group to the west.

The McArthur Group has been divided into the lower Umbolooga Subgroup and the upper Batten Sub-group (Jackson et al., 1987; Pietsch et al., 1991a,b; Fig. 2). The Teena Dolomite is part of the Umbolooga Sub-group and directly underlies the Barney Creek Formation, host to the Pb-Zn-Ag deposit at McArthur River. The Teena Dolomite was incompletely defined by Plumb and Brown (1973) and its upper part separated as the Coxco Dolomite Member. The lower Teena Dolomite is characterised by thin- to medium-bedded dololutite, medium grained dolarenite with sporadic oolitic and peloidal grainstone units. The Coxco Dolomite Member is predominantly thick-bedded dololutite with subordinate medium- and thin-bedded dololutite. Thin beds of pink- and buff-weathering 'tuff' have been described throughout the unit. The characteristic and definitive feature of the Coxco Dolomite Member is the presence of colloquially named 'Coxco needles' (Plate 1a), which are radiating clusters of acicular crystal casts up to 6 cm long. Coxco needles are a subtle feature that are best observed in preferentially weathered or silicified samples (Plates 1a,b,c).

Outcrops of Coxco Dolomite Member-equivalents with distinctive Coxco needle casts are noted in the Vizard Group, approximately 200 km to the northwest, on the Urapunga 1:250 000 Geological Mapsheet (Jim Jackson, pers comm. 1997), and in the Mt Shillingshaw Formation approx. 300 km to the southwest of the McArthur River area, on the Helen Springs 1:250 000 Geological Mapsheet (Peter Beier, pers comm. 1997).

Brown et al. (1969), as part of a detailed sedimentological study of the Barney Creek Formation and associated carbonates of the McArthur Group interpreted their shape and habit as indicative of aragonite pseudomorphs. However, Walker et al. (1977) put forward an alternative hypothesis that

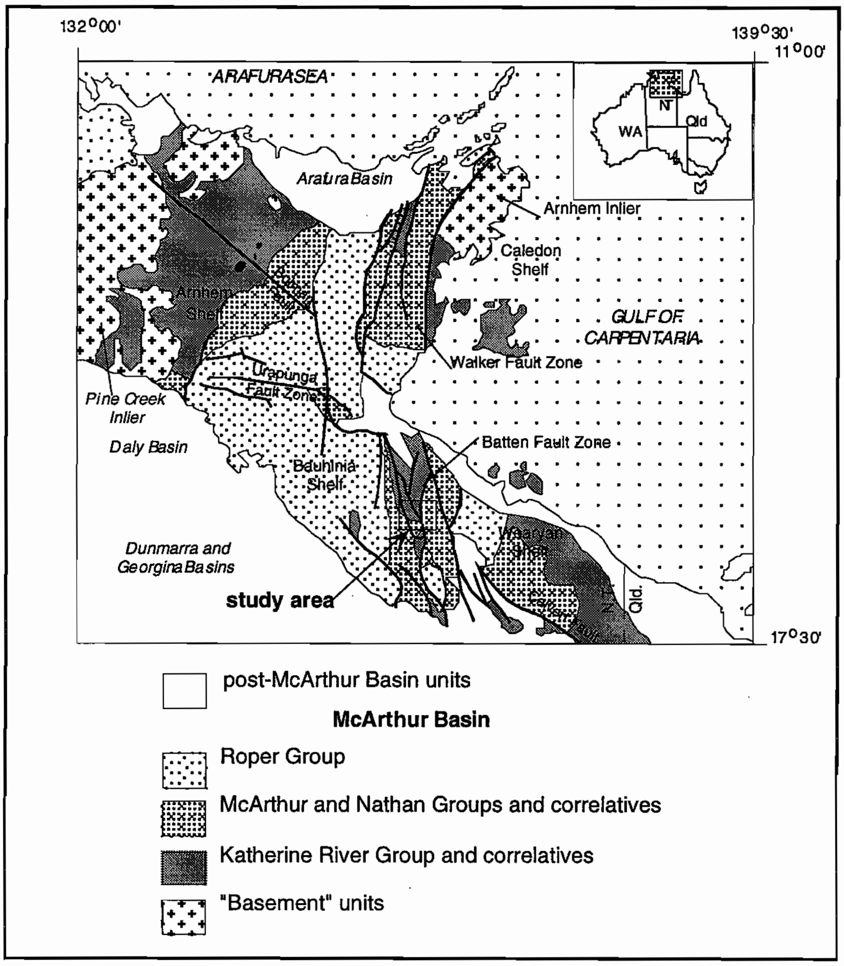

Figure 1. Major tectonic elements of the McArthur Basin (adapted after Piestch et al. 1991a).

they represented gypsum pseudomorphs, based largely on comparison of interfacial angles of the pseudomorphs with aragonite and gypsum, and purported analogies with modern examples growing in shallow brine pools on the sabkhat of the Trucial coast. A third alternative interpretation was put forward by Jackson et al. (1987), that at least some of the crystal casts were morphologically similar to trona described from the Eocene Green River Formation (Fahley, 1962). This tentative interpretation lead the authors to speculate that the depositional environment of the Coxco Dolomite Member was lacustrine as trona ($NaHCO_3.Na_2CO_3.2H_2O$) cannot be precipitated from normal seawater.

Methodology

As part of the measurement of regional sections through the Teena Dolomite and its contact with the overlying Barney Creek Formation, a large number of Coxco needle samples were collected and field relationships noted. Studies of drill core from the McArthur River area were also a source of additional, unweathered sample material. After discussion with NTGS (Alice Springs) geologists, further samples were also obtained from the Mt Shillingshaw Formation on the Helen Springs 1:250 000 Geological Mapsheet. The morphology of Coxco needles was studied both in outcrop and in hand-specimen, while several polished thin-sections were prepared for petrographic and microprobe work. As part of a larger geochemical study, samples of Coxco needles were drilled out for carbon and oxygen stable isotope analysis.

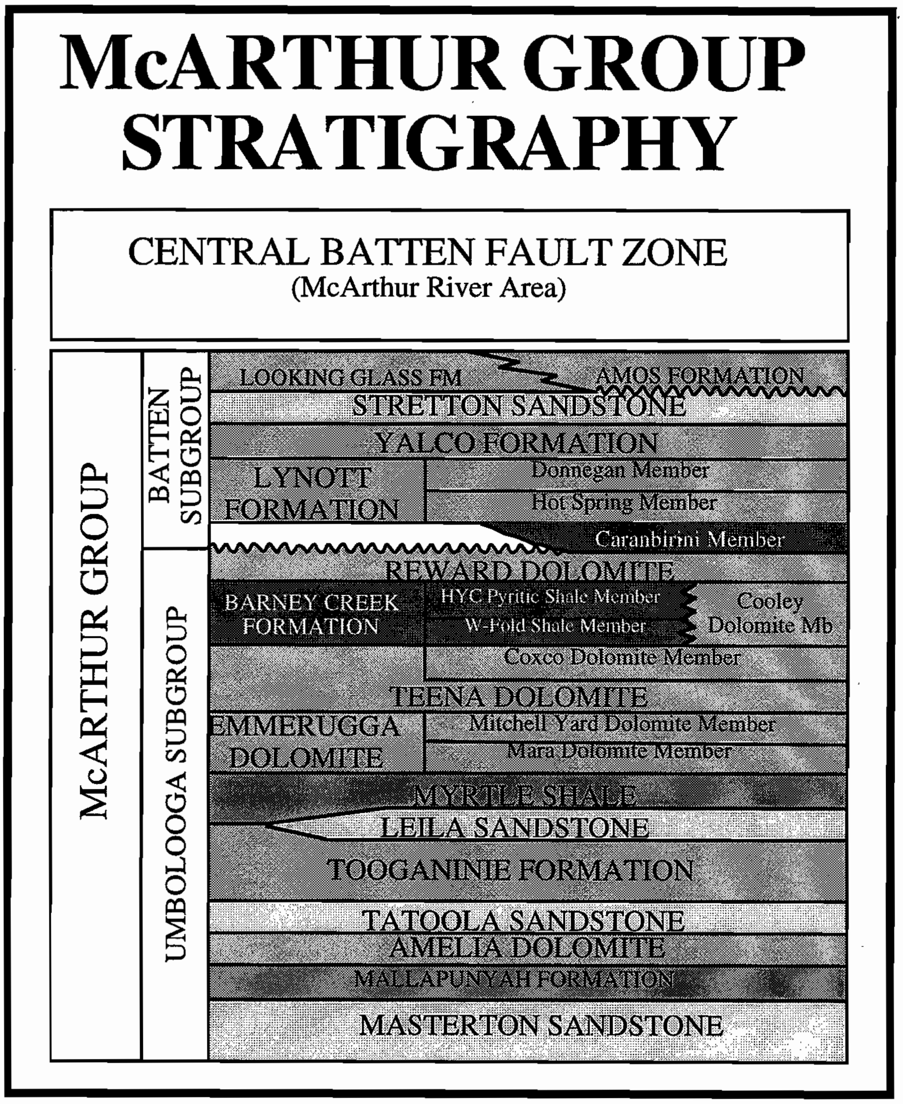

Figure 2. McArthur Group stratigraphy as defined by Jackson et al. (1987) and Pietsch et al. (1991a,b).

'Coxco needle ' lithofacies

The measurement of sections through the Teena Dolomite in the southern McArthur Basin has identified two distinctive lithofacies associated with Coxco needles. The first and most widespread lithofacies is largely composed of light- to dark grey crystalline dolostone and dololutite. Coxco needles up to 6 cm long are present and the acicular pseudomorphs form distinct rosettes or fans, either in isolation or as intergrown bundles forming distinct layers. Sedimentary laminae are commonly seen to onlap or drape the Coxco needle fans (Fig. 3). This lithofacies is particularly evident in the 'Gorge Prospect' and can be traced along strike for several kilometres. A representative section through the Coxco Dolomite Member and overlying Barney Creek Formation in the 'Gorge Prospect' area is included as Appendix 1.1. The gamma curve shows a distinctive inflection at the lithological contact between the Coxco Dolomite Member and the Barney Creek Formation and is inferred by Southgate et al. (1997) to represent part of a transgressive event toward an eventual maximum flooding surface further up-section in the Barney Creek Formation.

The second lithofacies is somewhat unusual in that the Coxco needles are observed in direct association with large (up to 1.5 m high) 'plumose' microbialites (Plate 1e,f). This lithofacies is unusual in that it is previously undescribed and that it appears cyclical with each microbialite/Coxco needles cycle overlain by 10–20 cm of detrital carbonate and then another cycle (Plate 1d). This association repeats itself up through a section of approximately 40 m (Appendix 1.2). The 'plumose' microbialites are themselves interesting in that they are morphologically unlike microbialites described in any other unit in the southern McArthur Basin area. Deep subtidal microbialites with very similar morphologies are observed in late Archaean carbonates of the late Campbellrand-Malrani (Sumner, 1995). A third lithofacies was also described in the Foelsche Inlier by Pietsch et al. (1991b). They noted that Coxco needles were abundant in massive dololutite interbedded with thick beds of dolomitic shale and siltstone similar to that of the Barney Creek Formation and on that basis, the unit was mapped as Coxco Dolomite Member.

In addition, there are numerous instances in the Coxco Dolomite Member (Gorge Prospect, Kilgour River) of brecciated Coxco needle clasts surrounded by isopachous, fibrous marine cement and sediment. Marine cement-infilled fissures or neptunian dykes also cross-cut beds of Coxco needles (Winefield et al., this report).

Pseudomorph morphology

Coxco needles consist of distinctive bottom nucleated, radiating fans of acicular crystal casts with the point of origin sometimes discernible. The dimensions of each 'needle' is approximately in the ratio of 1:10 (width:height) with 4 cm being the average length measured in this study. The terminations of each needle are commonly blocky and feathery (Fig. 3; Plate 1a,b), although pointed terminations are also present. In cross-section, 'Coxco' needles can appear pseudo-hexagonal (Plate 2a,b,c), with crystal casts generally having irregular six-sided forms.

The space between individual Coxco needles appears to be infilled by very fine-grained, micritic dolomite. Etching of selected samples and the observation of the etched surface under the SEM (Plate 2d,e,f), illustrates that the core of each needle is made up of relatively coarse crystalline dolomite that is lined by a sheath of fine-grained dolomicrite.

Under plain light, Coxco needles are made up of a mosaic of generally irregular and relatively coarse, equant dolomitic sparry cement (Plate 1g). The crystal boundaries commonly cross-cut the relics of the original Coxco needle structure, although there are a number of examples where there is a sharp boundary between the coarse dolospar cement, defining the Coxco needles shape, and the fine crystalline dolomicritic matrix. Both square and pointed terminations are evident under the microscope (Plate 1h).

Geochemical data

Initial microprobe work on the coarsely crystalline dolomitic cement pseudomorphing individual 'Coxco' needles shows that Ca and Mg contents average 21.01 and 13.32 wt% respectively. Fe contents range between 108 ppm and 13188 ppm (avg. 3618 ppm) while Mn concentrations range from 0 to 1667 ppm (avg. 675ppm). Sr, Zn and Ba contents generally lie below the detection limits for the microprobe (generally ± 150–180 ppm), although some analyses showed Sr contents up to 405 ppm, Zn up to 705 ppm and Ba up to 313 ppm. The relatively high value for Zn is attributed to the sample coming from below a slightly mineralised zone in the Coxco Dolomite Member intersected in DDH BJ1 (see Bull et al., this report).

Comparison of the elemental compositions of later burial sparry cements with results from dolomite pseudomorphing the Coxco needles shows that Fe and Mn contents are much lower in Coxco needle samples. In addition, the Fe and Mn compositions of fibrous marine cements and internal sediments are comparable to the Coxco needle analyses. Further microprobe work needs to be done to confirm and expand on these observations.

In addition to microprobe work, samples have also been drilled out for carbon and oxygen stable isotope work. The results will be compared with analyses from fibrous marine cements, internal sediments and later burial sparry cements from other McArthur Group samples (see Winefield et al., this report). Samples drilled out will also be analysed for Sr and Mn using Atomic Absorption Spectroscopy, as Sr contents are below detection limits for the microprobe.

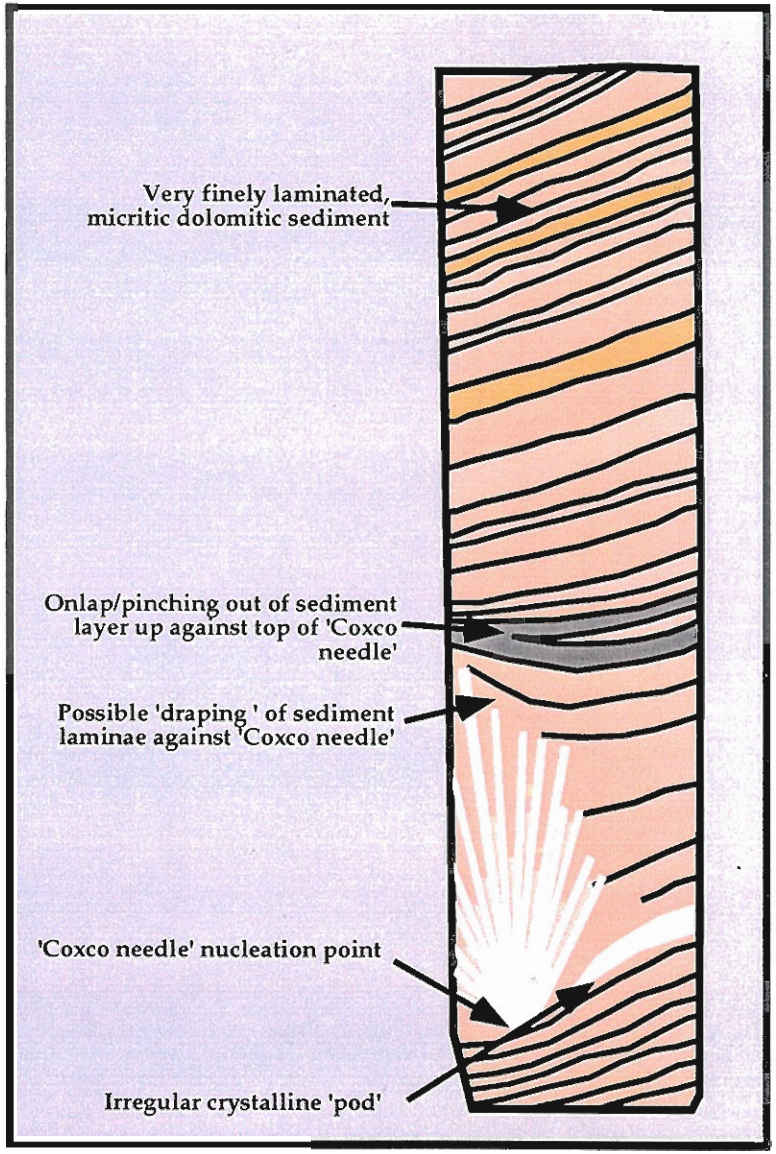

Figure 3. Photograph and schematic representation of a Coxco needle fan and associated features in a sample from DDH McA10 (132.35 m). Note particularly the onlapping and draping relationships of sediment laminae and the nucleation point of the 'Coxco' fan. There is only slight deformation of the underlying laminae beneath this point.

Plate 1

(1a) Radiating, acicular Coxco needles in the Coxco Dolomite Member from the Gorge Prospect, Kilgour River. The sample is °15cm wide.

(1b) 'Coxco' fans in the Mt Shillingshaw Formation, Helen Springs. The sample is 10 cm high. The Mt Shillingshaw Formation is overlain by sediments dated as being lateral equivalents of the Barney Creek Formation (Peter Beier, pers comm. 1997).

(1c) Silicified Coxco needles forming distinct subtly-weathered bands, 'Gorge Prospect', Kilgour River.

(1d) Laterally extensive (up to 500 m) benches of 'plumose', internally fibrous microbialites. Coxco needles form layers between microbialites, and are intimately associated with each individual microbialite. Note in plan view the circular, domal nature of microbialites of an underlying layer in the foreground. Microbialite layers are cyclical and are separated by planar- and wavy-laminated dololutite, which infills between microbialite forms. No Coxco needles are evident within this dololutite layer. Photo was taken at Weirk Waterhole on Balbirini Station.

(1e) Plan and cross-section view of microbialite bench shown in Plate 1d. Note the internally fibrous nature of each form. The overall shape of individual 'plumose' microbialites is elongate with a narrow base.

(1f) Close up view of 'plumose' microbialite forms, similar to Plate 1e.

(1g) Photomicrograph of a Coxco needles illustrating their radial form and acicular nature of individual 'needles'. Note particularly the irregular mosaic of pseudomorphic dolomite spar cement. This relationship is one of the criteria commonly used to infer calcitisation and dolomitisation of aragonite cements (Sandberg, 1985; Grotzinger, 1989; Sumner, 1995). Sample is from the Coxco Dolomite Member intersected in DDH Myrtle 5 (381.4 m). Scale bar = 1 mm.

(1h) Photomicrograph of the blocky and feathery terminations of individual Coxco needles. Note the finely crystalline dolomicritic matrix in the background and the sharp contact with pseudomorphic dolomite cement defining the needle shape. Sample is from the Coxco Dolomite Member intersected in DDH Berjaya 1 (91.30 m). Scale bar = 1 mm.

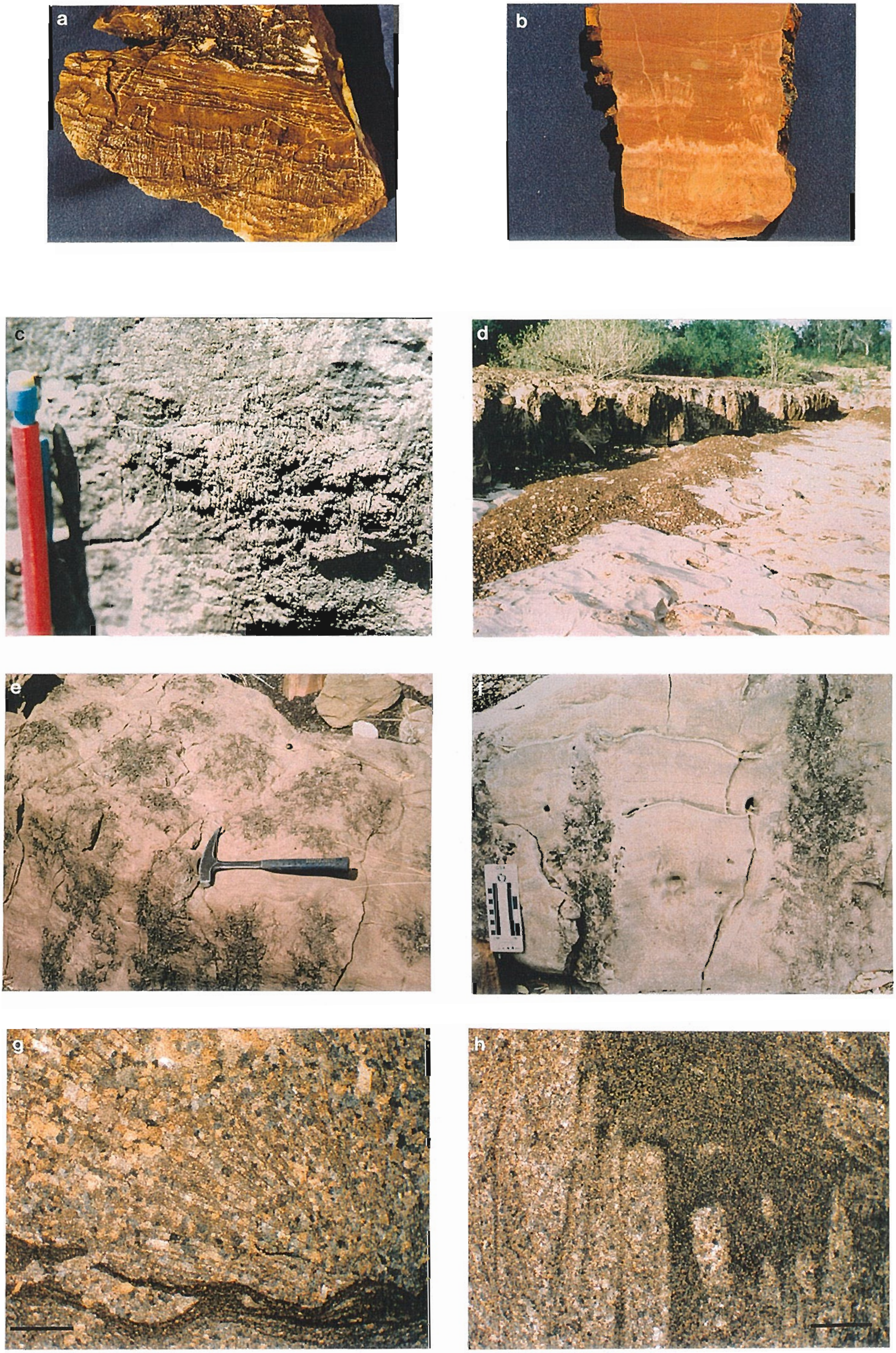
a
b
c
d
e
f
g
h

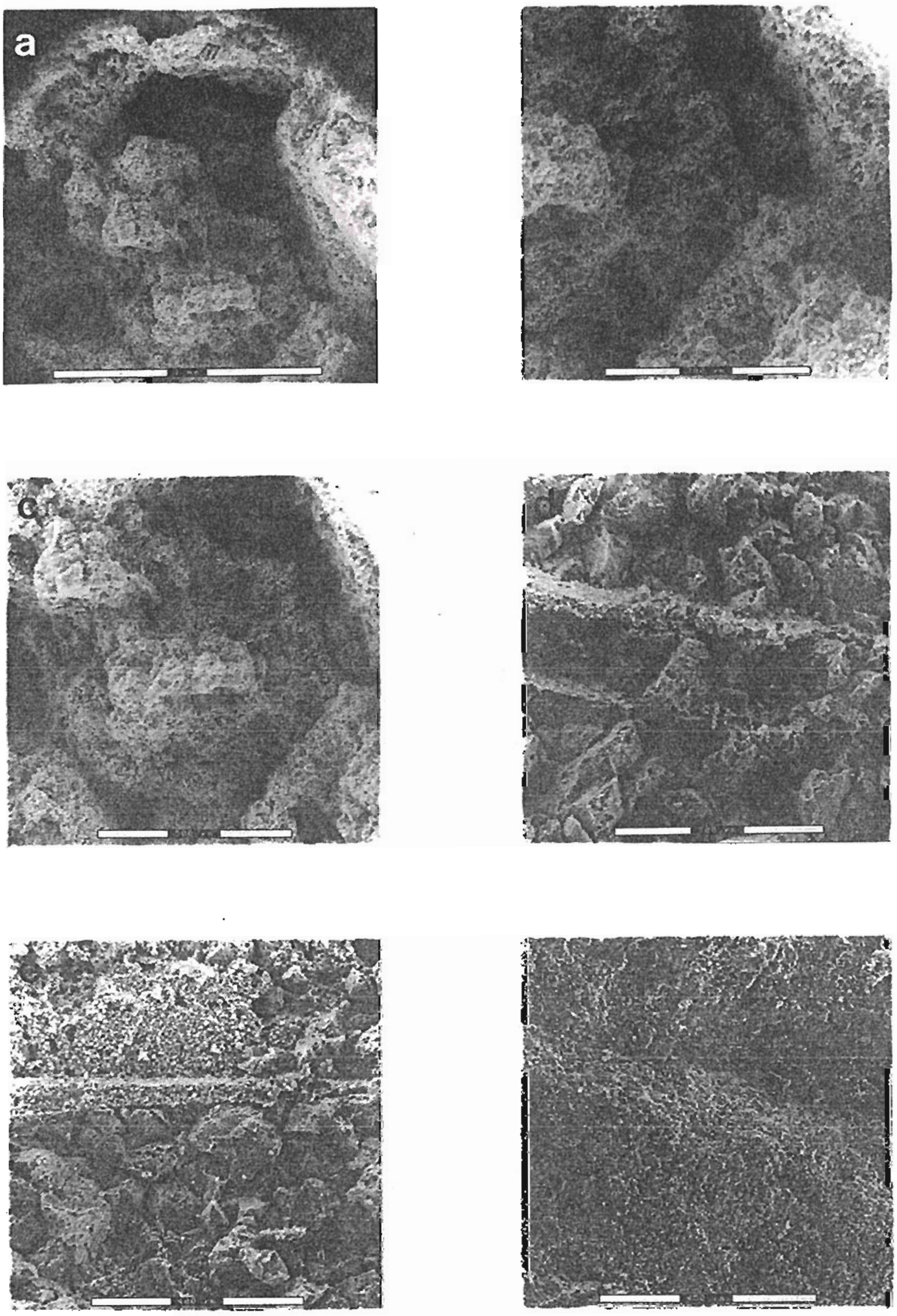

Plate 2

(2a), (2b) & (2c) Pseudo-hexagonal cross-section of Coxco needles under the SEM at various magnifications. Note the cross relationship between needles. Scale bar =1 mm(2a); 300 mm(2b); 500 mm(2c).Sample S96/130, Weirk Waterhole, Balbirini Station.

(2d), (2e) & (2f) Various SEM images of etched (2d, 2e) and unetched (2f) Coxco needles. Note the coarse dolomite cement which pseudomorphs each 'needle' is outlined by a finely crystalline dolomicrite layer, interpreted to be originally fine pelagic sediment that settled between individual acicular crystals. Scale bar = 300mm (2d); 400mm (2e); 450mm (2f). Sample S96/130, Weirk Waterhole, Balbirini Station.

Discussion

Field observations and the measurement of detailed sedimentological sections through the lower Teena Dolomite, Coxco Dolomite Member and Barney Creek Formation would appear to be inconsistent with the evaporative and/or emergent depositional environment interpreted for the Coxco Dolomite Member (Brown et al., 1969; Walker et al., 1977; Jackson et al., 1987; Pietsch et al., 1991a,b; Winefield and Bull, 1996). The general sequence (from the Emmerugga Dolomite/Teena Dolomite contact through to the upper Barney Creek Formation) appears to be broadly transgressive through coarse grained ooid/oncoid/ peloid grainstones interbedded with current rippled dololutite of the lower Teena Dolomite, subtidal columnar microbialite, planar laminated dololutite and interbedded dololutite/dolomitic shale lithofacies of the Coxco Dolomite Member, transitional oxidised/reduced sub-wave base lithofacies of the W-Fold Shale Member, and finally very coarse-grained mass-flows, turbiditic and slumped dolomitic siltstone and reduced shale of the lower part of the Barney Creek Formation. The distinct absence, in the Coxco Dolomite Member, of desiccation features (e.g. mud cracks, peritidal or lacustrine tepee structures), evaporite pseudomorphs (after anhydrite, halite, or gypsum) and supra-tidal lithofacies (microbially laminated dolostone with desiccation features coarser rippled layers; brecciation associated with post-depositional leaching of evaporites) support an entirely subaqueous depositional environment. This better fits a model of an overall transgressive sequence from the Coxco Dolomite Member into the Barney Creek Formation and is consistent with sequence stratigraphic interpretation of the gamma curve through KP96/1 by Southgate et al. (1997).

The fan-like geometry, pseudo-hexagonal cross-sections, acicular nature of individual Coxco needles and feathery to blocky crystal terminations are all consistent with primary aragonite precipitation (Loucks and Folk, 1976; Davies, 1977; Mazzullo, 1980). Subaqueous bottom-nucleated gypsum commonly has 'swallow-tail' or 'spear-like' terminations (John Warren, pers comm. 1996) and exhibits morphologies that are distinct from Coxco needles (see Fig 6a,b; Warren, 1996). The irregular coarse equant mosaic of pseudomorphing dolomite spar is consistent with criteria for identifying primary aragonite cements in ancient carbonate sequences (Sandberg, 1985).

Excellent fabric preservation of Coxco needles implies very early dolomitisation of the aragonite. Dolomitisation of gypsum requires a solid volume loss or the movement of large quantities of pore-water through the rock (Pierre and Rouchy, 1988). The absence of brecciation or solution-collapse phenomena, or evidence of significant pore-water movement (i.e vughs etc.) would appear to discount the latter process in this case.

Exclusively upright growth, sediment onlapping and draping relationships and the presence of Coxco needles in beds generally lacking in detrital carbonate all indicate that they grew either as positive relief features just below the sediment–water interface or nucleated directly at the sediment surface in a subaqueous environment. It is considered unlikely that they originated in the subsurface as diagenetic crystals.

The use of elemental geochemistry to distinguish whether there is elevated Sr, indicative of an aragonite precursor, has thus far proved unsuccessful. Elevated Sr compositions have been noted in Neoproterozoic ooids thought to have been originally aragonite (Kidder and Hall. 1993). Therefore, if the Coxco needles were originally aragonite and were dolomitised early, and the diagenetic system was closed, then an elevated Sr signature should be preserved. Carbon and oxygen stable isotope work should also aid in demonstrating an early marine, rather than a burial isotopic signature, for the dolomite cements pseudomorphing the Coxco needles.

Jackson et al. (1987) discussed the possibility that the Coxco needles could be pseudomorphs after trona evaporites. A review of the literature on trona indicates that it generally occurs in playa lake settings (e.g. Eugster and Hardie, 1978; Southgate et al., 1989) that exhibit distinctive lithofacies absent from the Coxco Dolomite Member. In addition, trona has a characteristic crystal morphology unlike that observed in Coxco needles samples collected as part of this study.

Other examples of aragonite fans

Massive submarine aragonite cements with large crystal sizes are recognised in many Phanerozoic sequences (Ginsburg and James, 1976; Yurewicz, 1977;

Davies, 1977). They are frequently composed of coarse aragonite and former aragonitic crystal arrays, now replaced by calcite or dolomite (Grotzinger, 1989).

In addition to Phanerozoic examples of giant aragonite arrays, there is an increasing recognition of crystal fans in the Precambrian carbonate rock record interpreted to have been originally aragonite (Table 1). These examples are all described as having features more diagnostic of aragonite than gypsum (i.e. radiating, upward-growing, acicular botryoidal form; sediment draping and onlap relationships with overlying sediment laminae; blocky or feathery terminations; pseudo-hexagonal cross-sections; irregular calcite/dolomite spar pseudomorph textures; intimate association with microbialites).

Significance of an aragonite precursor for Coxco needles

The presence of Coxco needles at a distinct stratigraphic interval, throughout a number of lithofacies and over a large area (from Helensprings through Bauhinia Downs up to Urapunga) indicates that their precipitation was a function of a subtle but widespread change in the water chemistry of the McArthur Basin. If the precursor of the Coxco needles was aragonite, then this change in water chemistry could be interpreted as an increase in the ratio of $[HCO_3^-]$ to $[Ca^{2+}]$ so that $CaCO_3$ precipitation was favoured.

A number of mechanisms could have affected the concentration of $[HCO_3^-]$ during deposition in the southern McArthur Basin. Grotzinger (1989) invoked atmospheric conditions to explain the large volume of carbonate precipitates (including aragonite fans) in the late Archaean/early Proterozoic. This is supported by the likelihood that the Archaean/early Proterozoic atmosphere contained more CO_2 than in the Phanerozoic. This increased the $[HCO_3^-]$ to $[Ca^{2+}]$ ratio allowing the greater precipitation of carbonate. Increased rates of carbonate production, is inferred by Grotzinger (1989) to have exhausted the concentration of Ca^{2+} and therefore only very limited calcium sulphate would have been precipitated. The change to conditions more akin to the Phanerozoic is thought to be recorded by the first appearance of bedded or massive gypsum in the McArthur Basin (1.6–1.5 Ga). The increased uptake of Ca^{2+} by $CaCO_3$ precipitation would have increased the ratio of Mg/Ca and provided a mechanism for the early dolomitisation of carbonate precipitates. The interpretation of aragonite fans in the Teena Dolomite would appear to complicate this model. A return to atmospheric conditions similar to that invoked in the late Archaean/Early Proterozoic is considered unlikely as there is no evidence of aragonite pseudomorphs or increased carbonate precipitation, that have been described, in stratigraphically equivalent carbonate sequences from the Lawn Hill Platform or Mt Isa Basin in Queensland, Australia.

A second mechanism that could have affected carbonate precipitation is tectonic induced changes in sea-level. Kennedy (1996) suggested that transgression and flooding (related to deglaciation) of carbonate shelves by bicarbonate-charged deep water caused the subsequent rapid precipitation of $CaCO_3$ related to deposition of Neoproterozoic cap dolostones in Australia. Therefore, it is thought likely that changes in the bathometry of a water body can influence that precipitation of carbonate cements through the upwelling of $[HCO_3^-]$ charged fluids onto carbonate platforms. Loutit et al. (1994) suggested, from Apparent Wander Polar Wander Path (APWP) data from the southern McArthur Basin, that there was a major tectonic event coincident with the deposition of the Teena to Reward Dolomite stratigraphic interval. A change in the bathometry of the southern McArthur Basin during the deposition of the Teena Dolomite could, therefore, possibly account for the precipitation of aragonitic Coxco needles.

Hydrothermal processes could also alter water chemistry in such a way as to favour the precipitation of aragonite fans and other carbonate cements (see Winefield et al., this report). Changes in the bathometry of the southern McArthur Basin related to the tectonic event recorded in the APWP, might also serve to 'restrict' the water body increasing the influence of this hydrothermal processes. However, it is unlikely that hydrothermal processes alone could explain the widespread occurrence of Coxco needles. Therefore, the combination of bathometric changes and hydrothermal activity, both related to a major tectonic event, is preferred as the major control on the precipitation of Coxco needles.

Table 1 Examples of radiating, acicular crystal fans in the literature.

Age	Stratigraphy/Location	Context	References
≈0.6 Ga	Nucculeena Fm, Adelaide Geosyncline, Australia	Relict crystal fans, now dolomite. Radiating, acicular form thought to have precipitated as aragonite.	Kennedy (1996)
1.9 Ga	Odjick-Rocknest Transition, Wopmay Orogen, Canada	Upward growing seafloor cement fans. Presence of square or feathery terminations and replacement by turbid neomorphic dolomite or calcite spar mosaics of randomly orientated crystals with ragged boundaries is inferred to be indicative of aragonite precipitation. Sr contents are typical of most ancient dolomites, some rare high Sr values.	Grotzinger and Read (1983)
2.52 Ga	Campbellrand-Malrani Carbonate Platform, Transvaal Supergroup, South Africa	Bundles of fibrous crystals forming crystal fans that grew upward in a radial pattern from a single point and reach heights of over 50 cm. Draped by micritic sediment and are commonly intricately associated with stromatolites. Combination of fibrous crystal habit, pseudo-hexagonal cross-sections and characteristics of the replacing mosaic suggest an aragonitic precursor.	Sumner and Grotzinger (1996); Sumner (1995)
2.7Ga	Steep Rock Group, southwest Province, Canada	Pseudofossil *Atikokenia* (up to 25 cm high) described as neomorphic carbonate that is pseudomorphed after a fibrous, radiating precursor mineral. Similar forms were also associated with stromatolites. Hoffman (1971) suggested an aragonite or calcium sulfate precursor. Later authors favoured gypsum due to the large crystal size (Walter, 1983; Wilks, 1986). Grotzinger (1989) prefers aragonite due to association with elongate marine stromatolites.	Hoffman (1971); Walter (1983); Wilks (1986); Grotzinger (1989)
2.7Ga	Cheshire Formation, Ngezi Group, Zimbabwe	Well-preserved, upward-diverging, botryoidal crystal bundles. 'Crystals' are composed of a calcite mosaic that is slightly coarser and 'cleaner' than groundmass. Martin et al. (1980) favoured a gypsum or aragonite precursor, while Walter (1983) preferred gypsum. Grotzinger (1989) argues for aragonite precipitation.	Martin et al. (1980); Walter (1983); Grotzinger (1989)

Conclusions

Sedimentological observations of the occurrence of Coxco needles in the Coxco Dolomite Member are inconsistent with the evaporative, emergent depositional environment previously proposed. The lack of desiccation features, other evaporite pseudomorphs and supratidal lithofacies would support the Coxco Dolomite Member being part of a broad transgressive sequence from the lower Teena Dolomite to the lower Barney Creek Formation.

The fan-like geometry, acicular nature of individual crystals, pseudo-hexagonal cross-sections, blocky or feathery terminations, excellent fabric preservation and irregular coarse mosaic of pseudomorphing dolospar cement is more indicative of an aragonite precursor for Coxco needles than of gypsum or trona. In the Proterozoic rock record, there are several other examples of carbonate crystal fans, interpreted as being originally aragonite, that display features very similar to Coxco needle fans. Sedimentological relationships and their exclusively upright growth suggests that the Coxco fans grew as either positive relief structures immediately below the sediment–water interface or nucleated directly on it. This is supported by their occurrence in beds lacking detrital carbonate and their intimate association with microbialites.

The observation of Coxco needles over a large lateral area, in a number of lithofacies and within a distinct stratigraphic interval is thought to be a function of a subtle change in the $[HCO_3^-]$ concentration. A major tectonic event is interpreted to have changed the bathometry of the southern McArthur Basin during Teena Dolomite deposition and, possibly in association with hydrothermal activity, created an environment favourable to the precipitation of aragonite fans in a number of sub-environments as evidenced in the Coxco Dolomite Member.

Acknowledgements

This work forms part of a PhD study on the sedimentology and diagenesis of Proterozoic McArthur Group carbonates of the southern McArthur Basin, northern Australia. Funding comes from an Australian Commonwealth Postgraduate Research Award and the AMIRA P384A Proterozoic Sediment-Hosted Base Metal Deposits project provides additional logistical support. The authors would like to thank Peter Beier (NTGS) for providing samples of the Mt Shillingshaw Formation for inclusion in this study. John Warren (JK Resources Pty Ltd) is thanked for providing the impetus for this report and discussions related to subaqueous gypsum precipitation. Jim Jackson and Peter Southgate (NABRE/AGSO) are thanked for fruitful discussions on various aspects of this report. Constructive criticism from John Dunster and David Rawlings (CODES) is also gratefully acknowledged.

References

Brown, M.C., Claxton, C.W., and Plumb, K.A., 1969. The Proterozoic Barney Creek Formation and some associated units of the McArthur Group, Northern Territory. Bureau of Mineral Resources, Australia, Record 1969/145

Bull, S.W., Cooke, D., and Winefield, P.R., this report. Progress report: Sedimentology and mineralisation at the Beryaya Prospect. AMIRA/ARC Project P384A.

Davies, G.R., 1977. Former magnesian calcite and aragonite submarine cements in upper Palaeozoic reefs of the Canadian Artic. Geology, v5, p11–15.

Eugster, H.P., and Hardie, L.A., 1978. Sedimentation in an ancient playa-lake complex: the Wilkins Peak Member of the Green River Formation of Wyoming. Bulletin of Geological Society of America, v86, p319–334.

Fahley, J.J., 1962. Saline minerals of the Green River Formation. U.S. Geological Survey, Professional Paper 405.

Grotzinger, J.P., 1989. Facies and evolution of Precambrian carbonate depositional systems: emergence of the modern platform archetype. *In* Crevello, P.D., Wilson, J.L, Sarg, J.F. and Read, J.R., eds, Controls on Carbonate Platform and Basin Development, SEPM Special Publication No. 44, p79–106.

Grotzinger, J.P., and Kasting, J.F., 1993. New constraints on Precambrian ocean composition. Journal of Geology, v101, p235–243.

Grotzinger, J.P., and Read, J.F., 1983. Evidence for primary aragonite precipitation, lower Proterozoic (1.9Ga) dolomite, Wopmay Orogen, north-west Canada. Geology, v11, p710–713

Ginsburg, R.N., and James, N.P., 1976. Holocene carbonate sediments of continental shelves. *In* Burk, C.A., and Drake, C.L., eds., The Geology of Continental Margins. Springer-Verlag, New York, p137–155.

Hofmann, H.J., 1971. Precambrian fossils, pseudofossils, and problematica in Canada. Geological Survey of Canada Bulletin, v189, 146p

Idnurm, M., Giddings, J.W., and Plumb, K.A., 1995. Apparent polar wander and reversal stratigraphy of the Palaeo-Mesoproterozoic southeastern McArthur Basin, Australia. Precambrian Research, v72, p1–41.

Jackson, M.J., Muir, M.D, and Plumb, K.A., 1987. Geology of the southern McArthur Basin, Northern Territory. Bureau of Mineral Resources, Australia, Bulletin 220.

Kidder, D.A., and Hall, S., 1993. Petrology and diagenetic evolution

15
colour

KP96/ 1

Gorge Prospect, Kilgour River

Base: 604552E; 8121760N

End: 604903E; 8121937N

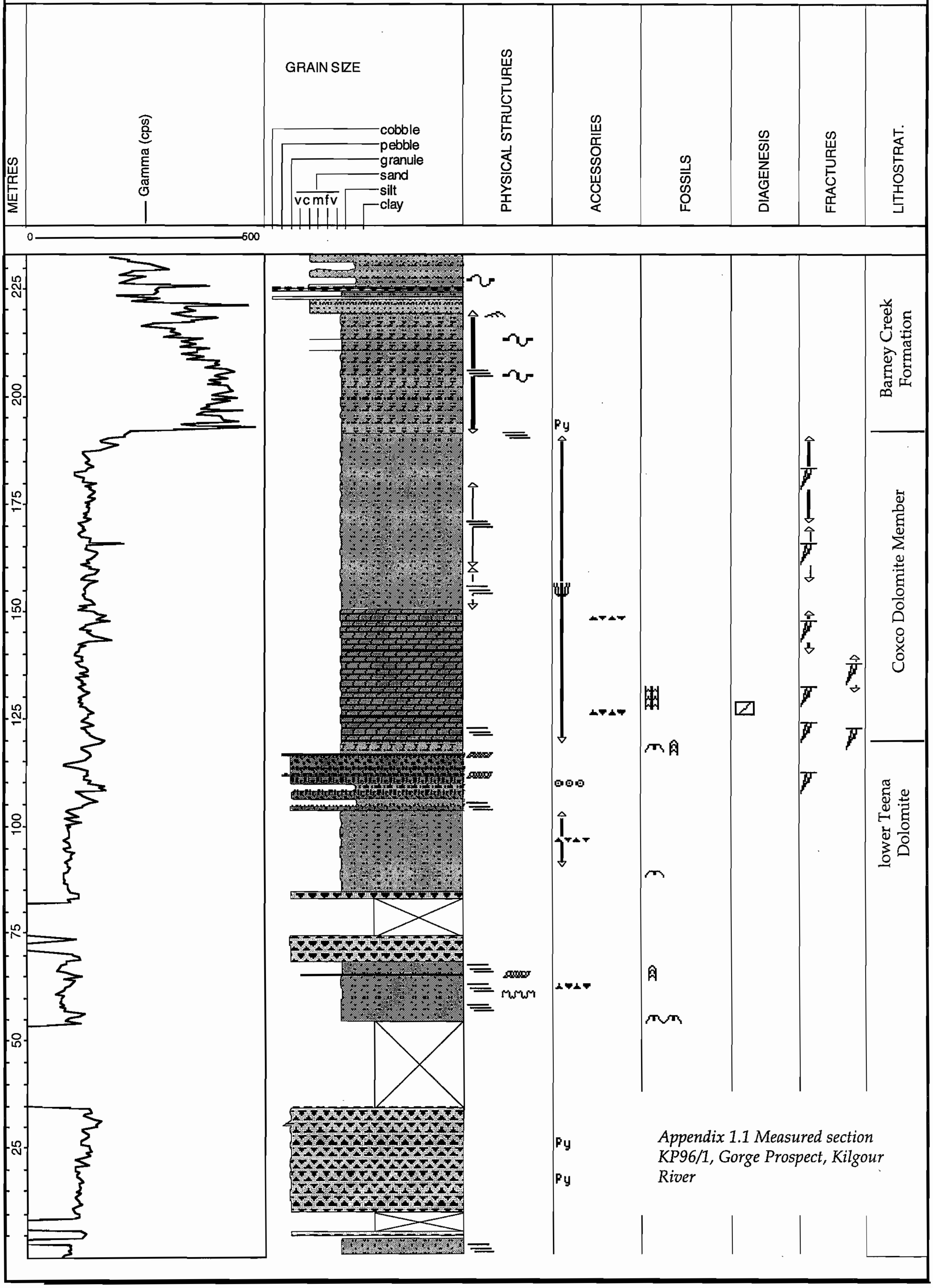

Appendix 1.1 Measured section KP96/1, Gorge Prospect, Kilgour River

colour

WE96/1

Weirk Waterhole, Balbirini Station

Start of section: 557232E; 81253389N
End of section: 555523E; 8124767N

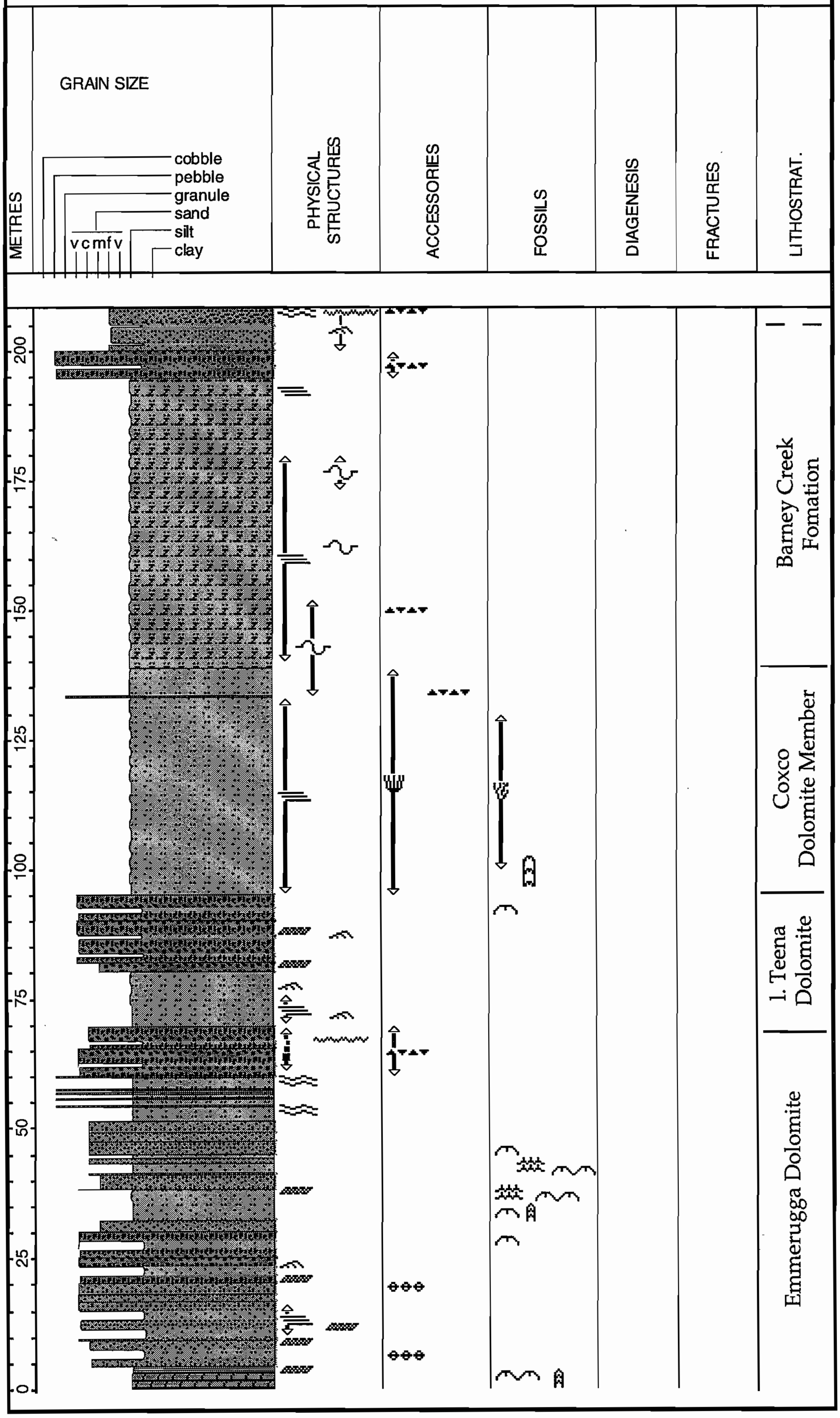

Appendix 1.2 Measured section WE96/1, Weirk Waterhole, McArthur River

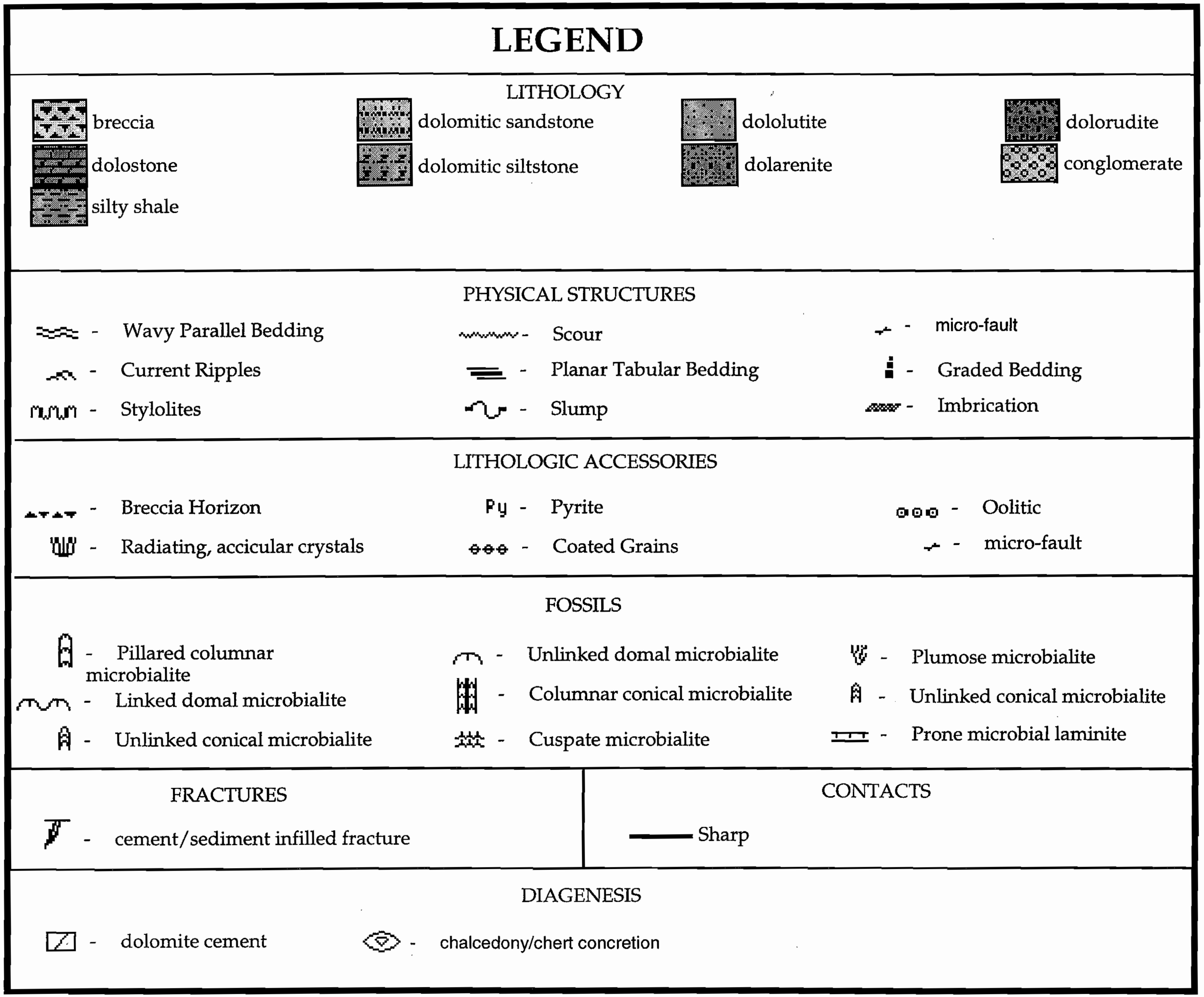

Appendix 1.3 Legend of symbols and lithologies used in Appendix 1.1 & 1.2

of Neoproterozoic ooids (Libby Formation, western Montana, U.S.A.). Precambrian Research, v63, p83–96.

Knoll, A.H., and Swett, K., 1990. Carbonate deposition during the late Proterozoic era: an example from Spitsbergen. American Journal of Science, v290A, p104–132.

Kennedy, M.J., 1996. Stratigraphy, sedimentology, and isotopic geochemistry of Australian Neoproterozoic Post-glacial Cap Dolostones: deglaciation, d[13]C excursions, and carbonate precipitation. Journal of Sedimentary Research, v66, no.6, p1050–1064

Louchs, R.G., and Folk R.L., 1976. Fan-like rays of former aragonite in Permian Capitan Reef pisolite. Journal of Sedimentology, v46, p483–485

Loutit, T.S., Wyborn, L.A.I, Hinman, M.C., and Idnurm, M., 1994. Palaeomagnetic, tectonic, magmatic and mineralisation events in the Proterozoic of northern Australia. AusIMM Annual Conference, Darwin, p123–156

Mazzullo, S. J., 1980. Calcite pseudospar replacive of marine acicular aragonite, and implications for aragonite cement diagenesis. Journal of Sedimentary Petrology, v50, p409–422

Martin, A., Nisbet, E.G., and Bickle, M.J., 1980. Archaean stromatolites of the Belingwe Greenstone Belt, Zimbabwe (Rhodesia). Precambrian Research, v13, p337–362

Pietsch, B.A., Rawlings, D.J., Creaser, P.M., Kruse, P.D., Ahmad, P., Ferenczi, P.A. and Findhammer, T.L.R., 1991a. Bauhinia Downs 1:250000 Geological Map Series. Northern Territory Geological Survey Explanatory Notes SE53–3

Pietsch, B.A., Wyche, S., Rawlings, D.J., Creaser, P.M., and Findhammer, T.L.R., 1991b. McArthur River Region 1:100000 Geological Map Series. Northern Territory Geological Survey Explanatory Notes SE53-3 (6065–6165)

Plumb, K.A. and Brown, M.C., 1973. Revised correlations and stratigraphic nomenclature in the Proterozoic carbonate complex of the McArthur Group, Northern Territory. In Geological papers 1970–71, Bureau of Mineral Resources, Australia, Bulletin 139, p103–115

Pierre, C., and Rouchy, J.M., 1988. The carbonate replacements after sulphate evaporites in the middle Miocene of Egypt. Journal of Sedimentary Petrology, v58, p446–456.

Sandberg, P., 1985. Aragonite cements and their occurrence in ancient limestones. *In* Schneidermann, N and Harris, P.M., eds, Carbonate Cements, SEPM Special Publication No. 36, p33–57

Southgate, P.N., Lambert, I.B., Donnelly, T.H., Henry, R., Etminan, H., and Weste, G., 1989. Depositional environments and diagenesis in Lake Parakeelya: a Cambrian alkaline playa from the Officer Basin, South Australia. Sedimentology, v36, p1091–1112

Southgate, P.N., Jackson, M.J., and Winefield, P.R.., 1997. Sequence stratigraphy of the upper McArthur Group: Teena Dolomite to Looking Glass Formations, NABRE Workshop, Extended Abstracts, AGSO Record 1997/12

Sumner, D.Y., 1995. Facies, palaeogeography, and carbonate precipitation on the Archaean (2250Ma) Campbellrand-Malrani Carbonate Platform, Transvaal Supergroup, South Africa (unpublished PhD thesis), Massachusetts Institute of Technology, 514p

Sumner, D.Y., and Grotzinger, J.P., 1996. Were kinetics of Archaean calcium carbonate precipitation related to oxygen concentration? Geology, v24, no.2, p119–122

Walker, R.N., Muir, M.D., Diver, W.L., Williams, N., and Wilkins, N., 1977. Evidence of major sulphate evaporite deposits in the Proterozoic McArthur Group, Northern Territory, Australia, Nature, v265, p526–529

Walter, M.J., 1983. Archaean stromatolites: Evidence of the Earth's earliest benthos, *IN* Scholf, J.W., ed., Earth's Earliest Biosphere. Princeton University Press, Princeton, p187–213

Warren, J.K., 1996. Evaporites, brines and base metals: what is an evaporite? Defining the rock matrix, Australian Journal of Earth Sciences, v43, p115–132

Wilks, M.E., 1986. The Geology of the Steep Rock Group, N.W. Ontario: A major Archaean unconformity and Archaean stromatolites (unpublished MSc thesis), University of Saskatachewan, 206p"

Winefield, P.R., and Bull, S.W., 1996. Carbonate-evaporite sediments in the McArthur River area: revision of middle McArthur Group lithofacies and recognition of key surfaces, AMIRA/ARC Project P384A Report 1, p23–39

Winefield, P.R., Bull, S.W., Selley., D., and Wallace, M.W, this report. Neptunian dykes and associated features within the Teena Dolomite, southern McArthur Basin: their formation and possible implications for the tectono-sedimentary setting of the Barney Creek Formation, AMIRA/ARC Project P384A

Yurewicz, D.A., 1977. Origin of massive Capitean Limestone (Permian), Guadalupe Mountains, New Mexico and West Texas. *In* Upper Guadalupe Facies, Permian Reef Complex, Guadalupe Mountains, New Mexico and West Texas. Society of Economic Palaeontologists and Mineralogists, Permian Basin Section Publication, 77–16, p45–62

Progress report: Sedimentology and mineralisation at the Berjaya Prospect

by Stuart Bull, David Cooke and Peter Winefield
CODES Special Research Centre, Geology Department, University of Tasmania

Introduction

The Berjaya Prospect is an occurrence of Pb-Zn mineralisation hosted in the middle McArthur Group approximately 17 km west of HYC Deposit. It was chosen for study for AMIRA/ARC Project P384 in the 1995 field season for two reasons:

(1) Unpublished company reports (e.g. Kneale et al., 1979) suggested that the Barney Creek Formation thinned to the north across a prominent east–west lineament in the Berjaya area. This linear feature, which extends to the west from the area of the HYC Deposit, is marked on published geological maps as a line of base metal prospects (e.g. W-Fold and Reward) in the area of a change in the level of exposure of the McArthur Group (Fig. 1). It is roughly coincident with a proposed east–west trending growth fault system bounding the northern margin of a half graben feature interpreted from enhanced airborne magnetics (Etheridge et al., 1994). It was postulated by the author, that if unit thickness changes towards this structure could be confirmed, then this would provided field evidence in support of east–west oriented syn-sedimentary growth fault active during McArthur Group deposition.

(2) Models for the genesis of the McArthur River base metal mineralisation (e.g. Walker et al., 1977) have proposed that the inter-ore breccia beds represent syn-sedimentary activity on an east–west trending growth fault to the north of the deposit, with the implication that this was a potential conduit for the mineralising fluids. If this is correct, and the east–west lineament in the Berjaya region is the westward continuation of the same growth fault structure, then the base metal mineralisation in this area potentially provides the opportunity to study the feeder system the HYC Deposit.

Initial sedimentological logging and sampling of two open file diamond drill cores, Berjaya 1 and 4 and one closed file core, DDH Boko 3 in the 1995 field season appeared, in general terms, to confirm the thickness changes in the McArthur Group units proposed by Kneale et al. (1979). However, the research program had to be put on hold when the area became both economically and academically sensitive. This was due to a renewed phase of exploration drilling of the prospect carried out by MIM Exploration in the 1994 and 1995 field seasons, the results of which were incorporated into confidential research being carried out by MIM geologists on the tectonostratigraphic setting of the McArthur Group. A summary of this work has now been published in abstract form (Neudert and McGeough, 1996), allowing the P384 research program to recommence in P384A.

Geological setting

Diamond drilling in the area of the Berjaya Prospect was initiated in 1978 to test airborne geophysical (INPUT) anomalies in the area of the prominent east–west lineament that extends west from HYC Deposit (Fig. 1). It penetrated middle McArthur Group stratigraphy, specifically; the upper Umbolooga Subgroup (Teena Dolomite, Barney Creek Formation, Reward Dolomite); and lower Batten Subgroup (Caranbirini Member of the Hot Spring Formation). Three types of base metal mineralisation were

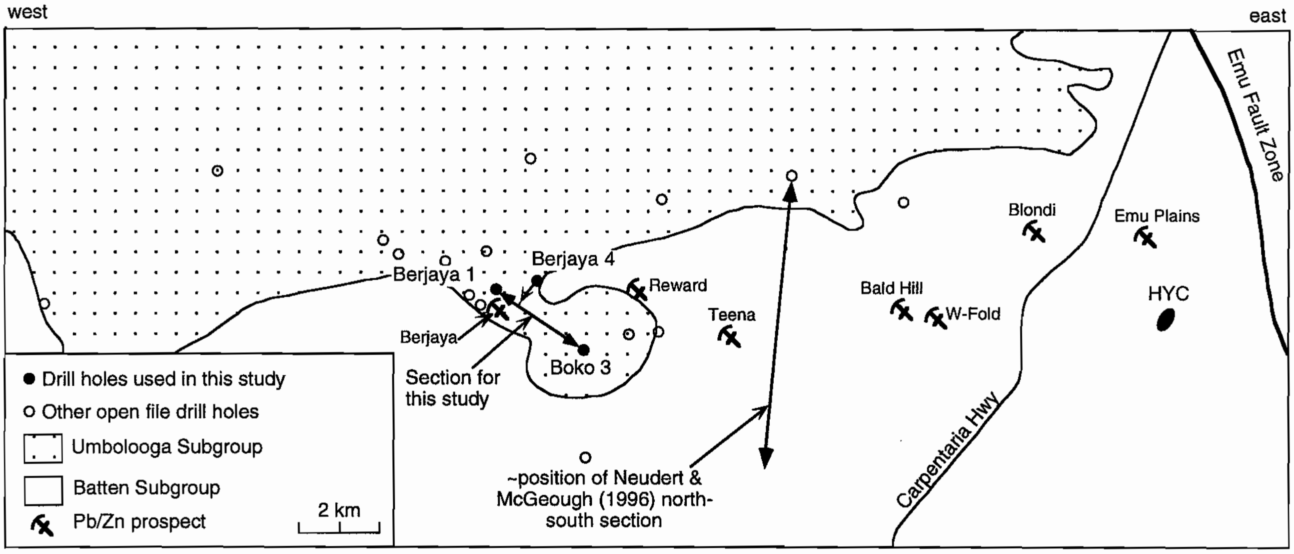

Figure 1. Location of the drill cores used in this study and other selected open file cores west of the HYC Deposit.

reported (Kneale et al., 1979). Finely disseminated pyrite in carbonaceous shales and discrete bands of pyrite on top of graded "tuffaceous" turbidites appear, from the assay data, to occur mainly in the Caranbirini Member with possible minor occurrences in the Barney Creek Formation. Coarsely crystalline sphalerite and chalcopyrite in vughs in dolomite occur in the Teena Dolomite. Although there are numerous faults in the area, two of the drill holes from this program (DDH Berjaya 1 and 4), in combination with a hole drilled in 1978 2.5 km to the southeast (DDH Boko 3), can be projected onto a northwest trending section that shows broad lateral changes in unit thickness and facies, as proposed in Kneale et al. (1979).

Drill core stratigraphy and correlations

Correlation between the three drill cores in the section examined is reliant on the recognition of key facies at the base and top of the intersections in each hole. These can be assigned to units of the current McArthur Group stratigraphy (Kneale et al., 1979) as follows; a pale coloured dolomite unit that forms the base of each intersection represents the Teena Dolomite; an interbedded dolomite and dolomitic siltstone unit that forms the upper part of each intersection represents the Hot Springs Formation. The characteristics of these units are described below:

Teena Dolomite

Thickness: DDH Boko 3; > 21 m, base not intersected, top defined by transition from pale dolomite with acicular needle pseudomorphs to darker more carbonaceous deposits.

DDH Berjaya 4; > 15 m, base and top as above.

DDH Berjaya 1; > 47.7 m, base and top as above.

Description: Massive/patchy/paisley patterned white to pale grey dolomite. Typical sedimentary features include faint lamination, bedding normal and radiating clusters of acicular needles, coarse-grained intraclastic dolomite, fine wavy carbonaceous lamination and small scour surfaces or hardgrounds in the DDH Berjaya 4 intersection between 137 and 138.5 m. Local post depositional features include irregular dark grey stylolitic bands up to 5 mm in width and stylo- or solution brecciation.

Interpretation; The acicular needles present in this units are characteristic of the Coxco Member of the Teena Dolomite (e.g. Jackson et al., 1987), however, the precise depositional mechanism for the dominant massive/recrystallised dolomite is unclear. Where lamination is present in the pale dolomite it is not obviously microbial in origin. However, some of the fine wavy carbonaceous lamination in DDH Berjaya 1 may represent in-situ microbial mat accumulated in the photic zone, and the scour surfaces and/or

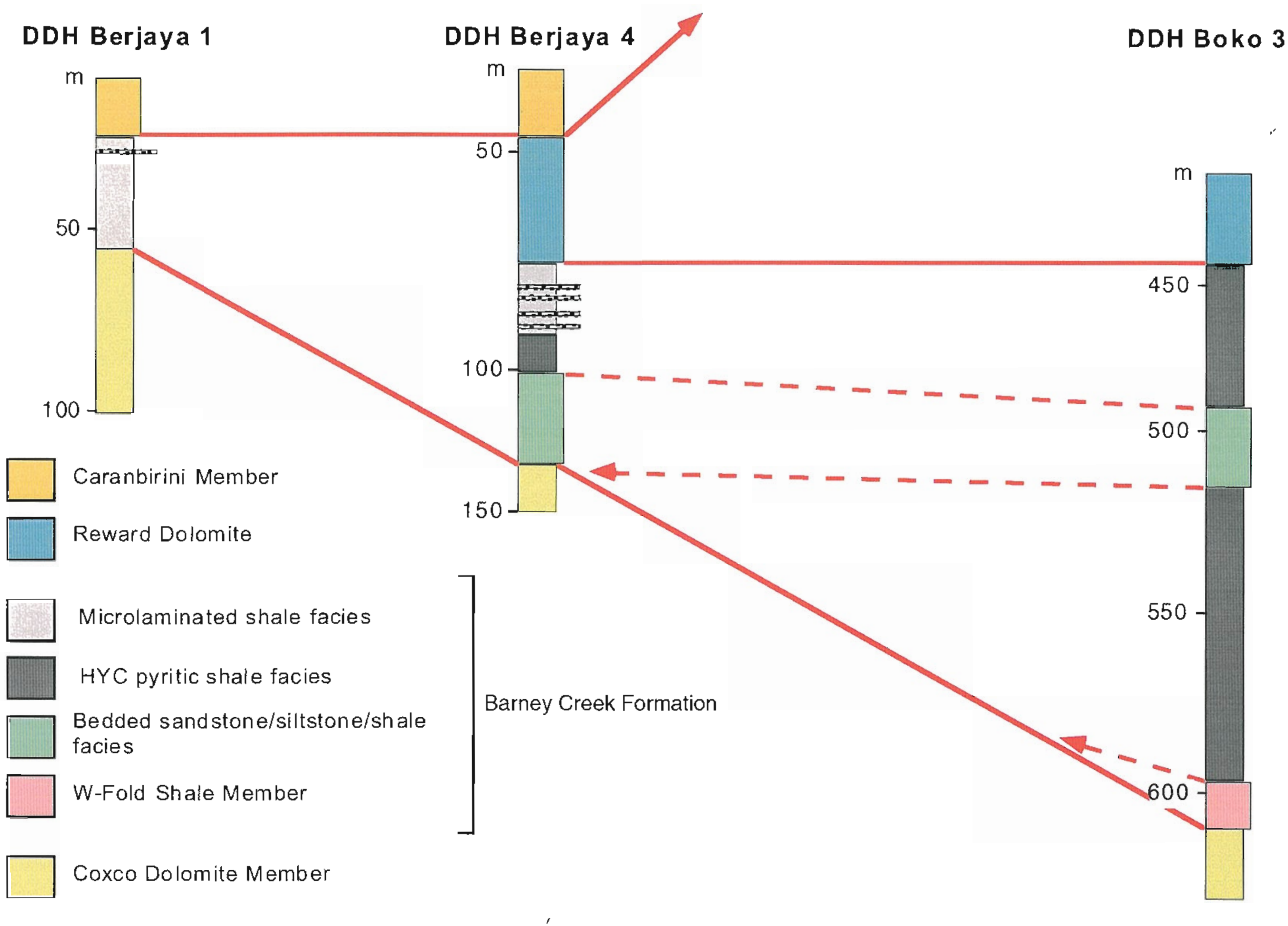

Figure 2. Facies logs for the three drill cores considered in this study. Tie lines are the suggested lithostratigraphic correlations.

Barney Creek Formation/Reward Dolomite

Thickness: DDH Boko 3; 519 m, base defined by interbedded carbonaceous siltstone and pale green dolomite characteristic of the W-Fold Shale Member (e.g. Jackson et al., 1987)

DDH Berjaya 4; 96 m, base defined by interbedded massive pale and finely laminated dark grey (relatively TOC-rich) dolomite

DDH Berjaya 1; 29 m, base defined by onset of thinly laminated wavy carbonaceous material that is locally disrupted

Description: In terms of published stratigraphic schemes for the McArthur Group (e.g. Jackson et. al., 1987; Pietsch et al., 1991), both a Barney Creek Formation and a Reward Dolomite intersection can be recognised in DDH Boko 3. The Barney Creek Formation intersection consists of a basal 13 m interval comprising interbedded grey to green dolomite and carbonaceous siltstone interpreted to represent the W-Fold Shale Member. It is overlain by a 146 m of HYC Pyritic Shale Member that can be subdivided into three; the lower and uppermost intervals are dominated by thinly bedded to laminated carbonaceous and pyritic siltstone; the middle interval is characterised by thicker bedding and a lightening of colour reflecting a decrease in the proportion of carbonaceous material. The overlying Reward Dolomite intersection has been interpreted to be 360 m thick in open file company drill logs (Kneale et al., 1979), however, only the basal few tens of metres were logged by the author. These comprised distinctive laminated to nodular pale grey dolomite.

Discrete Barney Creek Formation and Reward Dolomite intervals can also be recognised in DDH Berjaya 4. The Barney Creek Formation intersection in this case is a more complex mixture of facies that can broadly be subdivided into three intervals; the lowermost consists of 26.5 m where dolomitic mass flows up to 15 cm thick are interbedded with thinner deposits of massive or laminated carbonaceous siltstone; the middle interval consists of 10 m characterised by thinner and less abundant dolomitic mass flows and a higher proportion of carbonaceous and pyritic material; the upper interval consists of 12.5 m of interbedded finely laminated carbonaceous siltstone, locally crinkly/wavy, and massive grey dolomite. Intraclastic dolomitic breccia beds up to 1 m thick are also present at this level. The overlying Reward Dolomite intersection, although much reduced in thickness, is similar in overall appearance to that described from Boko 3. It can broadly be subdivided into a basal zone of 20 m of massive to faintly laminated/bedded pale grey dolomite with some nodule horizons and an upper zone of 23 m of interbedded pale grey dolomite and thinly laminated, dark grey, carbonaceous and pyritic siltstone.

The 29 m Barney Creek Formation/Reward Dolomite equivalent interval in DDH Berjaya 1 cannot obviously be subdivided into the constituent units. It is dominated by dark grey, thinly planar/wavy laminated, carbonaceous dolomitic siltstone. The lamination is disrupted in the basal metre of the unit. Scattered shallow scours are present throughout the unit and several distinct bleached zones (?hard-grounds) occur between 33 and 44 m. A pervasive network of fractures, some filled with pyrite, is locally present that is interpreted to have been generated during dewatering and/or compaction.

Interpretation: The Barney Creek Formation intersection in DDH Boko 3 is similar to other relatively thick drill core intersections of the unit described by the author (e.g. Bull, 1995). In the depositional model proposed from these studies; the basal W-Fold Shale Member is interpreted to represent a transitional oxidised facies from a pre-existing shallow water environment; the lower carbonaceous and pyritic siltstone dominated interval of the HYC Pyritic Shale is interpreted to record the deepest water conditions attained during accumulation of the McArthur Group. This was the result of a major transgression coincident with, and possibly generated by, a basin wide tectonic event that occurred at this time (e.g. Hinman et al., 1994; Neudert and McGeough, 1996). Sediment accumulation in this quiet reducing environment is by hemi-pelagic accumulation of carbonaceous matter periodically interrupted by the emplacement of dolomitic mass flows; the middle interval of the HYC Pyritic Shale Member is interpreted to represent a relative shallowing event where the mass flows are thicker and more proximal in character; the upper pyritic siltstone dominated interval of the HYC Pyritic Shale is interpreted to represent a further, less major flooding event with a resultant decrease in thickness of the dolomitic mass flows, accompanied by an increase in the proportion of hemi-pelagic carbonaceous material.

Thick Reward Dolomite intersections such as occurs in DDH Boko 3, that are characterised by an increase in the proportion of dolomitic mass flows with an accompanying decrease in carbonaceous and pyritic shale, have been observed by the author in other McArthur Group drillcores (Bull, 1995). They have been interpreted to represent shallowing and/or an increase in proximity to the mass flow source relative to, and genetically linked to, the depositional system responsible for the underlying Barney Creek Formation.

There are two possible origins for the nodular textures locally present in most Reward Dolomite intersections: (1) They may be primary depositional features, in which case their palaeoenvironmental significance is similar to that of the hardgrounds described from the Barney Creek Formation intersection in DDH Berjaya 1. (2) They may have a diagenetic origin in which case they have no palaeoenvironmental significance. The latter interpretation is preferred because the nodules often occur dispersed throughout areas of the host dolomite, not concentrated in discrete horizons as would be expected if they were developed at the sediment water interface.

The lower and middle Barney Creek Formation intervals of the Barney Creek Formation in DDH Berjaya 4 comprise facies described from thicker intersections such as DDH Boko 3. They can similarly be interpreted as representing hemi-pelagic accumulation of carbonaceous matter, periodically interrupted by the emplacement of dolomitic mass flows. It should be noted, however, that no W-Fold Shale Member interval is present. In addition, the facies arrangement within the HYC Pyritic Shale Member is different to that typical of the thicker Barney Creek Formation intersections studied, in that there is no clearly defined basal flooding event present. In fact, the deposits that appear to represent the deepest water conditions (i.e. where the proportion of carbonaceous material is highest and the dolomitic mass flows are less abundant and thinner) define the middle interval of the unit.

The facies association that comprises the upper interval of Barney Creek Formation in DDH Berjaya 4 has not been observed by the author in other intersections of the unit. The characteristic finely laminated carbonaceous siltstone has a distinctive wavy texture identical to that in the carbonaceous fragments in the storm deposited beds present in the Caranbirini Member, interpreted as evidence of accumulation as in-situ microbial mat in the photic zone (e.g. Scheiber, 1986). Prone mat in permanently submerged modern settings (e.g. Bermuda) occurs in areas of low sediment supply and slow current movement (Gebelein, 1969). The intraclastic dolomitic breccias must be sourced either from adjacent areas of steep topographic relief, or by erosion of consolidated substrate by energetic storm events. If the latter origin is correct, this provides further evidence for deposition in relatively shallow water above storm wave base. The Reward Dolomite intersection is analogous to that in DDH Boko 3 and is interpreted in the same manner to represent further shallowing and/or increased proximity to the source of the dolomitic mass flows.

The finely laminated wavy carbonaceous fabric that characterises the thin Barney Creek Formation intersection in DDH Berjaya 1 is also interpreted to represent in-situ microbial mat. In this case a relatively shallow depositional environment is supported by the scour surfaces present. Similar features to the bleached zones, here interpreted as hardgrounds, have been called crusts in other studies of the northern Australian Proterozoic sediments (e.g. Neudert and McGeough, 1996; Neudert, 1997), with the implication that they are evidence of subaerial exposure of the substrate. In the absence of supporting evidence of shallowing and emergence (e.g. plate breccias, evaporite pseudomorphs, oxidation etc.), the author believes they are more likely to be subaqueous hardground features. These have been reported from numerous modern carbonate settings (e.g. Fischer & Garrison, 1967) where they form in areas of sediment stability with low sedimentation rates and high initial sediment permeability (Schinn, 1969) and/or may be associated with bottom current activity (Stentoft, 1994).

Discussion

In terms of addressing the question proposed above, as to whether the progressive thinning of the Barney Creek Formation/Reward Dolomite interval to the northwest across the drill section studied is a result of removal of, or condension of, section, the litho-stratigraphic descriptions presented above are equivocal. This is due mainly to the lack of good stratigraphic markers at this level of the McArthur Group. Some observations can, however, be made and suggested correlations are shown by the tie lines on Figure 2:

(1) It is clear that the W-Fold Shale Member that occurs locally at the base of the Barney Creek Formation, has disappeared to the northwest over the 2 km between the 500 m thick section in DDH Boko 3 and the 100 m thick section in DDH Berjaya 4. In addition, the lack of the obvious basal flooding present in all of the thicker intersections of the HYC Pyritic Shale Member (Bull, 1995) in Berjaya 4, suggests that the lower part of this unit is also disappears across the section.

(2) The distinctive facies defined by finely laminated wavy carbonaceous fabric, and interpreted to represent accumulation of in-situ microbial mat in relatively shallow water conditions, appears to be restricted to the thinner HYC Pyritic Shale Member intersections.

Two possible mechanisms exist for the removal of the W-Fold Shale Member, and probably also the base of the HYC Pyritic Shale Member, over the relatively short distance between DDH Boko 3 and DDH Berjaya 4. These are onlap and faulting.

It is difficult to assess them quantitatively without more drilling and/or outcrop control. However, the fact that the section continues to thin past DDH Berjaya 4 into the area of DDH Berjaya 1 indicates that the system is more complex than simple removal of section across one fault. It must, therefore, either consist of multiple faults or onlap to the northwest.

The most recent model proposed for the tectono-stratigraphic development of this part of the McArthur Group (Neudert and McGeough, 1996), is based on drill core analysis, and extends an earlier regional model presented by Etheridge et al. (1994) that was based on enhanced airborne magnetics. In summary, this model contends that middle McArthur Group sedimentation was controlled by half grabens generated by a network of east–west trending, south dipping growth faults (e.g. the lineament that extends westward from the HYC Deposit through the Berjaya area) and north–south trending transfers (e.g. the Emu Fault). The east–west trending drill core based sections shown in Neudert and McGeough (1996) extend from the area of the HYC deposit as far west as Berjaya, and their north–south section showing a half graben geometry is taken approximately 5 km to east of the section documented in this study (Fig. 1). In their model, the south dipping normal fault inferred to form the northern boundary of the proposed half graben corresponds to the east–west trending map lineament through the Berjaya area.

If the thinning of the Barney Creek Formation/Reward Dolomite interval to the northwest in the Berjaya area documented in this study is due to onlap of the base of the package, then it supports the Neudert and McGeough (1996) model as schematically represented in Figure 3. In this case; the thick section in DDH Boko 3 would represent sediment accumulation on top of the most subsided part of the hanging wall block close to, but to the south of, the south dipping growth fault; the thinner section in DDH Berjaya 4 would be the result of the removal of the W-Fold Shale Member and the basal part of the HYC Pyritic Shale Member by onlap onto the elevated footwall block; the thinnest interval in DDH Berjaya 1 would represent deposition to the north of the growth fault on top of the elevated footwall block. This model is supported by the fact that the in-situ microbial mat facies, that must represent deposition in relatively shallow water (i.e. within the photic zone), occurs in relatively elevated parts of the Barney Creek Formation depositional system. It is also consistent with the presence of subaqueous hard-grounds in the thinnest intersection in Berjaya 1. These features are known to form in areas of low sediment supply and this elevated position, on top of the uplifted footwall block, would have been a site of sediment bypass and non-deposition for much of the Barney Creek Formation/Reward Dolomite time. It should be noted, however, that no evidence of the karstification which has been reported from such sites (Neudert and McGeough, 1996) was observed in this case.

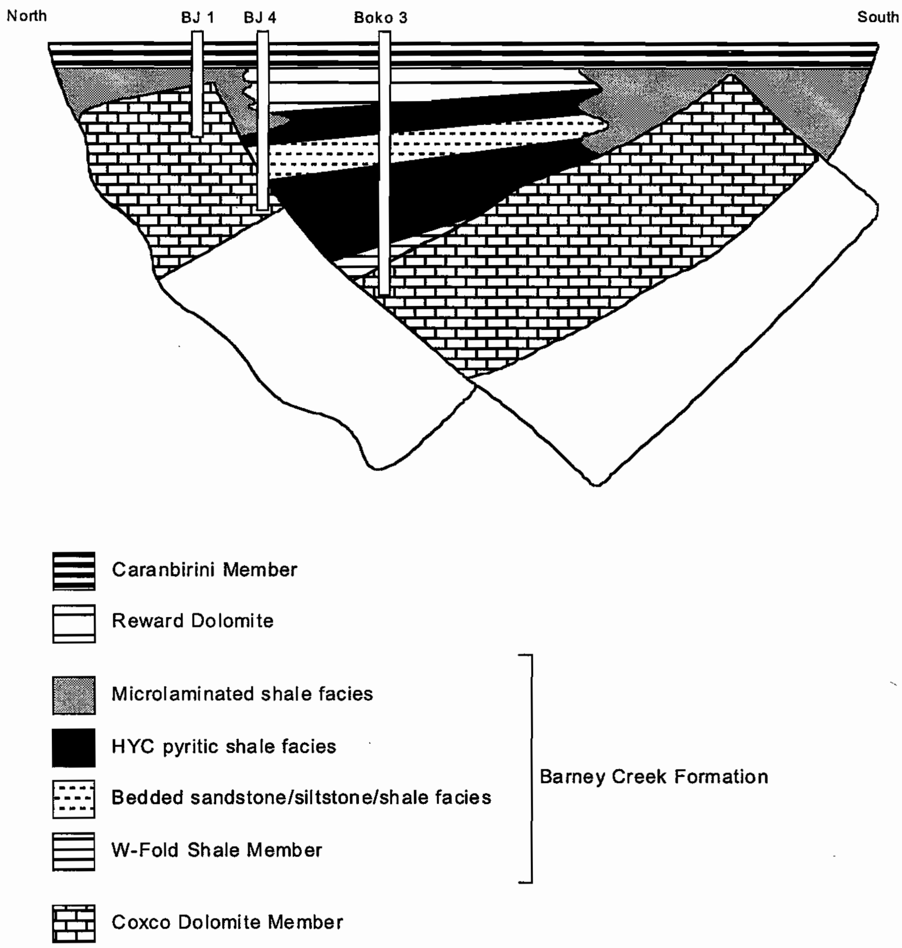

Figure 3. Cartoon (not to scale) of the suggested relationship between the drill cores studies and a half graben model for Barney Creek Formation time.

Conclusions

Drill core based studies in the Berjaya area indicate that:

(1) The stratigraphy is constrained by the recognition of the Coxco Member of the Teen Dolomite in the base of the drill core intersections, and the Caranbirini Member of the Lynott Formation in the top. The latter comprises a distinctive sedimentary facies interpreted to represent storm wave reworking and redeposition of originally in-situ microbial mat in relatively shallow water conditions.

(2) The intervening stratigraphic interval that represents Barney Creek Formation/Reward Dolomite time thins markedly over a distance of only 2.7 km from in excess of 500 m in DDH Boko 3 in the southeast, through around 100 m in DDH Berjaya 4, to less than 30 m in DDH Berjaya 1 in the northwest, as originally proposed by Kneale et al. (1979).

(3) Lithostratigraphic correlations within this package are uncertain due to a lack of good lithostratigraphic markers. However, the most likely mechanism for the thinning of the section appears to be onlap of the lower part of the

Barney Creek Formation (W-Fold and lower HYC Pyritic Shale Members) to the northwest (Fig. 2). This configuration supports tectono-stratigraphic models that invoke accumulation of the sediments at this level of the McArthur Group in half grabens controlled by east–west trending, south dipping growth faults and north–south trending transfers (Etheridge et al., 1994; Neudert and McGeough, 1996).

(4) In areas where the section is thinner, distinctive sedimentary features occur e.g. thinly planar to wavy laminated carbonaceous siltstone interpreted to represent in-situ microbial mat, and bleached zones interpreted as subaqueous hardgrounds. These occurrences can also be explained by the prevailing tectonic model, in which these areas would represent deposition in areas above the uplifted footwall block in a half graben system. Such settings would be relatively shallow water (or possibly emergent) because of the elevated structural position. The latter would also result in restriction of accommodation space and promotion of sediment bypass, which would be manifest in the rock record as thin/condensed sections, and by the promotion of sedimentary features characteristic of areas of low sediment supply in relatively shallow water (i.e. the in-situ microbial mat and subaqueous hardgrounds) respectively.

Future work

Mineralisation in the Berjaya Prospect will be studied using a number of geochemical techniques with the aim of better understanding the fluid dynamics of a mineralised system on the east–west trend away from HYC. This approach will include: sulphur isotope analysis (both whole rock and laser ablation) of diagenetic pyrite and pyrite associated with mineralisation; Pb isotope analysis of galena from discordant and stratiform mineralisation; carbon and oxygen analysis of sparry dolomite cements associated with pyrobitumen and sulphide mineralisation; carbon isotope analysis of organic carbon/pyrobitumen; and fluid inclusion analysis on selected coarse dolomite cements. In addition, dolomite cements and their association with sulphide minerals will also be studied using standard petrographic and cathodoluminescence techniques and the results included in a PhD study of the carbonate diagenesis of middle McArthur Group carbonates by Peter Winefield.

References

Brock, T. D. 1976. Environmental microbiology of living stromatolites. Developments in sedimentology, 20, Stromatolites. M. R. Walter. Elsevier, Amsterdam, 251–259.

Bull, S. W. 1995. Toward a regional depositional model for the Palaeoproterozoic Barney Creek Formation, southern McArthur Basin, Northern Territiory. CODES: AMIRA/ARC Project P384 Final Report, 133–157.

Chakraborty, C. 1995. Gutter casts from the Proterozoic Bijaygarh Shale Formation, India: their implicaiton for storm-induced circulation in shelf settings. Geol. J. 30(1), 69–78.

Gebelein, C. D. 1969. Distribution, morphology and accretion rate of recent subtidal algal stromatolites, Bermuda. J. Sed. Pet. (39), 49–69.

Fischer, A. G. and Garrison, R. E. 1967. Carbonate lithification on the sea floor. J. Geol. 75(4), 488–496.

Etheridge, M. and Wall, V. 1994. Tectonic and structural evolution of the Australian Proterozoic. Geol. Soc. of Aust. Abst. 37, 102–103.

Hinman, M., Wall, V. and Heinrich, C. 1994. The interplays between sedimentation, deformation and hydrothermal activity at the the McArthur River Pb-Zn(Cu) Deposit.Geol. Soc. Aust. Abst. 37, 176–177.

Kneale, C. M., MacDonald, I. A., Shannon, C. H. C. and Zeissink, H. E. 1979. Annual Report, Berjaya Prospect, A.O. (Australia) Pty. Ltd. Northern Territory Department of Mines and Energy, Open File Company Report 79/8c (unpublished).

Jackson, M. J., Muir, M. D. and Plumb, K. A. 1987. Geology of the southern McArthur Basin. B. M. R. Bull. 220, 173 pp.

Myrow, P. M. 1992. Pot and gutter casts from the Proterozoic Chapel IslandFormation, Southeast Newfoundland. J. Sed. Pet. 62(6), 992–1007.

Neudert, M. and McGeough, M. 1996. A new tectonostratigraphic framework for the deposition of the upper McArthur Group, N.T. New Developments in Metallogenic Research: The McArthur-Mount Isa-Cloncurry Minerals Province, MIC 96 Extended Abstracts, 90–93.

Neudert, M. 1997. The Mount Isa Group in the Mount Isa district sequence stratigraphy and accomodation history from core and outcrop. NABRE Workshop March 4–5, 1997, Abstracts. AGSO Record. 1997/12, 10pp.

Pietsch, B.A., Wyche, S., Rawlings, D.J., Creaser, P.M., and Findhammer, T.L.R., 1991b. McArthur River Region 1:100000 Geological Map Series. Northern Territory Geological Survey Explanatory Notes SE53-3 (6065-6165).

Schieber, J. 1986. The possible role of benthic microbial mats during the formation of carbonaceous shales in shallow Mid-Proterozoic basins. Sedimentology. 33, 521–536.

Shinn, E. A. 1969. Submarine lithification of Holocene carbonate sediments in the Persian Gulf. Sed. 13, 109–144.

Stentoft, N. 1994. Early submarine cementation in the fore-reef carbonate sediments, Barbados, West Indies. Sed. 41, 585–604.

Walker, R. N., Logan, R. G. and Binnekamp, J. G. 1977. Recent geological advances concerning the H.Y.C. and associated deposits, McArthur River, N.T. J. Geol. Soc. Aust. 24, 365–380.

Progress report: Neptunian dykes and associated features within pre-Barney Creek Formation sediments, southern McArthur Basin

by Peter R. Winefield, Stuart W. Bull, David Selley & Malcolm Wallace*
CODES Special Research Centre, Geology Department, University of Tasmania
**Department of Earth Sciences, University of Melbourne*

Summary

Sediment- and fibrous cement-infilled fractures (or neptunian dykes) have been identified in the Teena and Emmerugga Dolomites within the southern McArthur Basin. They are commonly infilled by successive generations of radial-axial fibrous dolomite cement and internal sediment, and intraclasts rimmed with fibrous dolomite cement are occasionally observed as part of the infilling sequence. The fibrous dolomite cements display very similar characteristics to radial-axial fibrous calcite cements commonly inferred to be of a marine origin in Phanerozoic carbonate sequences.

At each locality, the structural orientation of neptunian dykes and sills is remarkably consistent and there is strong evidence for surfical extension, sliding and slumping of lithified carbonate sediments creating open spaces within the displaced mass. Individual neptunian dykes display fitted and regular features with little evidence of dissolution associated with subaerial exposure. This is supported by the lack of sedimentological evidence for emergence. Two possibilities are suggested for neptunian dyke formation; slumping of lithified sediment as a function of 'tilt-block' formation or deformation directly related to syn-sedimentary fault development.

Sedimentological relationships between the Teena Dolomite and Barney Creek Formation in the 'Gorge Prospect' area would support the 'tilting' of the Coxco Dolomite Member and older units and subsequent deposition of Barney Creek Formation sediments into the resultant sub-basin. Further structural work is needed to better constrain neptunian dyke formation and its relationship to Barney Creek Formation deposition.

Introduction

Neptunian dyke definition

Neptunian dykes are syn-sedimentary dykes formed by the infilling of submarine fissures or cavities by sedimentary material (Playford, 1984; Bates and Jackson, 1987). Strauch (1966) described sedimentary dykes as fissures filled with sediment penetrating other rock units at various angles and cited Pavlow (1896) as the initiator of the term 'neptunian dyke' for submarine sedimentary dykes. The term 'neptunian dyke' is applied to sediment- and or cement-infilled fissures that cut bedding of the host rock, while neptunian sills are related fissure fillings that are essentially bedding parallel (Playford, 1984).

Neptunian dyke formation

The mechanism that commonly results in the formation of neptunian dykes is the extensional or dilatational movement of lithified and indurated sediment layers due to gravitational mass movement or differential tectonic movement. Wendt (1971) attributed submarine fractures (or neptunian dykes) in Jurassic shallow-water limestone of western Sicily to tensional stress as evidenced by parallelism of successive submarine fissure generations. Lehner (1991) observed that successive neptunian dyke generations along drowned carbonate platform margins could be caused by repeated extensional brittle faulting of lithified periplatform deposits. The study of neptunian dyke formation can therefore allow a better understanding of the regional history of vertical movement with regard to sea-level (tectonic and/or eustatic). If the cavities were formed by subaerial processes, e.g. by karstic dissolution of a host carbonate sequence, then emergence is required, followed by resubmergence if the infilling cements and or sediments are of marine origin. Alternatively, if the cavities were formed by fracturing and dilation of the host rocks in a submarine environment, then emergence would be an unnecessary over-interpretation (Winterer and Sarti, 1994).

Neptunian dykes are commonly infilled with at least one generation of fibrous radial-axial calcite (RFC) cement. It was originally described as a replacement texture after aragonite, but work by Kendall (1985) and Sandberg (1985) has proven it as a primary precipitate that forms in the marine phreatic environment. Marine cements are commonly: the first cement generation; fibrous (acicular or columnar); isopachous fringes around grains or cavities; associated with internal sediments; succeeded by sparry calcite or dolomite; non-ferroan and non-luminescent under cathodoluminescence (CL); and may occur in intraclasts (Tucker and Wright, 1990).

Examples of neptunian dykes studies

There are several examples in the literature where neptunian dykes have been recognised (e.g. Bernouli and Jenkins, 1974; Lehner, 1991; Winterer et al., 1991 and Winterer and Sarti, 1994). The best known occurrence of neptunian dykes is in the Devonian Reefs of the Canning Basin, western Australia. They were first recognised by Playford and Lowry (1966) and further described by Playford (1980) and Playford (1984). The neptunian dykes are interpreted to have formed relatively soon after deposition in early-cemented limestone due to the effects of local tectonism on carbonate platform margins. The open fissures were infilled by combinations of sediment infilling from above, encrusting organisms, fossil debris, oolites, spar balls (RFC cement isopachously rimming brecciated dyke fillings) and syn-sedimentary marine RFC cement (Playford, 1984). Neptunian sills are most abundant in marginal-slope deposits and are interpreted to be the result of downslope sliding of cemented blocks of fore-reef and reefal-slope sediments on uncemented interbeds of mud or sand. Some sills are also the result of bedding-subparallel fissuring of reef-margin and reef-flat limestone.

Most of the dykes and sills are not directly related to faults (Playford, 1984), although a major exception is neptunian dyke system that follows the Cadjebut Fault at the south end of the Emanuel Range (Playford and Lowry, 1966). Recent work by Dörling et al. (1996) has shown that the distribution of lithofacies in the Pillara Range is controlled by basement-hosted faults. These faults focused syn-sedimentary deformation along the edge of the platform margin, with zones of sediment- and cement-filled neptunian dykes forming above the basement faults.

Controls on fracturing and neptunian dyke formation are often a source of conjecture. An example of this is the Mesozoic Tethys in the Mediterranean region, which display a great variety of neptunian dykes. Some have been interpreted as marine infilling of subaerial karstic cavities, while others have been interpreted as having been formed by surficial fracturing, dilation and infilling entirely within the submarine environment (Winterer and Sarti, 1994).

Therefore where any set of neptunian dykes is present, the following fundamental questions must be answered:

1. How, where and when were the cavities formed? Do they relate to relatively passive, gravity driven downslope sliding and platform failure (e.g. Playford, 1984) or are they more directly linked to active faults that focus syn-sedimentary deformation along the edge of the lithified platform (e.g. Dörling et al., 1996)? Are they cavities formed by dissolution associated with subaerial exposure of a carbonate succession (e.g. Vera et al., 1987) or is the open space generated in the subaqueous environment?

2. How, where and when were the cavities infilled? Are they filled with marine carbonate cements and laminated sediments (e.g. Playford, 1984; Dörling et al., 1996)? Do they display terra rosa

features etc? Was hydrostatic pressure a factor in the infilling of cavities (Lehner, 1991)?

Once these questions have been answered, then questions about the larger palaeogeographical and tectonic environments can be resolved.

Regional geological setting

The McArthur Basin is an extensive Proterozoic sedimentary system located along the southern and western margins of the Gulf of Carpenteria in northern Australia (Fig. 1). McArthur Group carbonates are best exposed in the southern McArthur Basin as two N-S trending bands, separated by the N-S trending Tawallah Fault (Fig. 2).

The McArthur Group is sub-divided into the lower Umbolooga Sub-group and the upper Batten Sub-group (Jackson et al., 1987; Pietsch et al., 1991a,b; Fig. 3) with the contact between the two sub-groups defined on the basis of local unconformities adjacent to the major fault zones (Pietsch et al., 1991a) and the presence of local palaeo-karst and palaeo-regolith (Jackson et al., 1987). The Teena Dolomite directly underlies the Barney Creek Formation, host to the

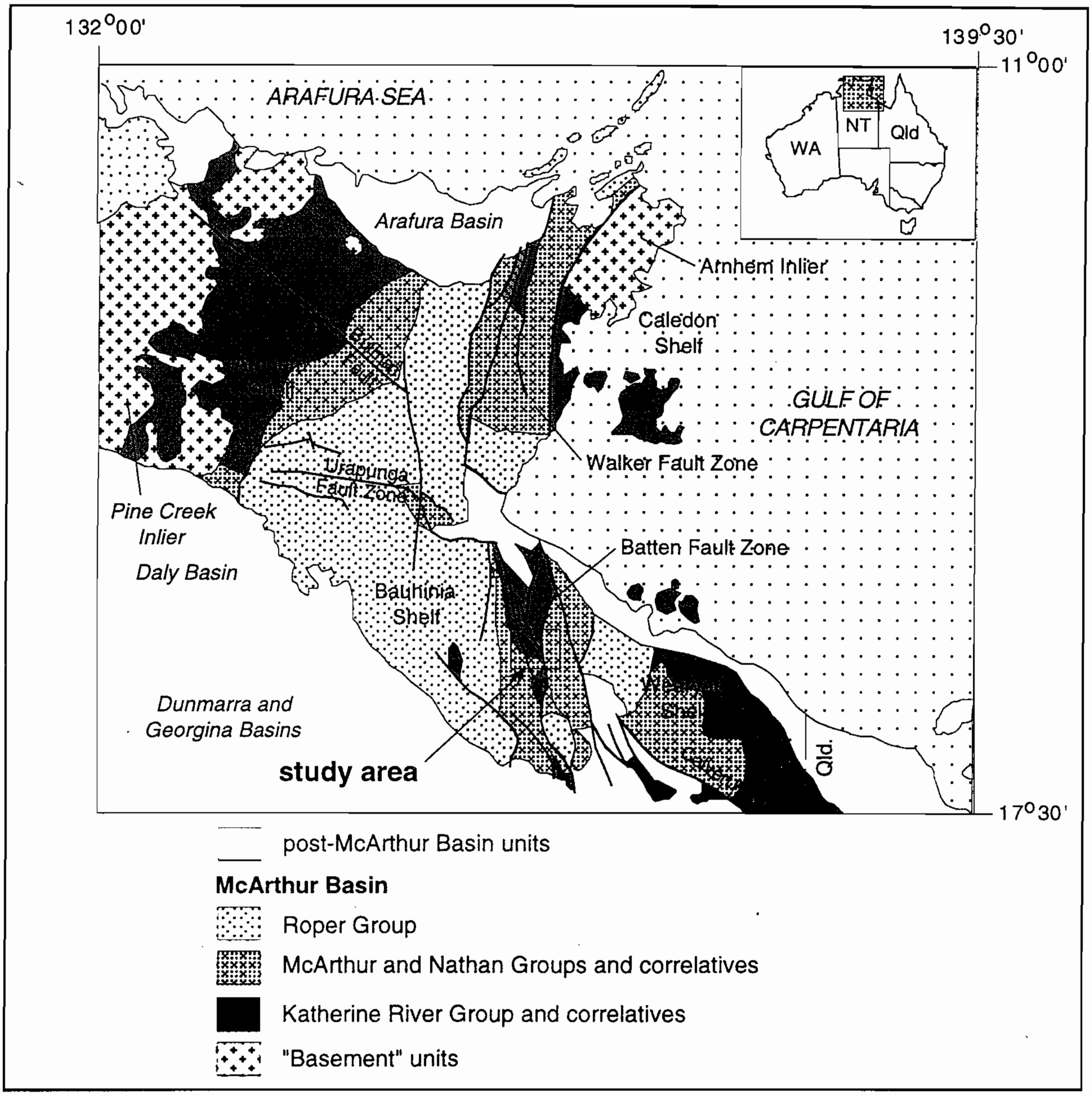

Figure 1. Major tectonic elements of the McArthur Basin (adapted after Pietsch et al., 1991a).

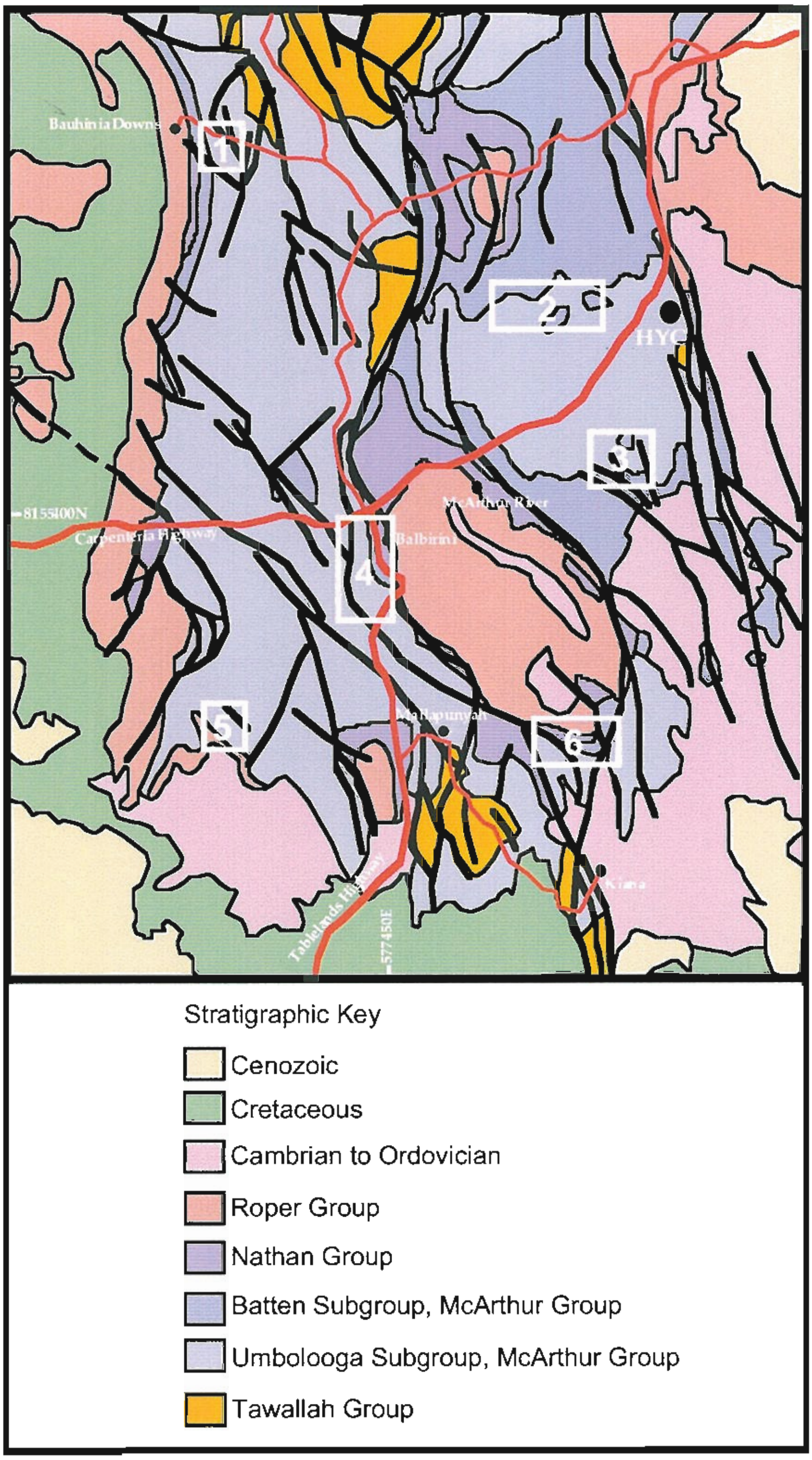

Figure 2. Geology of the central Batten Fault Zone with selected field localities marked. 1-Bauhinia Downs; 2-McArthur River area; 3-Lynott Fm. type section; 4-Top Crossing; 5-Weirk Waterhole; 6-Gorge Prospect.

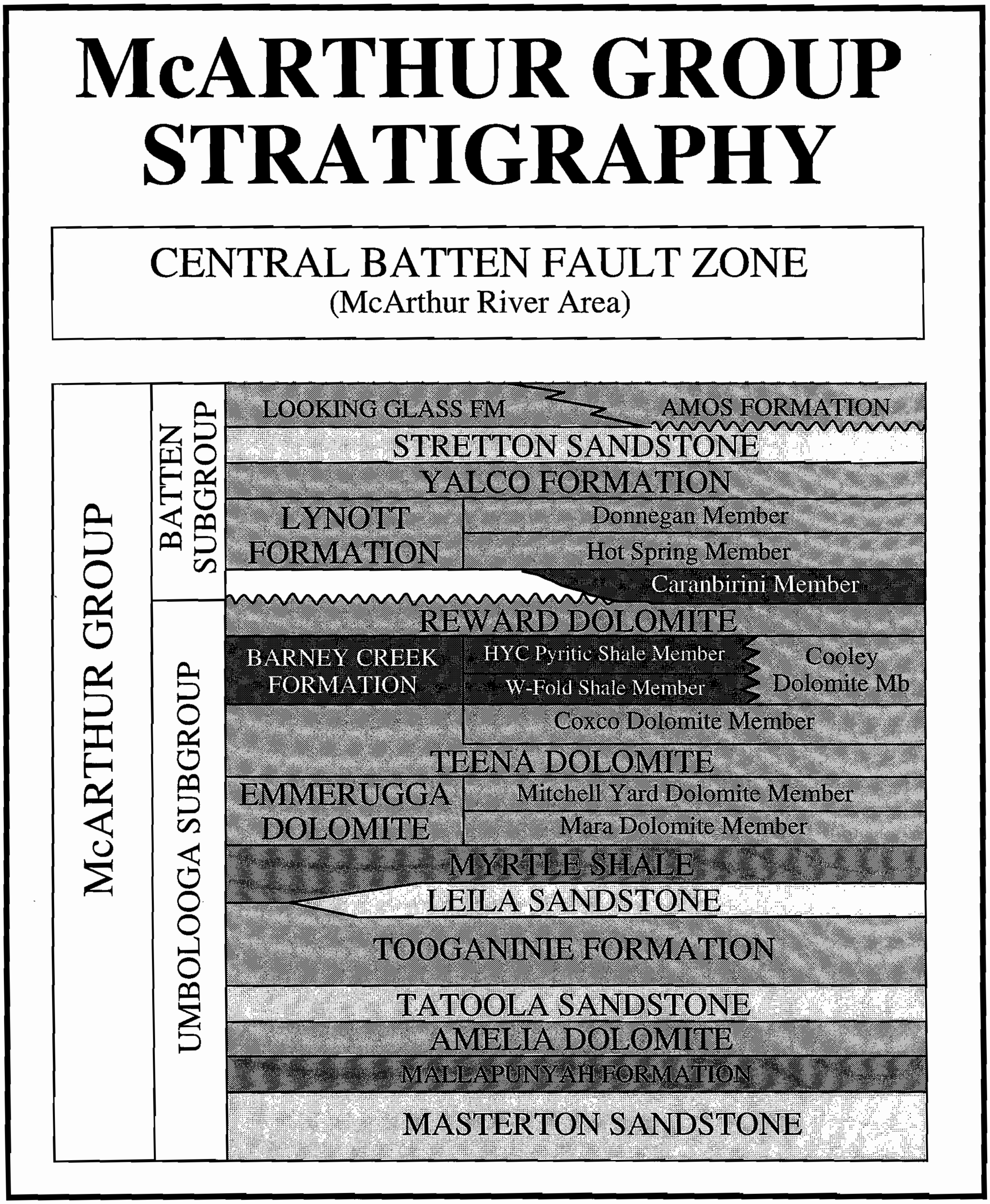

Figure 3. McArthur Group stratigraphy as defined by Jackson et al. (1987) and Pietsch et al. (1991a,b).

HYC Pb-Zn-Ag deposit at McArthur River, near the top of the Umbolooga Sub-group. The Teena Dolomite was incompletely defined by Plumb and Brown (1973) and is divided into the lower Teena Dolomite and the Coxco Dolomite Member. The lower Teena Dolomite is characterised by thin- to medium-bedded dololutite, medium grained dolarenite with occasional oolitic and peloidal grainstones (Plate 1c). 'Coxco needles', the definitive feature of the Coxco Dolomite Member, were originally interpreted as aragonite pseudomorphs by Brown et al. (1969). Later work by Walker et al. (1977) using interfacial and analogies with gypsum from the Trucial Coast inferred that gypsum forming in shallow brine pools was the precursor of 'Coxco needles' and on this basis the depositional setting were thought to be evaporative and emergent. New research has placed doubt on whether gypsum was the precursor for the 'Coxco needles' and aragonite is now preferred (see Winefield, this report). In addition, regional sedimentological sections through the Teena Dolomite are inconsistent with an evaporative, emergent setting for the Coxco Dolomite Member. The lack of supratidal features, desiccation features and other evaporative features would support an overall transgressive event from the lower Teena Dolomite into the upper Barney Creek Formation. This is supported by sequence stratigraphic interpretations of a major erosive event at the base of the Teena Dolomite followed by a transgression toward a major flooding event in the Barney Creek Formation (Southgate et al., 1997).

Localities

In this report, we describe four key localities in the southern McArthur Basin where neptunian dykes and associated features are evident (Fig. 3).

Gorge Prospect, Kilgour River

The Gorge Prospect is located along the Kilgour River approximately 60km southwest of HYC immediately south of the Abner Range. Mapping of the area indicates that Emmerugga Dolomite to upper Batten Sub-group sediments outcrop in the area striking NW-SE with a distinctive swing in strike to N-S towards the southeast (see Appendix 1). The Gorge Prospect lies adjacent to the southern extension of the Tawallah Fault, where is swings approximately NW/SE south of the Abner Range. AGSO mapping (Abner Range 1:100 000 Geological Mapsheet) implies that there is a significant thickness of Barney Creek Formation (up to 650m) in this area, and work done in the 1996 field season confirms this. MIMEX and Perilya drilled one diamond and three percussion drill-holes in the Gorge Prospect area in 1994 to test stream sediment Pb-Zn geochemical anomalies.

Neptunian dykes are recognised in the Emmerugga Dolomite, lower Teena Dolomite and Coxco Dolomite Member in the Gorge Prospect area. They are generally up to 8 cm in width and cross-cut bedding. The margins of each dyke or fracture appear to be fitted, with no evidence for dissolution (e.g. rounded fluted cavity walls rather that sharply angular wall forms), and are lined with distinctive fibrous dolomite cement. Internal sediment is commonly observed intimately associated with several generations of fibrous cement (Plate 1a). Porosity is generally occluded by a subsequent coarsely crystalline cement which is preferentially silicified in outcrop. In larger cavities are laminae in internal sediment are at an angle to the original lamination. At the top of one particular cavity, bacterial growths are observed in growing downward (Fig. 4). Figure 5 illustrates a typical infill sequence for neptunian dykes and sills in the Gorge Prospect area.

In addition to neptunian dykes, there are a number of neptunian sills or fractures orientated sub-parallel to bedding in the lower Teena and Emmerugga Dolomites. Interestingly, they are not as common in the Coxco Dolomite Member. They do display very similar infill to neptunian dykes (Plate 1d).

Both neptunian dykes and sills are associated with intraclasts that have been isopachously rimmed by fibrous cement (Plate 1b). These display very similar characteristics to the 'spar balls' described by Playford (1984).

The structural orientation of the neptunian dykes is remarkably consistent in that they strike approximately N-S (Fig. 6). There are obvious complications in the Gorge Prospect area, most notably the 'fold' structure that defines the change in strike from NW-SE to N-S. Neptunian dyke orientation changes slightly around the fold, although the dominant N-S orientation is preserved. Future structural work in the Gorge Prospect will attempt to constrain the age

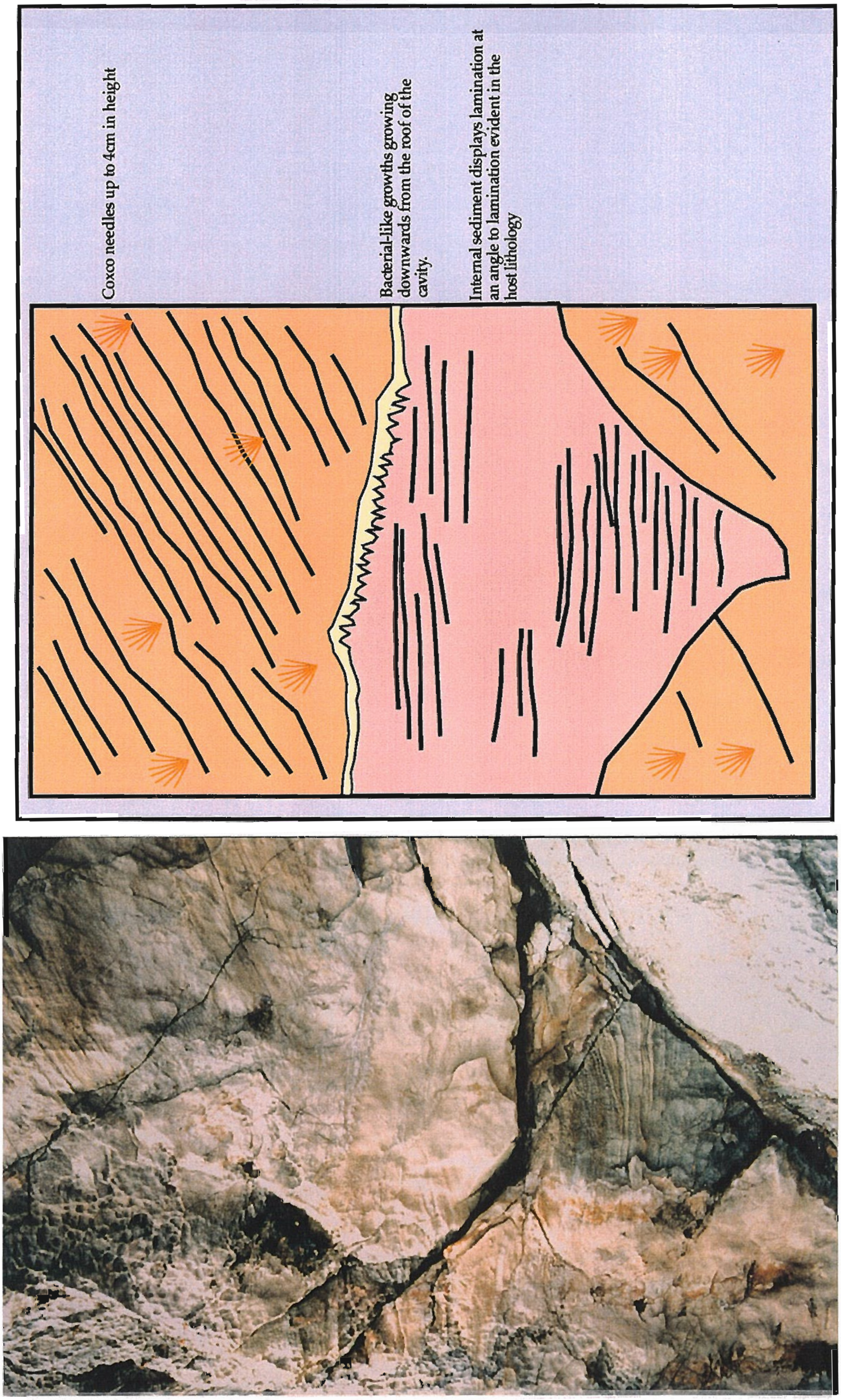

Figure 4. Cavity infilled with internal sediment displaying lamination at angles to bedding in the host sequence. Note the bacterial-like growths growing downwards from the cavity roof. Cavity is approximately 1.5m wide. Coxco Dolomite Member, Gorge Propect, Kilgour River.

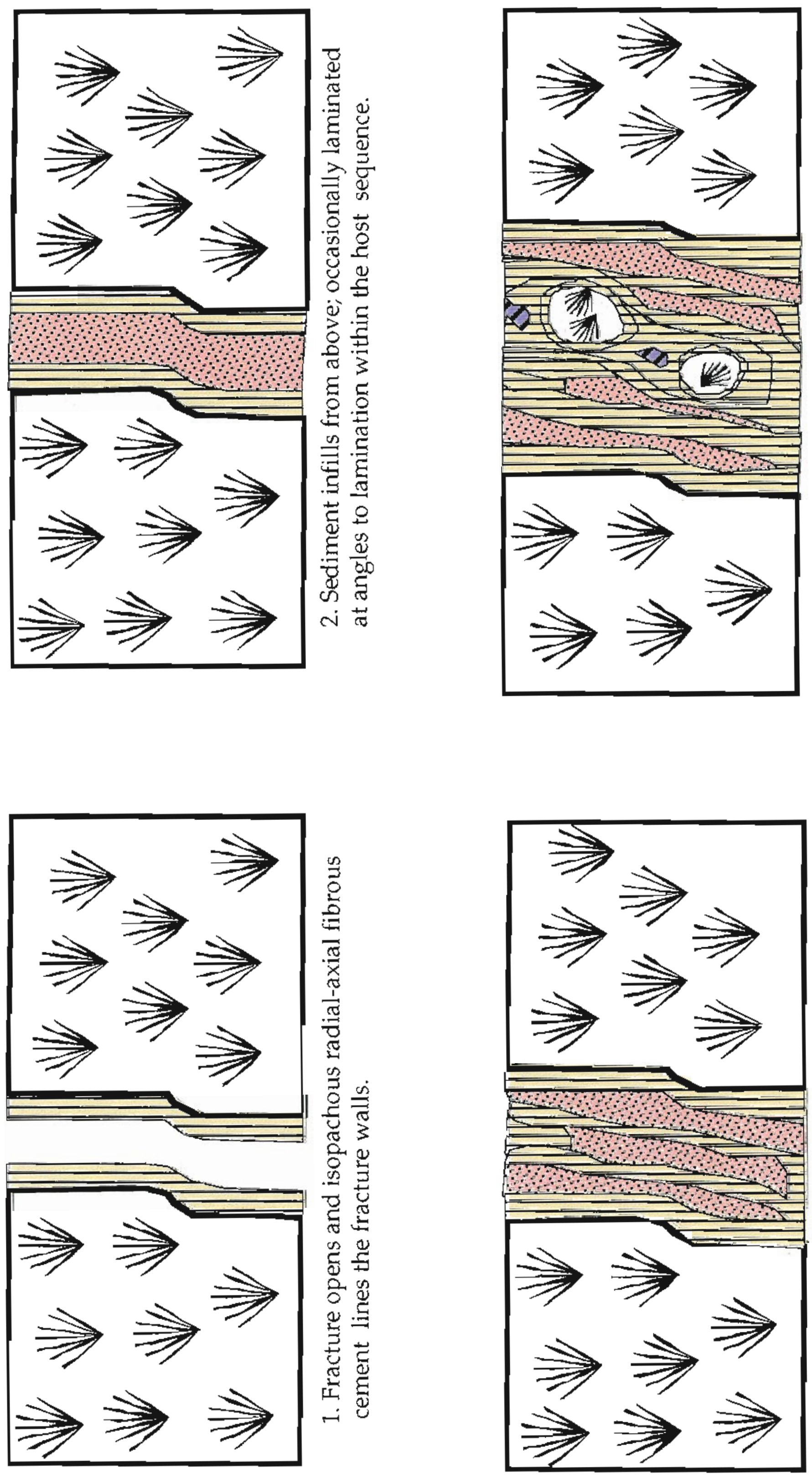

1. Fracture opens and isopachous radial-axial fibrous cement lines the fracture walls.

2. Sediment infills from above; occasionally laminated at angles to lamination within the host sequence.

3. Refracturing and infilling by sucessive generations of radial-axial fibrous cement and sediment.

4. Refracturing and infilling of sucessive generations of radial-axial fibrous cement and sediment. Brecciated clasts of host-rock lined with isopachous fibrous cement are sometimes included in the infill. Remaining porosity is occluded by a coarse crystalline sparry dolomite cement.

Figure 5. Typical infill sequence for neptunian dykes and sills observed in the Gorge Prospect, Kilgour River.

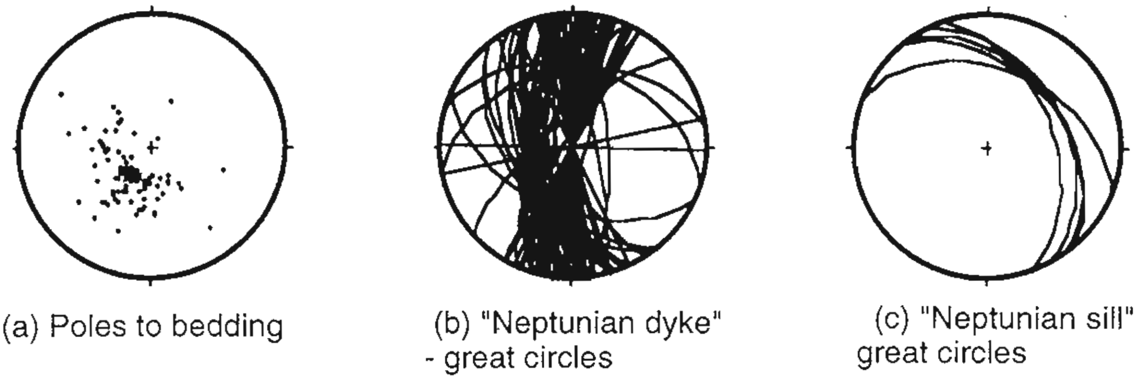

Figure 6. Structural data from the Gorge Prospect, Kilgour River.

Plate 1

1a Fibrous dolomite cement and internal sediment infilling a cavity in brecciated pelloidal grainstone from the lower Teena Dolomite, Gorge Prospect, Kilgour River.

1b Rounded intraclasts rimmed by isopachous, fibrous dolomite cement. Gorge Prospect, Kilgour River.

1c Photomicrograph of isopachous fibrous cement lining peloids in a peloid grainstone. Note the coarse dolomite cement occluding porosity. Scale bar = 1mm. Sample S96/80a, lower Teena Dolomite, Gorge Prospect, Kilgour River.

1d Complicated infill of a neptunian sill in a medium- to coarse-grained dolarenite from the lower Teena Dolomite. Note that there are several generations of infilling dolomite cement with a coarse dolomite cement particularly evident. Sample S96/107, Gorge Prospect, Kilgour River.

1e Photomicrograph of successive generations of fibrous dolomite cement infilling a cavity in the Teena Dolomite intersected in DDH Boko 4. Note the coarse sparry dolomite cement (top right) which is later than the fibrous cement and occludes porosity. Scale bar = 1 mm. Sample Bok4/1, DDH Boko 4 (243.70m).

1f 'Fibrous dolomite veins' from the Cooley I Pb-Zn deposit.

1g Polished slab of a 'fibrous dolomite vein' from the Cooley I Pb-Zn deposit. The 'zebra-stripped' herringbone calcite can just be made out lining the cavity. Sparry dolomite cements with coarse galena infill cross-cutting fractures throughout the cavity.

1h Fibrous dolomite cement isopachously rimming intraclasts. Internal sediment is also observed infilling cavities. Sample S96/137, Coxco Dolomite Member, base of the Lynott Formation type section.

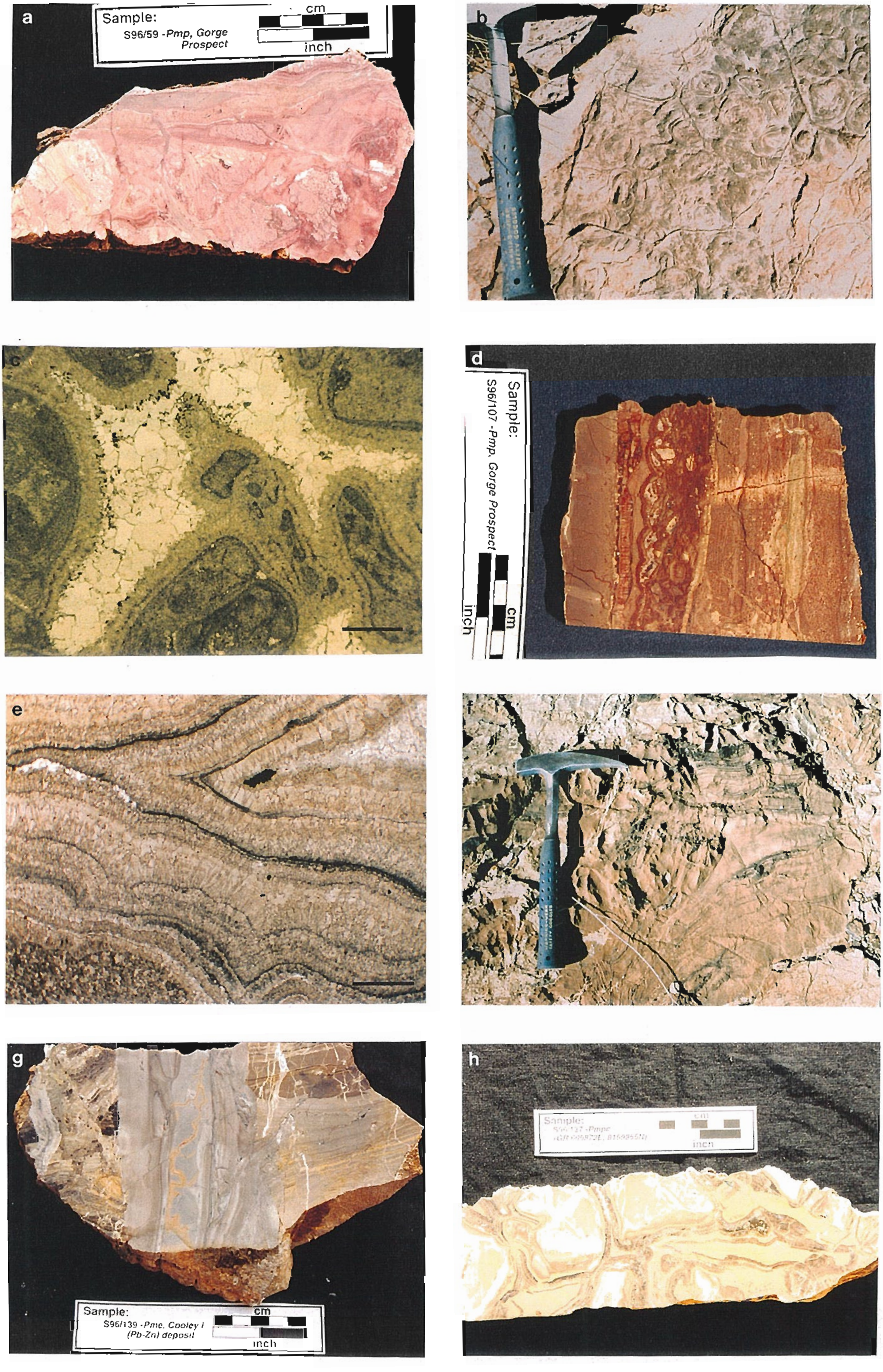
a
Sample:
S96/59 -Pmp, Gorge Prospect
cm
inch
b
c
d
Sample:
S96/107 -Pmp, Gorge Prospect
cm
inch
e
f
g
Sample:
S96/139 -Pmc, Cooley I (Pb-Zn) deposit
cm
inch
h
Sample:
cm
inch

of this 'fold' with respect to the formation of neptunian dykes and the deposition of the overlying Barney Creek Formation.

Mass-flow and turbiditic sediments of the Barney Creek Formation overlie the Coxco Dolomite Member in the Gorge Area. The mass flows are poorly sorted clasts, and contain clasts up to boulder size of planar laminated dololutite, some of which are suspected to contain 'Coxco needles'. The matrix is generally fine- to medium-grained dololutite, dolomitic siltstone and dolomitic sandstone. Up-section, a thick sequence of dolomitic turbidites display abundant slump structures and convolute bedding. The mass-flow lithofacies are interpreted to represent the basal part of the Barney Creek Formation, with the upper part defined by the dolomitic siltstones which grade into dolomitic sandstones and cuspate microbialites of the Reward Dolomite. Mapping done in the area would indicate that there is a pronounced change in the thickness of the Barney Creek Formation from approx. 100 m in the west of the Gorge Prospect area to approx. 650 m in the southeast (Appendix 1). The contact between the Coxco Dolomite Member and the basal Barney Creek Formation is illustrated in measured section KP96/1 (included as Appendix 2.1). Note the sharp change in the gamma curve at the lithostratigraphic contact of the Coxco Dolomite Member and the basal Barney Creek Formation. The upper part of the Barney Creek Formation and Reward Dolomite is shown in measured section KP96/2 (Appendix 2.2).

McArthur River area

Neptunian dyke features are evident in the Teena Dolomite intersected in several drill-cores along the east-west trend away from HYC. Neudert and McGeough (1996) proposed the formation of tilt blocks to explain the localised distribution of Barney Creek Formation and the extreme facies variations in the Reward Dolomite in this area. In this model the most elevated structural position, above the uplifted footwall block, was interpreted to be emergent as evidenced by localised karstic weathering. A number of drill-holes were logged in detail to document the sedimentary lithofacies and obtain unweathered samples of neptunian dyke infill (e.g. DDH's Lynott West 3,4 and 5; Boko 4 & 5; Beryaya 1). These drill holes were also selected because they were interpreted to intersect karstic textures (Neudert and McGeough, 1996; Fig. 7).

The detailed study of samples collected from the aforementioned drill-holes is presently incomplete, however, there are several features worth noting here. Fibrous, radial-axial dolomite cements are noted

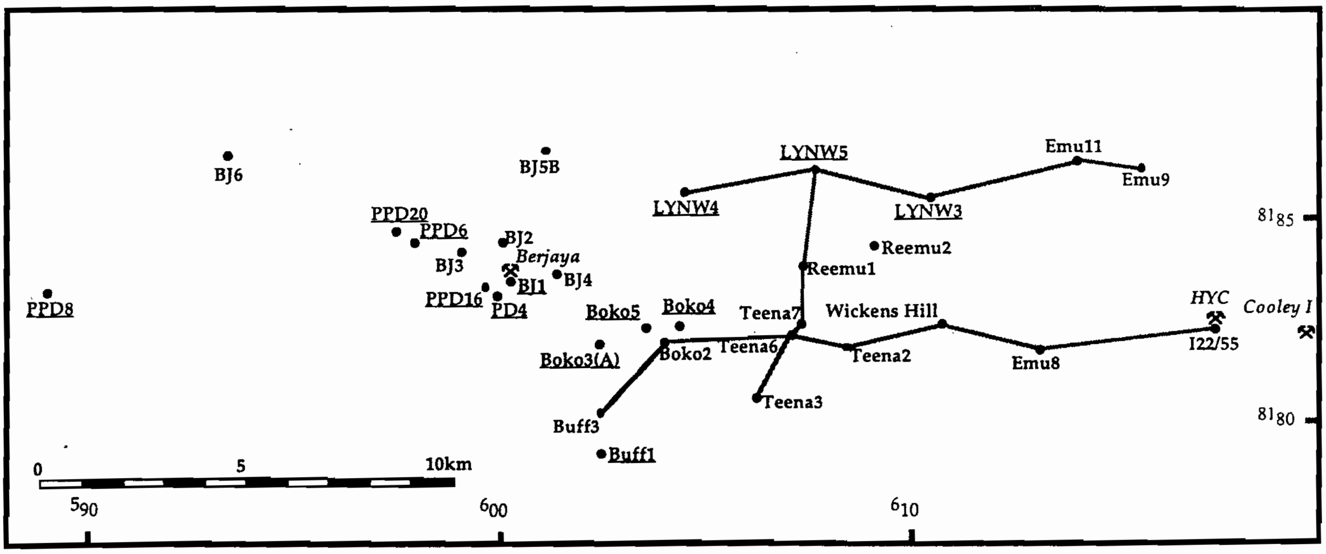

Figure 7(a). Location of selected McArthur River DDHs (adapted from Neudert and McGeough, 1996).

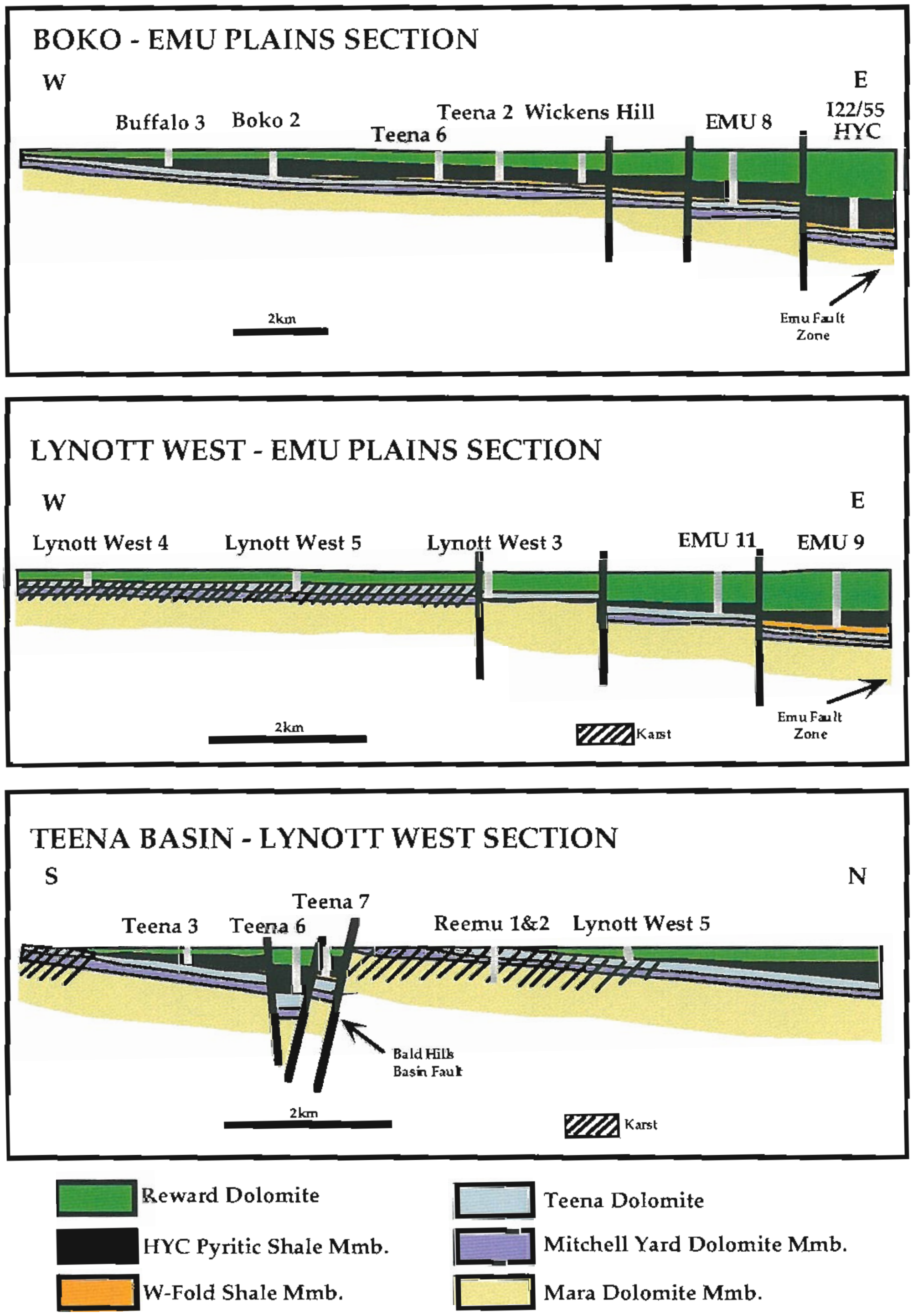

Figure 7(b). Selected McArthur River stratigraphic sections (adapted from Neudert and McGeough, 1996).

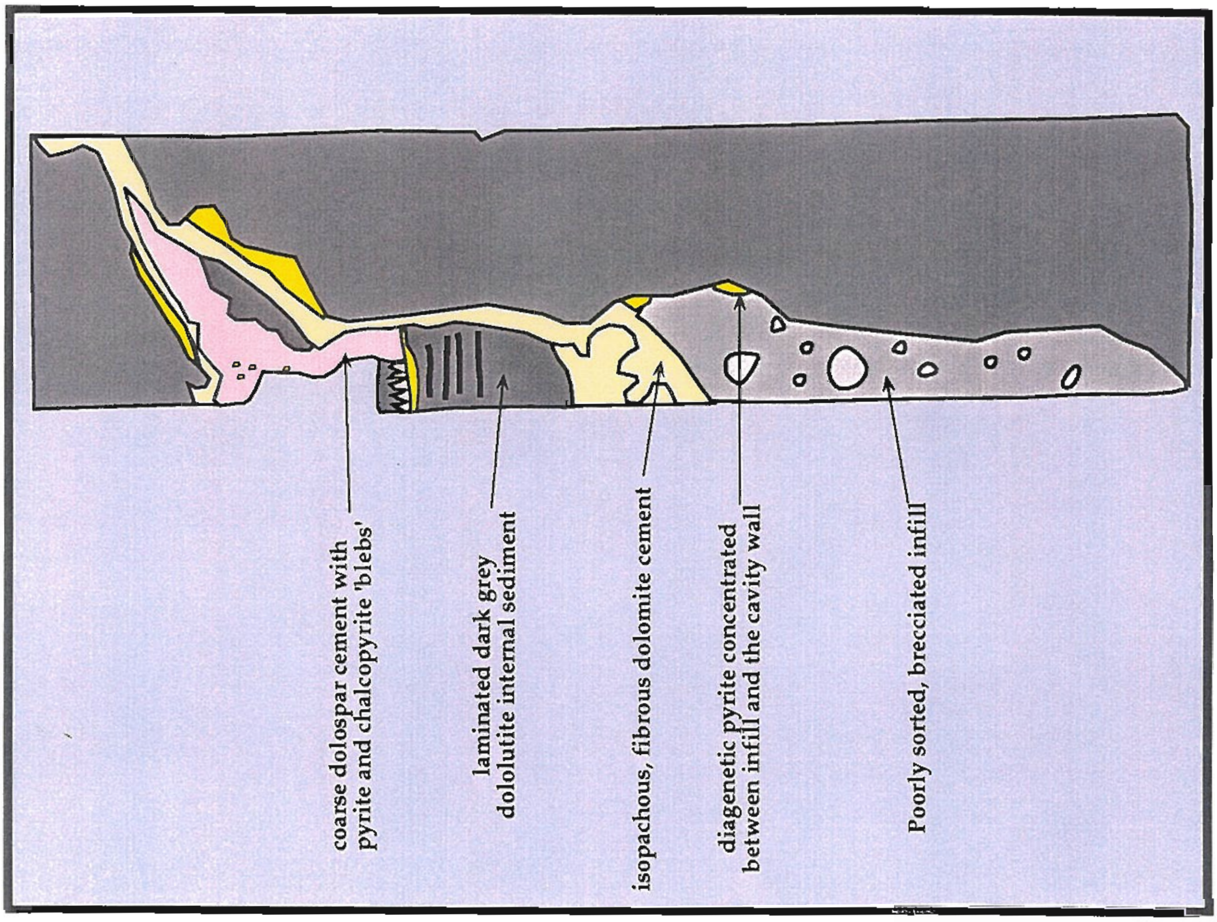

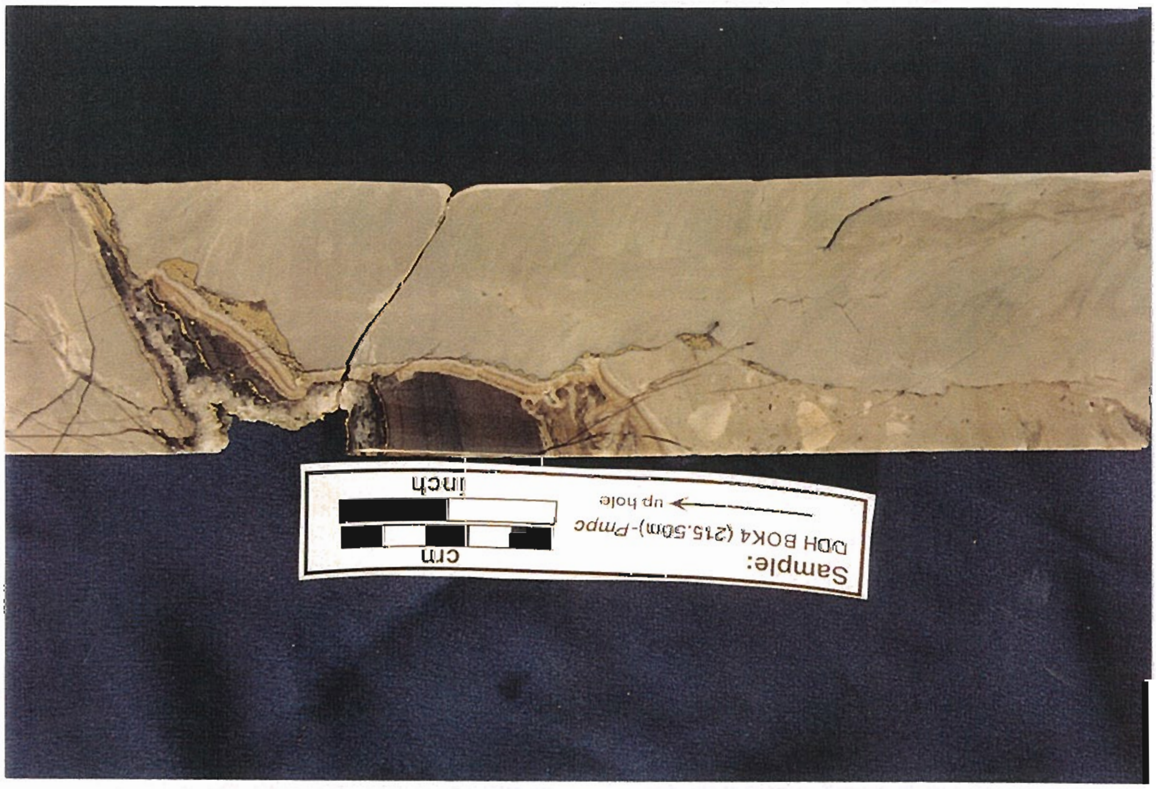

Figure 8. Cement- and sediment-infilled cavity, DDH Boko 4 (215.50m)

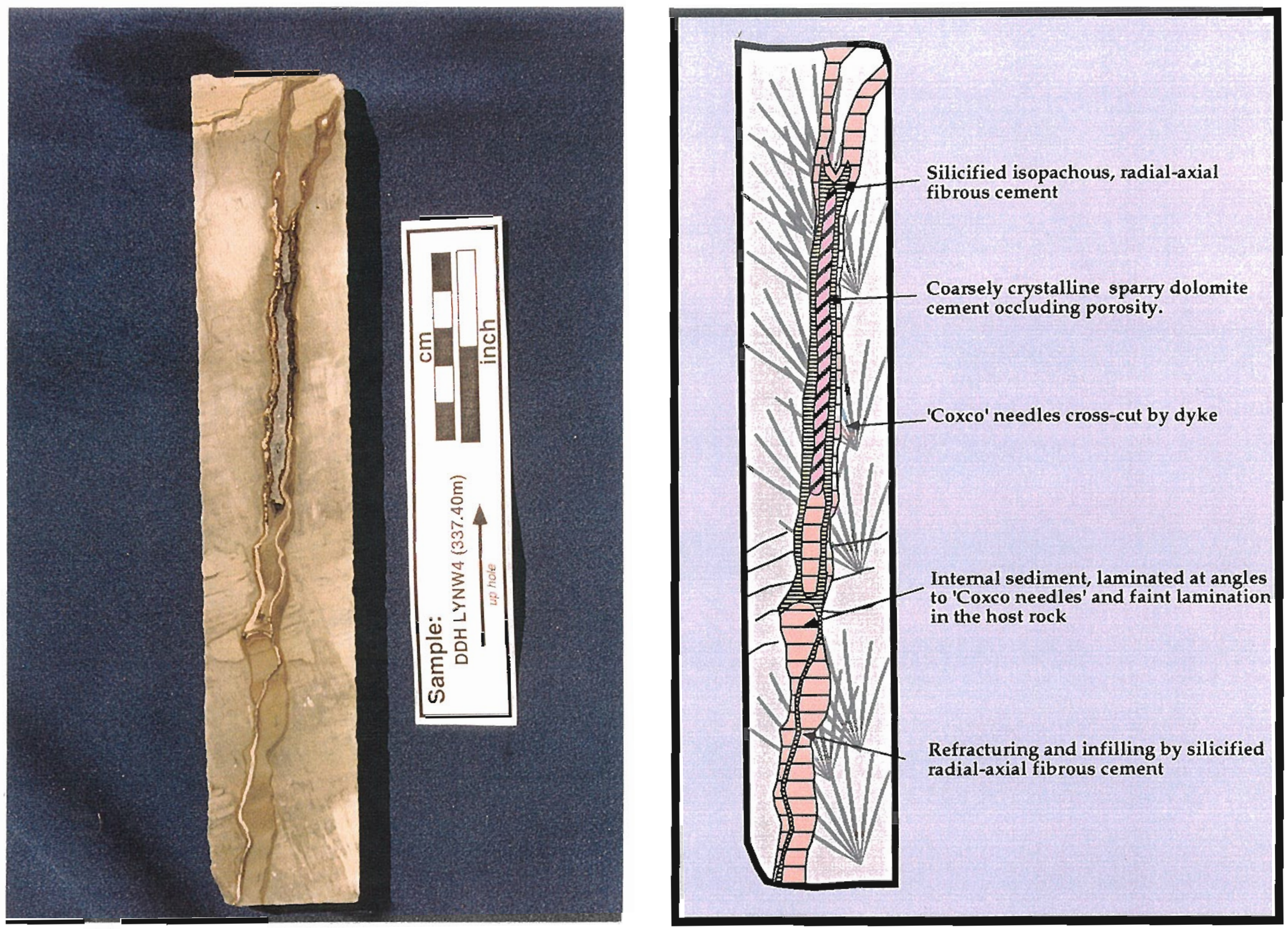

Figure 9. Various stages of neptunian dyke infill observed in DDH Lynott West 4 (337.40m). Note the regular, fitted nature of the fracture and the cross-cutting relationship with Coxco needles. Coarse crystalline sparry dolomite cement occludes porosity.

infilling neptunian dykes and cavities in most of the drill-holes logged. Interestingly, no neptunian dyke material was evident in DDH Boko 5 where a thick section of Barney Creek Formation (approx. 500m) was intersected overlying Teena Dolomite. DDH Boko 4, which was drilled approximately only 1 km to the east of DDH Boko 5, intersected significantly less Barney Creek Formation (approx. 100m) and contained a number of fibrous cement- and internal sediment-infilled fractures in the Coxco Dolomite Member.

Petrographic work on the material from DDH Boko 4 has confirmed the radial-axial nature of the fibrous cement (Plates 1e; 2), implying that it represents dolomitised equivalents of the marine radial-axial fibrous calcite cements documented by Playford (1984) and Kendall (1985). Similar dolomitised, radial-axial fibrous marine cements have also been identified in Neoproterozoic Cap Dolomites of the Adelaide Geosyncline (Kennedy, 1996). Poorly sorted, brecciated material is observed infilling a large cavity in DDH Boko 4, with successive generations of fibrous radial-axial cement and laminated internal sediment (Fig. 8). Later coarse crystalline dolomite cement partly occludes porosity in the cavity and contains chalcopyrite and pyrite. The association between coarse dolomite cement and chalcopyrite is repeated in late-stage vughs in DDH Beryaya 1 (Bull et al., this report).

Figure 9 illustrates the cross-cutting relationship between neptunian dykes and 'Coxco needles'. The neptunian dyke shown contains a number of generations of infill including laminated internal sediment, silicified fibrous radial-axial cement and a later coarsely crystalline sparry dolomite cement occluding porosity. Also evident is the fitted, regular nature of the cavity.

The Cooley I Pb-Zn deposit is hosted in Emmerugga Dolomite. The presence of 'veins' infilled with fibrous dolomite was recognised by Pietsch et al. (1991a). Outcropping Emmerugga Dolomite in the area of the deposit strikes N-S, dips moderately to the west and consists of well-bedded microbial dolostone. The 'veins' are NW striking, steeply NE dipping (Fig. 10) and up to 1m wide (Plate 1f). These have been described as 'dykes' by Pietsch et al. (1991a). These 'dykes' carry galena-bearing sparry dolomite in layers running parallel to their walls. In places, the Emmerugga Dolomite is brecciated and carries galena-sphalerite pods as breccia infill (Plate 1g). Williams (1978) studied the mineralisation and brecciation in the Cooley I deposit, although the origin of the dolomite 'dykes' was not discussed. Pietsch et al. (1991a) postulated that they may represent channelways for the mineralising fluids. Initial petrographic samples of dyke material from the Cooley I deposit has tentatively identified the fibrous dolomite cement as displaying very similar characteristics to the herringbone calcite of Sumner and Grotzinger (1996). Herringbone calcite is interpreted to be a sea-floor precipitate and carbonate cement that is common in Archaean carbonates but less evident in Proterozoic and Phanerozoic rocks. It generally occurs in carbonate sediments associated with anaerobic depositional environments or organic-rich sediments.

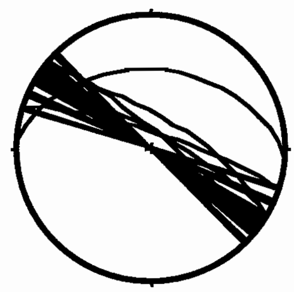

Figure 10. Structural orientations of 'fibrous veins' from the Cooley I Pb-Zn deposit.

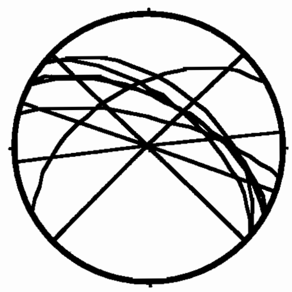

Figure 11. Structural orientations of neptunian dykes observed in the Coxco Dolomite Member at the base of the Lynott Formation type-section.

Plate 2 (opposite)

Two photomicrographs of fibrous dolomite cement showing sweeping extinction under cross-polarised light. The sweeping extinction which moves in the same direction as the microscope stage is the diagnostic feature of radial-axial carbonate cements. Scale bar = 0.15 mm. DDH Boko 4 (241m).

Lynott Fm. Type-section

The Barney Creek Formation and Coxco Dolomite Member outcrop poorly at the base of the type-section of the Lynott Formation, which is approximately 7 km southeast of the confluence of the Kilgour and McArthur Rivers. The outcrop of Coxco Dolomite Member in this area is interesting due to the presence of neptunian dykes described in the 1993 Carpenteria Zinc Belt Geological Excursion Guide as '... numerous veins both bedding parallel and cross-cutting filled with fibrous dolomite and laminar chert similar to the mineralised veins in the Emmerugga Dolomite at the Cooley I deposit. This outcrop is fairly typical of the Coxco Member ...'. Measurement of the structural orientation of neptunian dykes confirms an approximate NW-SE orientation (Fig. 11). Plate 1h illustrates fibrous dolomite lining cavities in brecciated dololutite.

Top Crossing

Features described in this report are contained in Emmerugga and Teena Dolomite correlates located adjacent to the segment of the Tawallah Fault which extends northward from Gum Flat to the McArthur River. The stratigraphy in this region is of particular interest due to its anomalously high volume of brecciated material. Breccias are dominantly intraformational, but possess a range of dimensions, morphologies, relationships to enclosing coherent strata and potential origins. Various lines of evidence involving clast morphology as well as textural and compositional features of matrix and/or cement, indicate a potential early diagenetic origin for many of these breccia units.

The most volumetrically significant breccia units occur towards the base of the Emmerugga Dolomite and potentially extend downward into underlying evaporitic Myrtle Shale correlates. Chaotic deposits are widespread throughout the McArthur Basin at this level of the stratigraphy and have been attributed to solution collapse mechanisms triggered by removal of halite within the Myrtle Shale (Jackson et al., 1987). Along the E-W section between the Tablelands Highway and the Tawallah Fault, south of the McArthur River (a distance of approximately 7km), there is a dramatic increase in the thickness of breccia units positioned at the Myrtle Shale-Emmerugga Dolomite boundary range from roughly 2-5m to at least 30m as the Tawallah Fault is approached from the east. Breccia units within the lower Emmerugga Dolomite are generally stratabound, but laterally discontinuous, with crude convex-downward bases. The nature of their lateral margins is varied and includes sharp, fault-defined contacts with coherent dolostone, or transition boundaries marked by a progressive reduction in the degree of brecciation. The attitude of small-scale faults associated with breccia units range from steeply- to shallowly-dipping, the latter showing listric morphologies which rapidly sole out into bedding surfaces. These faults exhibit consistent normal displacements, with breccia units having accumulated in (or on) downthrown hangingwall blocks. The strike of fault surfaces is roughly NNW and parallels the main Tawallah Fault trace.

Clast-types in stratabound breccia units are limited and include dolomitic mudstone and graded silty mudstone. The internal structure of breccia units is disorganised and lacking in stratification or grading. Clasts are poorly sorted, non-imbricated, angular and enclosed by a volumetrically sub-ordinate matrix of finer-grained sedimentary fragments and chalcedonic quartz. Internally, clasts show ductile folding and/or disaggregation of silty layers without an associated tectonic fabric (eg. cleavage development). Similarly, the external form of clasts is highly irregular, with ragged clast shapes and common impingement of neighbouring clasts. These features of the clast morphology tend to suggest that the sedimentary precursor was incompletely lithified at the time of brecciation.

Monomict breccia zones, ranging 20-100cm in width, were also observed locally along the surfaces of steeply-dipping brittle faults. These breccia zones clearly cross-cut stratigraphy, but are texturally similar to stratabound examples. The internal texture involves angular silty dolostone fragments contained within a matrix of fine-grained sediment, with local coarse-grained carbonate cement filling open pore space. Neither pervasive cleavage development, nor granulation of fine quartz grains were observed. A later phase of deformation has resulted in thin, regularly oriented quartz veins, which overprints the pre-existing breccia fabric. Although no unequivocal evidence has been found to prove an early diagenetic origin for these fault-related breccias, the lack of a pervasive tectonic fabric or an association of high-T hydrothermal mineral phases with the initial phase of brecciation indicates that such an origin cannot be discounted.

The upper portion of the Emmerugga Dolomite and the overlying Teena Dolomite involves a complex association of brittle deformation features including dilational fracturing, block faulting and brecciation. Dilation fractures are oriented sub-perpendicularly to bedding and are best developed in sub-horizontally oriented strata. They possess a consistent NNW strike, but range in width from a few millimetres to at least 4m. Narrow dilational fractures are rarely infilled by fine-grained sediment, but more commonly by a distinctive, fibrous cement, similar to that associated with neptunian dykes from the Kilgour Gorge. Broader fractures contain brecciated dolostone fragments which are both texturally and compositionally identical to strata contained in the immediately adjacent wall-rock.

As the Tawallah Fault is approached, the dip of strata rotates abruptly about a NNW-trending, shallowly plunging axis, from sub-horizontal to approximately 60° to the west. The fold geometry produced is a monoclinal closure, with domains of irregular, small-scale extensional block-faulting and brecciation localised along the hinge line. Fault surfaces are steeply-dipping, sub-planar and sharp, but appear to die out vertically over distances of less than 5m. There is little evidence for brecciation or veining along fault surfaces.

Summary of main features

The main features of neptunian dykes and sills observed in each of the localities are:

1. neptunian dykes are most common in the Coxco Dolomite although they are also developed in the underlying lower Teena and Emmerugga Dolomites;
2. the overlying Barney Creek Formation sediments generally show at least some evidence of slumping or mass-movement;
3. the fracture/cavity walls are generally fitted and regular with limited evidence for dissolution;
4. the first generation of cavity infill is isopachous, fibrous radial-axial dolomitic cement;
5. the fibrous cement is often intimately associated with internal sediment. Lamination in the internal sediment is commonly at an angle to bedding in the host-rock;
6. occasionally brecciated intraclasts isopachously rimmed by fibrous dolomite cement (i.e. spar balls) are included in neptunian dykes;
7. the structural orientation of neptunian dykes is consistent within a particular locality.

Discussion

Creation of space

Style of deformation leading to dilation

In the Gorge Prospect area, there is strong evidence for surficial extension, sliding and slumping of indurated, lithified carbonate sediments, thereby creating open spaces within the displaced mass. The coherent structural orientation of neptunian dykes within each locality studied is consistent with systematic, but localised extension under a stable stress field. In both Top Crossing and the Gorge Prospect, domains of syn-sedimentary/early diagenetic dilational structures are closely positioned with the Tawallah Fault. Furthermore, dilational structures are intimately associated with monoclinal folds adjacent to the trace of the Tawallah Fault. The geometry of folds in these regions and their spatial association with a major fault zone are consistent with roll-over geometries related to normal fault movement. In the Gorge Prospect, folding can be demonstrated to have been restricted to syn/pre-Barney Creek Formation sediments. These features are supportive of localised block rotation associated with major extensional faults. In addition, evidence for early diagenetic extension and brecciation has also been documented at the Emmerugga Dolomite/Myrtle Shale contact, adjacent to the Tawallah Fault in the Top Crossing area.

Karstic dissolution vs. mechanical dilation

Neudert and McGeough (1996) documented karstic features in drillcore interpreted to intersect the uplifted edges of 'tilt blocks' in the McArthur River area (Fig. 7). Work done in the 1996 field season on some of the drilling referred to by Neudert and McGeough (1997) has identified several features that are strongly indicative of neptunian dyke formation. These include: fitted, regular fissures; fibrous radial-axial marine cement; and internal sediment intimately associated with fibrous cements.

While there are numerous examples of dissolution related to subaerial exposure of carbonate sequences in the literature, there is also a similar number on submarine carbonate dissolution by undersaturated bottom-waters. Therefore, dissolution of carbonates is not in itself unequivocal evidence of subaerial karst formation, and additional sedimentological (e.g. shallowing upward sequences, tepee structures, birdseyes, desiccation cracks etc) and geochemical (e.g. carbon and oxygen stable isotopes) evidence of emergence is required.

Regional sedimentological sections through the Teena Dolomite are inconsistent with a period of emergence. Instead, the inclusion of the Coxco Dolomite Member into an overall trangressional sequence from the lower Teena Dolomite to the upper Barney Creek Formation is favoured. The lack of sedimentary features indicative of emergence is major problem in interpreting a karstic origin for the fissures and cavities forming neptunian dykes. In addition, the generally regular and fitted nature of neptunian dykes, and their consistent structural orientation at each locality is better explained by extension related to the tilting of strata, or slumping associated with platform margin failure.

Episodic dilation and timing

Playford (1984) described very large (up to 1 m) neptunian dykes that appear to have been repeatedly infilled and refractured. Generally, the neptunian dykes observed as part of this study are much thinner, and although there is some evidence for refracturing, it would appear that they have not had such a long and protracted infill history as those described in the Canning Basin. Therefore, they are unlikely to be related to a well-defined platform margin but to topographically minor, short lived fault scarps as predicted under a tilt-block model.

Infilling of spaces

Submarine vs. meteoric-water cements

Meteoric-water carbonate cements have distinctive characteristics and chemistries. They grow as meniscus or gravity cements which are generally observed growing downwards. The fibrous radial-axial dolomite cement observed isopachously (or rimming) infilling fractures and cavities in the McArthur River region is almost identical to RFC cement from neptunian dykes in the Canning Basin interpreted as being precipitated in the marine phreatic environment by Kendall (1985). The early dolomitisation that has affected much of the McArthur Basin carbonate sequences has also dolomitised these infilling cements. In addition to its occurrence as neptunian dyke and cavity infill, fibrous dolomite cement is also observed isopachously rimming brecciated fragments of neptunian dykes (spar balls) and in oncoid grainstones of the lower Teena Dolomite. The intimate association with internal sediments is very indicative of marine cements (Tucker and Wright, 1990) and the fact that it is commonly overlain by later sparry dolomite cements is also supportive of a marine origin. Under CL, the fibrous cements appear non- to dull-luminescent, while the sparry cements commonly exhibit bright and dull intricate zoning. Microprobe analysis of each type of cement confirms that there is a difference in the Fe and Mn contents of each, which would explain the differing CL responses.

Possible implications for Barney Creek Formation deposition

The formation of neptunian dykes has important implications for the deposition of the Barney Creek Formation. Syn-sedimentary faulting and the development of tilt blocks is likely to be a major control of the development of neptunian dykes either directly, or indirectly via platform edge collapse related to tilting. It appears that cavities created in the Coxco Dolomite Member in the Gorge Prospect, where infilled after tilting as evidenced by the angular relationship between lamination in internal sediments and that inherent in the host sequence (Fig. 4). Therefore, the 'tilting' of pre-Barney Creek Formation sediments is recorded by neptunian dyke formation in the Teena and Emmerugga Dolomites. Development of tilt blocks created accommodation space for the deposition of the Barney Creek Formation into the resulting 'sub-basin' initially as mass-flows and carbonate turbidites that record slope-related slumping in proximal areas. Both the relationship between neptunian dyke formation and tilting of sediments, and the subsequent deposition of Barney Creek Formation can be observed in the Gorge Prospect area. Further work will attempt to better understand the possible relationship between neptunian dykes and syn-sedimentary fault movement.

Conclusions

Neptunian dykes and their associated features have been recognised at the Gorge Prospect and several other localities. They are evident in the Coxco Dolomite Member and Teena Dolomite intersected in drillcore in the immediate McArthur River area, in the Coxco Dolomite Member at the base of the Lynott Fm. type section and in the Emmerugga and Teena Dolomites at Top Crossing.

Consistent structural orientations, the absence of sedimentological evidence for subaerial exposure, and the regular, fitted nature of fissures and cavities suggests mechanical dilation as the major control of dyke formation. The infill of neptunian dykes consists of successive generations of radial-axial fibrous dolomite cement and internal sediments. Fibrous, radial-axial dolomite cements are interpreted to be dolomitised equivalents of marine radial-axial calcite cements. Their isopachous nature and association with internal sediments further supports a marine origin. Later sparry dolomite cements are also recognised occluding porosity.

Two possibilities are suggested for neptunian dyke formation: slumping of lithified sediment related to block rotation, or surfical deformation developed above a major syn-sedimentary fault zone. Both possibilities support the tilt-block model of Neudert and McGeough (1996), except that no evidence of karstification has been found and therefore we would propose an alternative origin for breccias associated with the Teena Dolomite. Further structural work in needed to better understand neptunian dyke formation and its relationship to Barney Creek Formation deposition.

Further work

Additional structural data will be gathered during the 1997 field season. The Gorge Prospect and Top Crossing are key areas in attempting to gain a better understanding of syn-sedimentary deformation of pre-Barney Creek Formation sediments and its relationship with neptunian dyke formation and Barney Creek Formation deposition. Work done in these areas will hopefully allow us to better constrain the tectono-sedimentary setting for the Barney Creek Formation within the southern McArthur Basin.

Conventional petrography and CL work on neptunian dyke samples will further aid in developing a diagenetic cement stratigraphy for the Teena and Emmerugga Dolomites. This will allow insights into the regional diagenetic and fluid-flow history of pre-Barney Creek Formation sediments. In addition, detailed isotopic and elemental work will hopefully aid in the characterisation of diagenetic environments and fluid chemistries. Mineralisation case studies will be used to test whether the regional diagenetic history can constrain the age of mineralisation at the Beryaya and Cooley I Pb-Zn prospects.

Acknowledgements

This work forms part of a PhD study of the sedimentology and diagenesis of Proterozoic McArthur Group carbonates of the southern McArthur Basin, northern Australia. Funding for this research comes from an Australian Commonwealth Postgraduate Research Award and the AMIRA P384A Proterozoic Sediment-Hosted Base Metal Deposits project provides additional logistical support. The authors would like to thank MIMEX for granting access to drillcore that has proved very important for this study and also for allowing us to stay at the MIMEX McArthur River depot during part of the 1996 field season. We are also very grateful to Eoin Rothery (MIMEX) for helping with tracking down open-file drillcore and for the many stimulating discussions. Perilya is also thanked for allowing access to DDH GPD4. Constructive criticism from John Dunster, Steve Hunns, and David Rawlings (CODES) is also gratefully acknowledged.

References

Bates, R.L. and Jackson, J.A., 1987. Glossary of Geology, 3rd edition. American Geological Institute, Alexandria, Virginia, p335 and 446

Bernouli, D. and Jenkins, H.C., 1974. Alpine, Mediterranean, and central Atlantic Mesozoic facies in relation to the early evolution of the Tethys. SEPM Special Publication, v19, p129-160

Brown, M.C., Claxton, C.W., and Plumb, K.A., 1969. The Proterozoic Barney Creek Formation and some associated units of the McArthur Group, Northern Territory. Bureau of Mineral Resources, Australia, Record 1969/145

Bull, S.W., Cooke, D., and Winefield, P.R., this report. Progress report: Sedimentology and mineralisation at the Beryaya Prospect. AMIRA/ARC Project P384A

Dörling, S.L., Dentith, M.C., Groves, D.I., Playford, P.E., Vearncombe, J.R., Muhling, P., and Windrim, D., 1996. Heterogeneous brittle deformation in the Devonian carbonate rocks of the Pillara Range, Canning Basin: implications for the structural evolution of the Lennard Shelf. Australian Journal of Earth Sciences, v43, p15-29

Jackson, M.J., Muir, M.D, and Plumb, K.A., 1987. Geology of the southern McArthur Basin, Northern Territory. Bureau of Mineral Resources, Australia, Bulletin 220

Kendall, A.C., 1985. Radialaxial fibrous calcite: a reappraisal. *In* Schneidermann, N and Harris, P.M., eds., Carbonate Cements. SEPM Special Publication, v36, p59-77

Kennedy, M.J., 1996. Stratigraphy, sedimentology, and isotopic geochemistry of Australian Neoproterozoic Post-glacial Cap Dolostones: deglaciation, d^{13}C excursions, and carbonate precipitation. Journal of Sedimentary Research, v66, no.6, p1050-1064

Lehner, B.L., 1991. Neptunian dykes along a drowned carbonate platform margin: an indication for recurrent extensional tectonic activity? Terra Nova, v3, p593-602

Neudert, M. and McGeough, M., 1996. A new tectonostratigraphic framework for the deposition of the upper McArthur Group, N. T. New Developments in Metallogenic Research: The McArthur-Mount Isa-Cloncurry Minerals Province, MIC 96 Extended Abstracts, 90-93.

Pavlov, A.W., 1896. On dykes of Oligocene sandstone in the Neocomian clays of the district of Altayr in Russia. Geol. Mag., v3, p49-53

Pietsch, B.A., Rawlings, D.J., Creaser, P.M., Kruse, P.D., Ahmad, P., Fererczi, P.A. and Findhammer, T.L.R., 1991a. Bauhinia Downs 1:250000 Geological Map Series. Northern Territory Geological Survey Explanatory Notes SE53-3

Pietsch, B.A., Wyche, S., Rawlings, D.J., Creaser, P.M., and Findhammer, T.L.R., 1991b. McArthur River Region 1:100000 Geological Map Series. Northern Territory Geological Survey Explanatory Notes SE53-3 (6065-6165)

Playford, P.E., 1980. Devonian 'Great Barrier Reef' of Canning Basin, Western Australia. American Association of Petroleum Geologists Bulletin, v62, p814-840

Playford, P.E., 1984. Platform-margin and marginal-slope relationships in Devonian Reef Complexes of the Canning Basin. *In*: Purcell, P.G., ed., The Canning Basin, western Australia, p189-214. Proceedings of the Geological Society of Australia and the Petroleum Exploration Society of Australia Symposium, Perth

Playford, P.E., and Lowry, D.C., 1966. Devonian reef complexes of the Canning Basin, Western Australia. Geological Survey of Western Australia Bulletin, v118, 150p

Plumb, K.A. and Brown, M.C., 1973. Revised correlations and stratigraphic nomenclature in the Proterozoic carbonate complex of the McArthur Group, Northern Territory. In Geological papers 1970-71, Bureau of Mineral Resources, Australia, Bulletin 139, p103-115

Sandberg, P., 1985. Aragonite cements and their occurrence in ancient limestones. *In* Schneidermann, N and Harris, P.M., eds, Carbonate Cements, SEPM Special Publication No. 36, p33-57

Southgate, P.N., Jackson, M.J., and Winefield, P.R.., 1997. Sequence stratigraphy of the upper McArthur Group: Teena Dolomite to Looking Glass Formations, NABRE Workshop, Extended Abstracts, AGSO Record 1997/12

Strauch, F., 1966. Sedimentgänge von Tjörnes (Nord-Island) und ihre geologische Bedeutung. N. Jb. Geol. Paläont. Abh., v124/3, p259-288

Sumner, D.Y., and Grotzinger, J.P., 1996. Herringbone calcite: petrography and environmental significance. Journal of Sedimentary Research, v66, no.3, p419-429

Tucker, M.E., and Wright, V.P., 1991. Carbonate sedimentology. Blackwell Scientific Publications, 482p

Vera, J.A., Molina, J.M., Molina-Diaz, A., and Ruiz-Ortiz, P.A., 1987. Bauxitas karsticas jurasicas en la zona subbetica (Zarzadilla de Totana, prov. de Murcia, sureste de Espana): Interpretacion paleogeografica. Acta geol. Hisp., v21-22, p351-360

Walker, R.N., Muir, M.D., Diver, W.L., Williams, N., and Wilkins, N., 1977. Evidence of major sulphate evaporite deposits in the Proterozoic McArthur Group, Northern Territory, Australia, Nature, v265, p526-529

Wendt, J., 1971. Genese und Fauna submariner und sedimentärer Spalten-füllungen im mediterranen Jura. Palaeontographica, v136, p122-192

Williams, N., 1978. Studies of the base metal sulphide deposits at McArthur River, Northern Territory, Australia I: The Cooley and Ridge deposits. Economic Geology, v73, p1005-1035.

Winefield, P.R., this report. Coxco needles: are they necessarily gypsum pseudomorphs? AMIRA/ARC Project P384A

Winterer, E.L., Metzler, C.V., and Sarti, M., 1991. Neptunian dykes and associated breccias (Southern Alps, Italy and Switzerland): role of gravity sliding in open and closed systems. Sedimentology, v38, p381-404

Winterer, E.L., and Sarti, M., 1994. Neptunian dykes and associated features in southern Spain: mechanics of formation and tectonic implications. Sedimentology, v41, p1109-1132

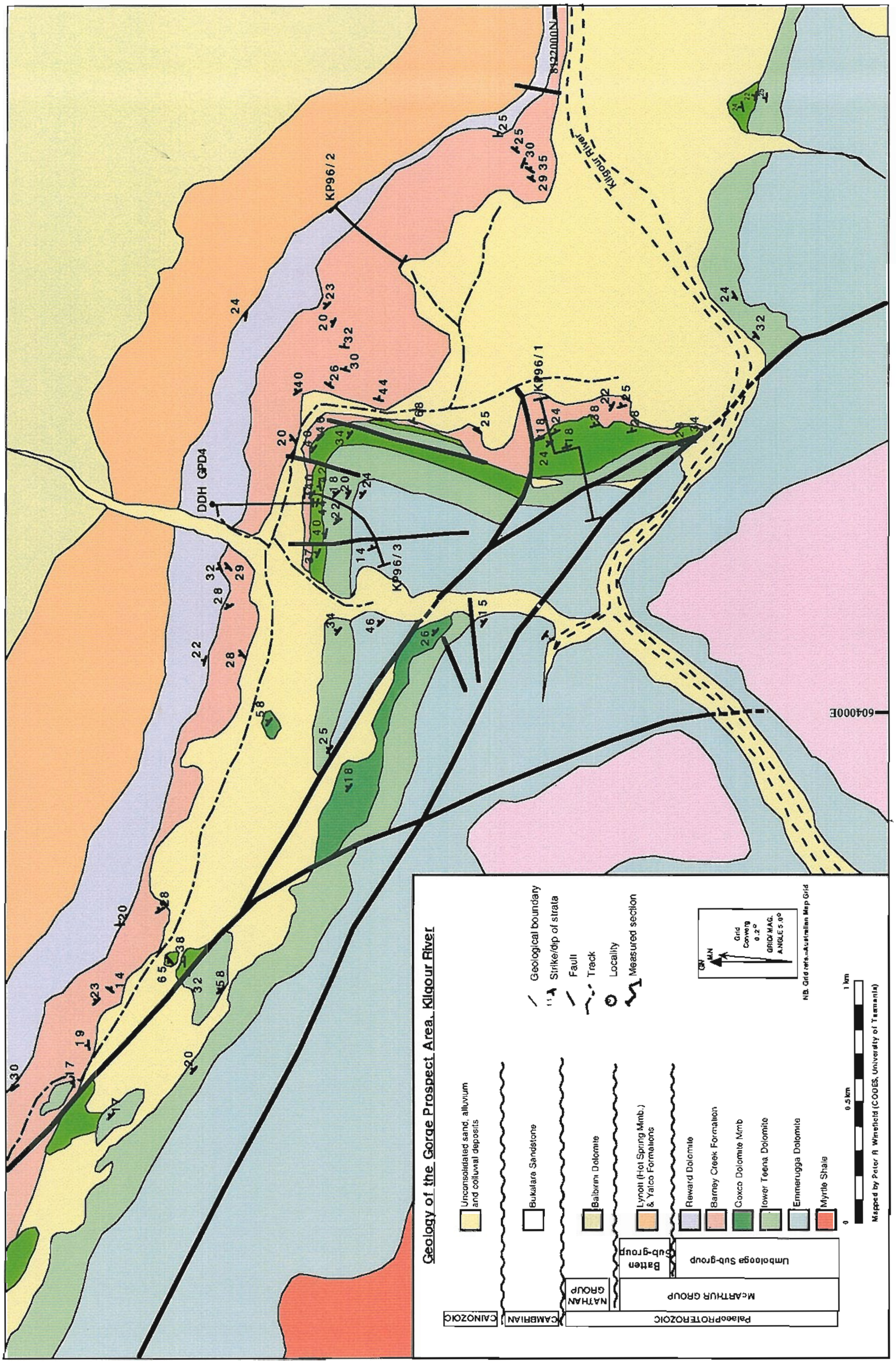

Appendix 1. Geology of the Gorge Prospect Area, Kilgour River

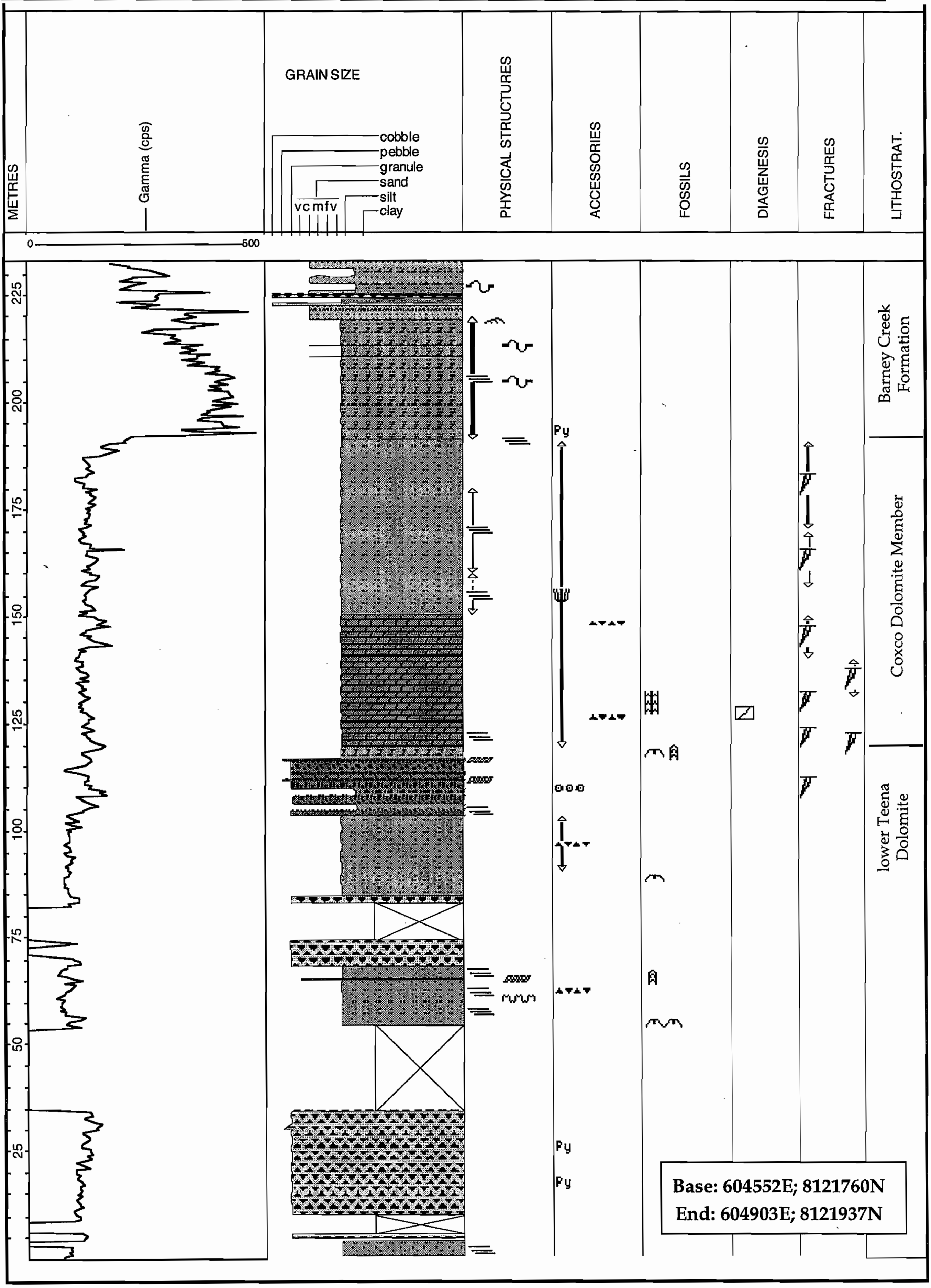

Appendix 2.1 Measured section KP96/1.

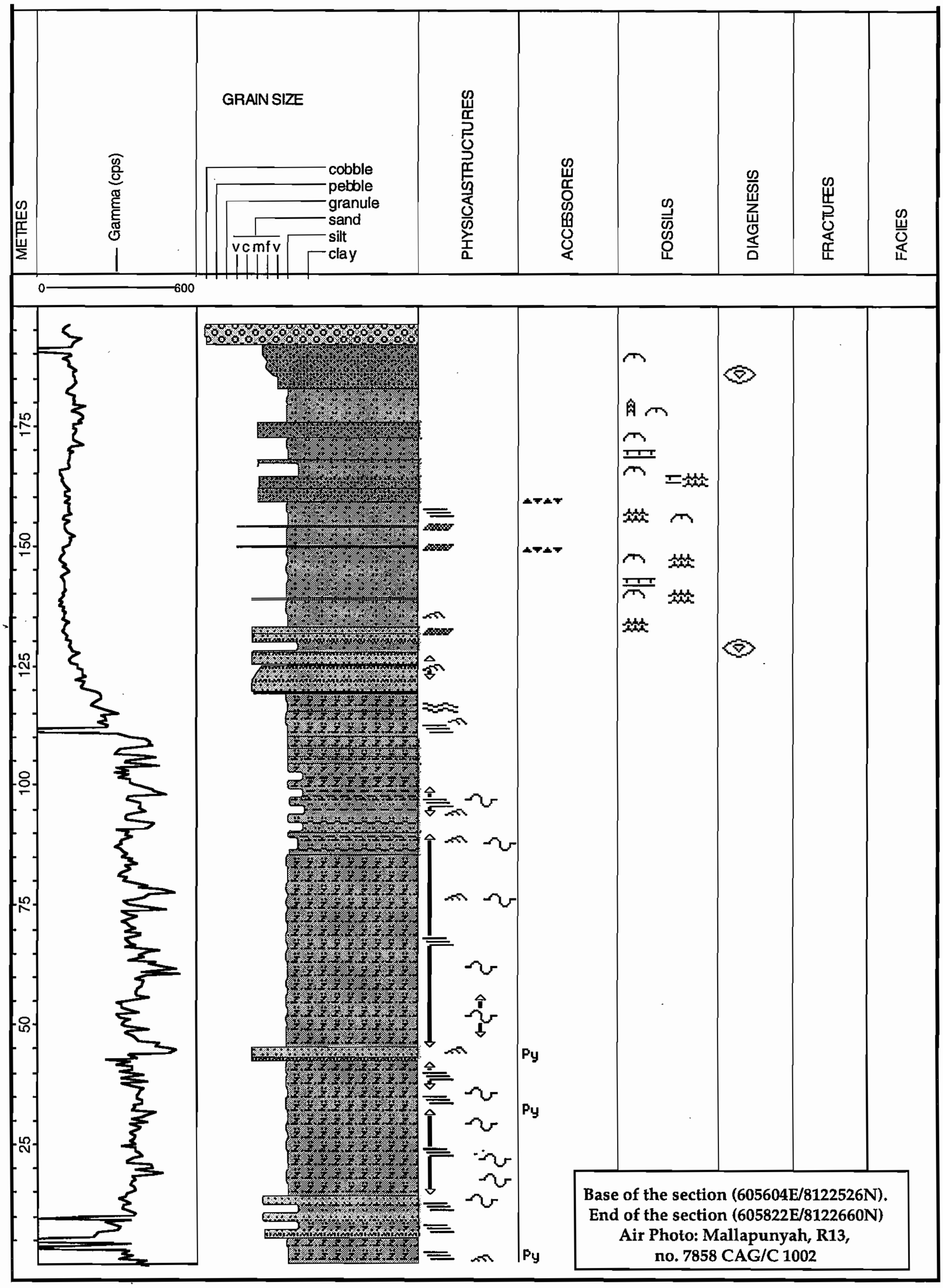

Appendix 2.2 Measured section KP96/2.

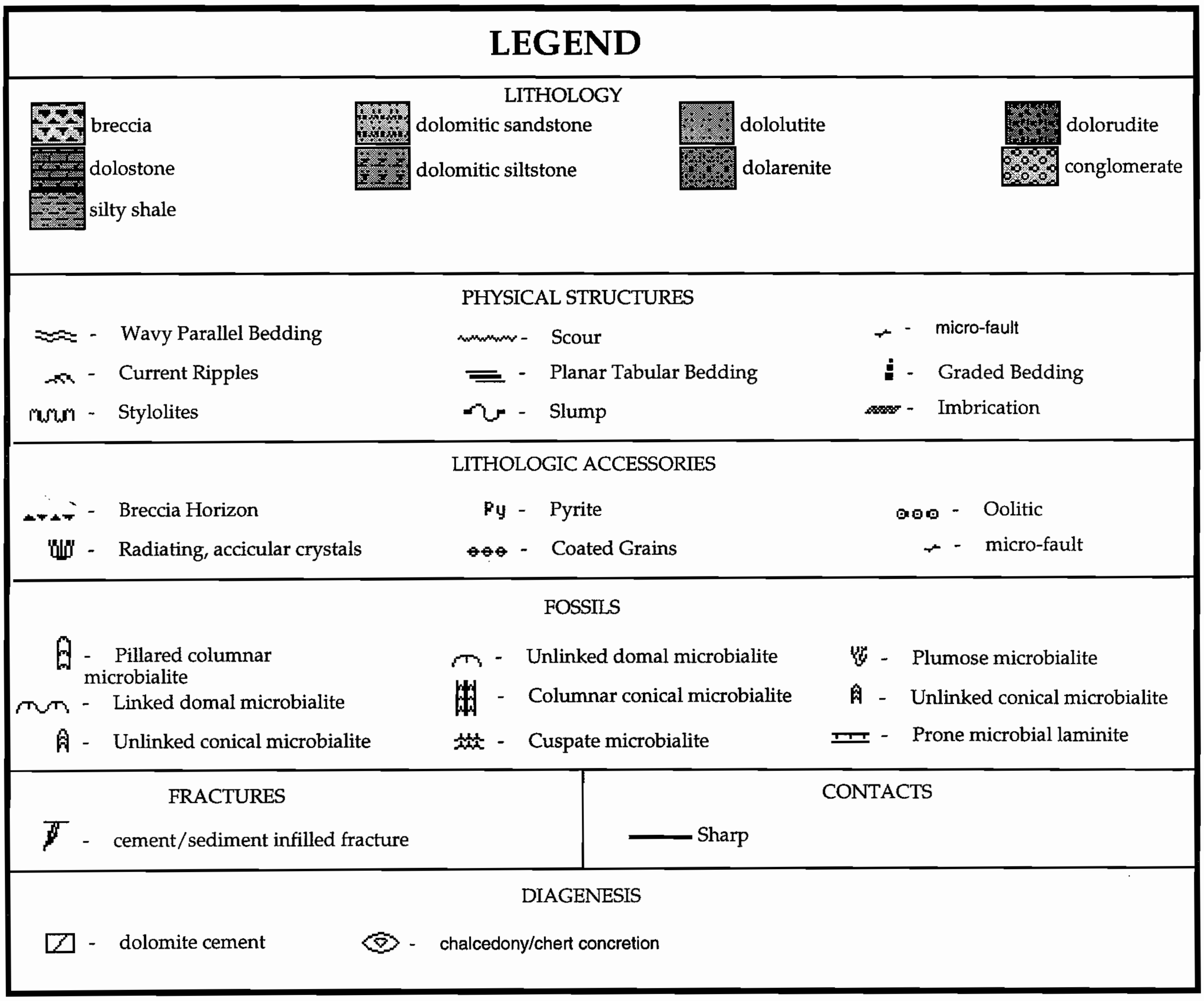

Appendix 2.3 Legend of symbols and lithologies used in Appendix 2.1 & 2.2

The Grevillea Prospect, Riversleigh area, north west Queensland: ore texture and primary lithogeochemical characteristics

Peter McGoldrick
CODES Special Research Centre, Geology Department, University of Tasmania

Summary

The Grevillea prospect comprises stratiform base metal mineralisation in pyritic black shales and siltstones of the lower Riversleigh Siltstone. The surface expression of the mineralisation is a prominent baritic gossan located 8 km south east of Riversleigh Homestead. Drilling in the immediate vicinity of the gossan revealed several intersections of between 15 an 25 m true thickness with Zn grades of 4-5%, up to 1% Pb, and about 35 g/t Ag in primary mineralisation. Although not outcropping, the pyritic horizon has a recognisable geophysical signature for at least 1.5 km north of the gossan. The pyritic sequence has been sampled by percussion drilling 250 m and 450 m to the north of the gossan, however, only low levels of base metals were encountered.

For this study quarter core was collected from cored holes near the gossan, and assay pulps from percussion holes to the north. Core samples were used to document the lithogeochemistry of barren siltstones and shales interbedded with pyritic and base metal sulphide-rich horizons, and for petrographic study of sulphide textures. The percussion hole samples provided examples of low-grade equivalents of the mineralisation to test the persistence of mineralisation-related geochemical signatures.

All the base metal mineralisation is associated with highly pyritic lithologies. Barite is locally abundant and associated with pyrite. Much of the pyrite is 'reactive' and has a 'spongy' appearance in hand specimen. Siltstones often display brown discolouration very similar in appearance to sideritic siltstones from the Lady Loretta deposit. Gypsum mush textures indicate the former presence of sulphate evaporites in the mineralised sequence. Macroscopic and microscopic textures of spongy pyrite are consistent with pyrite formation by replacement of prone microbial mat. Base metal sulphides occur as infilling within the spongy pyrite.

Twenty three samples of core and thirty two percussion pulps were analysed for major elements and selected trace elements. As in all previous case studies, sulphide-rich samples were avoided where possible. The analyses were used to calculate modal mineralogies, carbonate compositions, and alteration index parameters for all the samples. Five of the core samples contain siderite as the major carbonate phase, and in many of the remaining samples the carbonate is ankerite, not dolomite. Alteration indices (AI3 and SedexAI) and MnOd/s are often elevated in both core and pulp samples. Thallium levels are strongly anomalous in all the core samples, and many of the pulps. The best combined response comes from samples spanning the most strongly mineralised fifty metres of the core. None-the-less, the response from the pulps is still very encouraging, and would warrant follow-up drilling within a radius of 500 m.

A comparison of sedimentological, lithogeochemical and gamma log features in DDH LA 64, Lady Loretta area, north west Queensland

Peter McGoldrick and John Dunster
CODES Special research Centre, Geology Department, University of Tasmania

Summary

Drill hole LA 64 is collared approximately 4 km NNE of the Lady Loretta mine site, and provides a cored interval of about 600 m of Lady Loretta Formation from beneath thin Cambrian and Meszoic cover east of the Western Border Fault. Pyritic interbeds from this hole and several others in the area are the stratigraphic equivalents of the mineralised sequence at the mine. The area has been considered favourable for Lady Loretta style mineralisation and has undergone several base emtal exploration phases without any significant discoveries.

This report presents results form fifty four new whole rock major and trace element analyses from siltstone and shale samples from LA 64, and compares theses results with the sedimentological and gamma logs for the hole. Geochemical vectors developed from the Lady Loretta deposit have been calculated for these samples. For virtually all samples these indices (AI3, SedexAI, MnOd, Ankerite Ratio, and TI) are low and consistent with LA 64 being in a distal position with respect to Zn-Pb mineralisation. Graphical comparisons of K_20 and Al_2O_3 with gamma logs will be made at the meeting.

Iron transport in sedimentary brines — Implications for SEDEX deposits

David R Cooke
CODES Special Research Centre, Geology Department, University of Tasmania

Summary

Calculations presented in this report illustrate that iron is soluble in acidic hydrothermal solutions at 150°C, and is insoluble in neutral to alkaline solutions. Redox processes are mostly unimportant for Fe deposition over the common range of f_{O2} values in hydrothermal systems, with Fe soluble in acid, oxidised and acid, reduced waters.

Based on fluid chemistry, Cooke et al. (1995) proposed two subdivisions for stratiform sediment-hosted ("SEDEX") Pb-Zn deposits — *McArthur-type*, which form from oxidised fluids, and *Selwyn-type*, which form from reduced, acid fluids. Based on calculated solubilities, Selwyn-type fluids can carry the requisite Fe, Mn, Ba, Pb and Zn required to form a Selwyn-type deposit. However, acid Selwyn-type fluids cannot form a McArthur-type deposit during early diagenesis, because interaction with the host dolomitic siltstones would cause carbonate dissolution and generation of secondary porosity, and the development of metasomatic fronts. In contrast, if McArthur-type SEDEX deposits form from relatively oxidised, near-neutral to alkaline fluids that are in equilibrium with thick packages of carbonates and oxidised clastic sediments, then only Pb and Zn can be introduced by the mineralising solution. As proposed by Large et al. (1995), a second, low-T reduced fluid is required to introduce the necessary Fe and Mn into the HYC system prior to each pulse of mineralised brine, thus accounting for the textural evidence for pyrite predating galena and sphalerite in each ore horizon.

Introduction

Although not mined for their Fe content, Paleoproterozoic and Paleozoic SEDEX-style Zn-Pb-Ag deposits are also major accumulations of iron, both as iron sulfides (many millions of tonnes) and Fe-bearing carbonates. At the HYC deposit, two generations of pyrite have been recognised. They have distinct sulfur isotope characteristics and textural characteristic that have been interpreted to indicate that pyrite deposition pre-dated galena and sphalerite, a key observation that lead to the diagenetic replacement models for Pb-Zn deposition (e.g. Eldridge et al., 1993; Hinman et al, 1994). Large et al (1995) provided an alternative interpretation, whereby Pb and Zn were products of pulses of hot, dense, metalliferous brines into an euxinic basin, with Fe and Mn added by expulsion of low-temperature, reduced Fe- and Mn-bearing waters prior to and following mineralised brine expulsion. McGoldrick et al. (1995) proposed a similar model for Lady Loretta, although they proposed that the low temperature Fe-Mn-bearing fluid was relatively oxidised (pyrite-stable, but near the hematite-pyrite boundary)

Because Fe deposition appears to be de-coupled from Pb and Zn in Paleoproterozoic SEDEX deposits, the mobilisation and deposition of Fe warrants consideration, as it could provide important insights into the variations in fluid compositions and depositional processes that lead to metal deposition. It is well-documented that redox processes are important for Fe transport and deposition in low temperature groundwaters and surface waters (e.g. Drever, 1982). This report discusses the geochemistry of iron in 150°C, 10 eq. wt. % NaCl hydrothermal brines, and comments on the implications for SEDEX genesis.

Iron transport in hydrothermal solutions

Fe commonly occurs in one of two oxidation states in hydrothermal environments (Fe^{II}, Fe^{III}). Iron is most soluble in the ferrous form (Fe^{+2}), and in saline brines, will typically be transported as chloride complexes ($FeCl^+$ and $FeCl_{2\,(aq)}$). Iron can be precipitated as ferrous iron (e.g., pyrite, pyrrhotite, siderite), ferric iron (Fe^{+3}; e.g., hematite), or as a combination of ferrous and ferric iron (magnetite). Iron solubilities are very low in oxygenated surface waters, where iron occurs in the ferric state (Drever, 1982).

Figure 1 shows the stability fields for the Fe-O-S minerals and siderite, the predominance fields for the important aqueous sulfur species, and Fe solubility contours for 10 eq. wt % NaCl brines that contain 1 wt % $CO_{2\,(aq)}$ and a total sulfur concentration of 0.001 molal. From this diagram, it can be seen that large quantities of Fe can be transported in *acid fluids*, whereas Fe is insoluble in neutral to alkaline brines. As for Mn, and in contrast to Pb and Zn, redox changes have only a minimal effect on Fe solubilities in hydrothermal environments. For the common range of pH values in hydrothermal systems (≈ 3–7), the minimum solubility of Fe occurs in the pyrite field, at the SO_4^{-2} / H_2S predominance field boundary (Figure 1).

Pyrrhotite solubility

With regards to specific iron-bearing minerals, Fe has vertical solubility contours in the pyrrhotite field of Figure 1. This is because temperature, pH, ΣS concentrations and salinity control pyrrhotite solubility via reaction 1:

$$FeCl_{2\,(aq)} + H_2S_{(aq)} <=> FeS_{(s)} + 2\,H^+ + 2\,Cl^- \quad (1)$$

Iron deposition as pyrrhotite is therefore favoured by increasing pH and/or dissolved H_2S concentrations, and/or by decreasing salinity and/or temperature.

Pyrite solubility

For pyrite, Fe solubility contours have a negative slope in the H_2S predominance field (Fig. 1), because ***increasing*** pH and f_{O2} cause Fe deposition via reaction (2):

$$FeCl_{2\,(aq)} + 2\,H_2S_{(aq)} + 0.5\,O_{2\,(g)} <=> FeS_{2\,(s)} + 2\,H^+ + 2\,Cl^- + H_2O \quad (2)$$

Fe deposition also occurs via temperature decrease, dilution and/or increased H_2S concentrations for pyrite-stable H_2S-bearing fluids. A key point to note is that at constant pH for reduced, H_2S-rich fluids, decreasing f_{O2} can cause pyrite ***dissolution*** (as shown by the arrow on Fig. 1), in contrast to the widespread dogma about the importance of reduction for pyrite deposition from reduced hydrothermal solutions.

When fluids are pyrite-stable and sulfates (SO_4^{-2} or HSO_4^-) are the predominant sulfur-bearing aqueous species, Fe solubility contours have a positive slope (Fig. 1). This is because ***decreasing*** pH and f_{O2} cause Fe deposition via reactions such as reaction (3):

$$FeCl_{2\,(aq)} + 2\,SO_4^{-2}{}_{)} + 2\,H^+ <=> FeS_{2\,(s} + 2\,Cl^- + 3.5\,O_{2\,(g)} + H_2O \quad (3)$$

In other words, the Fe solubility minimum occurs in the pyrite field at the SO_4^{-2} /H_2S predominance field boundary, and Fe deposition as pyrite can occur via opposing processes above and below this boundary. However, pyrite deposition also occurs via temperature decrease, dilution and/or increased aqueous sulfate concentrations for pyrite-stable SO_4^{-2}–bearing fluids.

Siderite solubility

As for pyrrhotite, Fe has vertical solubility contours in the siderite field, although this is difficult to see from Figure 1. Decreasing temperature and salinity, or increasing pH and/or ΣC concentrations can cause siderite deposition via reaction 4:

$$FeCl_{2\,(aq)} + H_2CO_{3\,(aq)} <=> FeCO_{3\,(s)} + 2H^+ + 2Cl^- \quad (4)$$

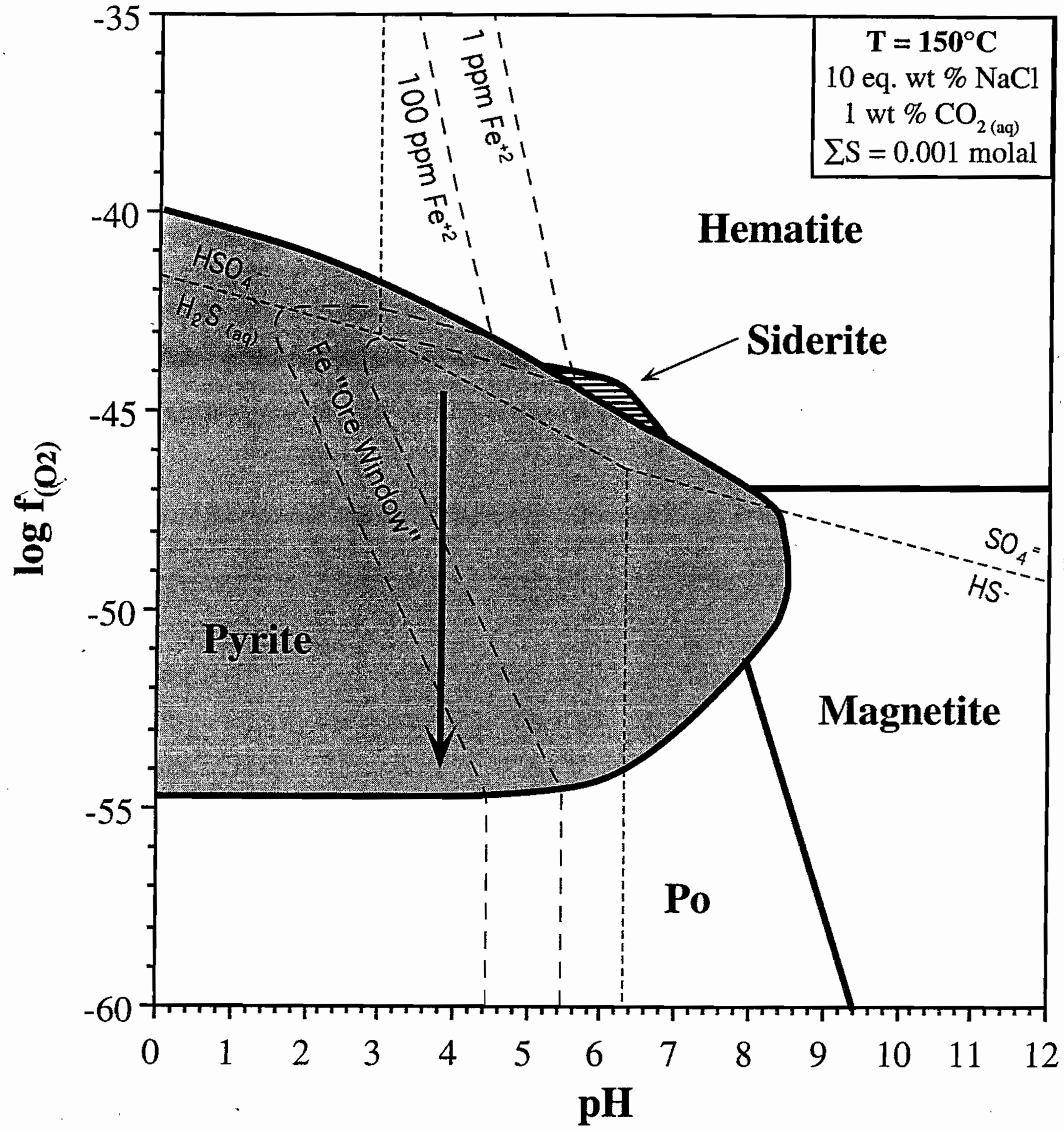

Figure 1: Log f_{O_2}-pH diagram showing the stability fields of the common Fe-O-S minerals (hematite, magnetite, pyrite, pyrrhotite) and siderite, the predominance boundaries between oxidised and reduced sulfur species, and Fe solubility contours (as $\Sigma Fe = m(Fe^{+2}) + m(FeCl^{+}) + m(FeCl_2)$) at 150°C. If a hydrothermal fluid evolved along the trajectory indicated by the bold arrow (reduction without pH change) pyrite would dissolve, liberating Fe into the hydrothermal fluid. This diagram has been constructed for a 10 eq. wt. % NaCl solution that contains 0.001 molal ΣS and 0.256 molal ΣC ($\approx$ 1 wt. % $CO_{2\,(aq)}$).

Hematite solubility

For hematite, Fe solubility contours have a negative slope(Fig. 1). Increasing pH and f_{O2}, and decreasing salinity and/or temperature cause Fe deposition via reaction (5):

$$FeCl_{2\,(aq)} + H_2O + 0.25\ O_{2\,(g)} \Longleftrightarrow 0.5\ Fe_2O_{3\,(s)} + 2\ H^+ + 2\ Cl^- \qquad (4)$$

ΣC and ΣS concentrations are unimportant for Fe solubilities in the hematite field, unless they increase to the point where siderite or pyrite is stabilised respectively.

Implications for Pb–Zn mineralisation

Figure 2 illustrates hematite, pyrite, siderite, galena and sphalerite solubility contours, together with the stability fields for siderite and the common iron oxides and sulfides at 150°C and 10 eq. wt. % NaCl. Fe is soluble in acid fluids with pH < 3, and is insoluble at pH > 5.5.

Pb and Zn are soluble in acid, reduced fluids (pH < 4), and over the full pH range in oxidised fluids (Fig. 2), where reduction is a key process for Pb-Zn deposition. In contrast, Fe solubility is mostly independent of redox changes for the common range of hydrothermal conditions at 150°C (Fig. 2).

At 150°C, Mn can be transported by reduced, acid brines (Region 1), oxidised, acid to neutral brines (Region 2a), and reduced, neutral to alkaline brines (Region 3a). Mn solubilities are low in Region 2b (oxidised, neutral to alkaline brines), with the exact amount of Mn able to be transported in solution depending on the amount of dissolved CO_2 in solution, and on the amount of Mn substitution into carbonate minerals.

Region 1 on Figure 2 corresponds to the type of fluids Cooke et al. (1995) inferred were responsible for the formation of *Selwyn-type* SEDEX deposits. Based on the calculations presented here and in previous reports, these fluids are predicted to be capable of transporting Pb, Zn, Ba, Mn and Fe.

Within region 2 (Fig. 2), oxidised hydrothermal solutions can transport Fe, Mn, Pb and Zn if they are acid (region 2A), whereas neutral to alkaline oxidised solutions can only transport Pb and Zn, with Fe, Mn and Ba insoluble.

Conclusions

Hot (T > 200°C), reduced (pyrite- and H_2S stable), acid fluids (pH < 4–5) can transport sufficient Pb, Zn, Mn, Ba, Pb and Zn to form a SEDEX deposit. This scenario is most likely to occur in clastic basins such as the Selwyn Basin, because clays are required to buffer fluid pH to acid values. A magmatic heat source (e.g. dolerite intrusion) is probably required to heat the solutions to high enough temperatures to transport Pb, Zn and Fe under sericite-stable conditions (T > 200°C). The principal base metal depositional mechanism is most likely to be quenching via mixing with seawater, which will also cause pH increase and salinity decrease.

Reduced (pyrite-stable) fluids in equilibrium with carbonates (i.e., pH > 5–6) will not be able to transport Pb, Zn or Fe. If the diagenetic model for HYC is correct, the mineralising reduced fluids would have to be highly acidic (pH < 2) to transport Fe, and moderately acidic (pH < 5) to transport Zn and Pb. Such acid fluids would dissolve the host carbonates, producing secondary porosity and metasomatic fronts (as in skarns). Such textures are not observed in Paleoproterozoic SEDEX deposits, and it is therefore concluded that an early diagenetic model for Pb-Zn deposition from reduced fluids is unworkable on chemical and textural grounds.

For oxidised, neutral to alkaline fluids in equilibrium with carbonates, sulfates and/or hematite (as is expected for a brine that passes through the McArthur Group carbonates, sandstones and evaporites), a 150°C brine will only be capable of transporting Pb and Zn, and would not be capable of introducing sufficient Fe (or Mn?) to account for the major Fe accumulation in this deposit. Large et al's (1995) two-stage fluid model for HYC and Lady Loretta are consistent with the predicted solubility relationships for Fe, Pb and Zn. For the HYC deposit, low-temperature reduced pore waters may have been expelled from the HYC shale within an anoxic sub-basin in response to fault movements. Deeper, warmer, oxidised Pb-Zn bearing brines would have also been tapped by these fault movements, expelling

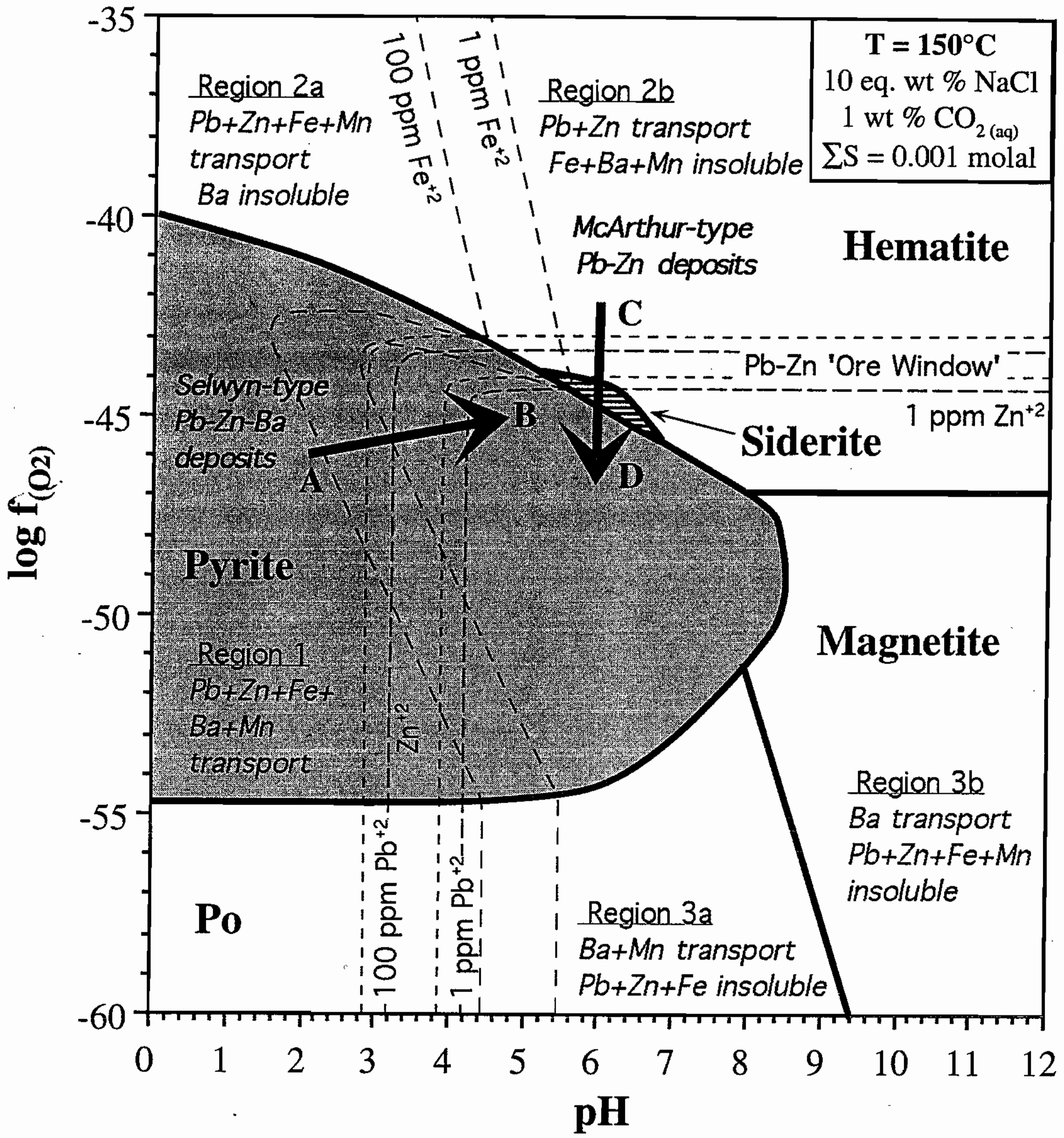

Figure 2: Log f_{O3}-pH diagram showing the stability fields of the common Fe-O-S minerals (hematite, magnetite, pyrite, pyrrhotite) and siderite, Fe, Pb and Zn solubility contours at 150°C. This diagram has been constructed for a 10 eq. wt. % NaCl solution that contains 0.001 molal ΣS and 0.256 molal ΣC (≈ 1 wt. % $CO_{2\,(aq)}$). A-B shows a possible evolutionary path for deposition of base metals from a Selwyn-type fluid (pH & fO2 increase). C-D is the predicted fluid evolution for Pb-Zn-bearing McArthur type brines (reduction)

into the anoxic basin after release of the low-T Fe- and Mn-bearing pore waters. The early low-T relatively oxidised fluid at Lady Loretta proposed by McGoldrick et al (1995) has a composition in the Fe solubility minimum, and would be a poor Fe transporter. The Lady Loretta model needs to be modified in the light of these findings, to account for the abundance of pyrite in that deposit.

References

Cooke, D.R., Large, R.R., McGoldrick, P.J., and Bull, S.W., 1995. Two classes of sediment-hosted Pb-Zn deposits. AMIRA/ ARC p.384, Final Report, 345-370.

Eldridge et al., 1993. Sulphur isotope variability in sediment-hosted massive sulphide deposits as determined using the ion microprobe SHRIMP II: a study of the HYC deposit at McArthur River, NT., Australia. Econ. Geol., 88: 1-26.

Drever, J.I., 1982. The geochemistry of natural waters. Prentice-Hall, N.J.,p. 234.

Hinman, M, Wall., V., and Heinrich, C., 1994. The interplay between sedimentation, deformation and hydrothermal activity at the McArthur Pb-Zn(-Cu) deposit. Geol. Soc. Aust. Abst. 37, pp. 176-177.

Large, R.R., Bull, S.W., Cooke, D.R., and McGoldrick, P.J., 1995. Review of genetic models at HYC: constraints from new sedimentology, alteration halo studies and fluid chemical modelling. AMIRA/ARC p.384, Final Report, 371-408.

McGoldrick, P.J., Dunster, J., and Aheimer, M., 1995. The Lady Loretta zinc-lead-silver deposit: primary dispersion halos, sedimentology, ore textures, stable isotopes, and metal distributions - towards a genetic model. AMIRA/ARC p.384, Final Report, 409-446.

Salinity controls on mineral stabilities and metal solubilities in 150°C sedimentary brines

David R Cooke
CODES Special Research Centre, Geology Department, University of Tasmania

Summary

This report compares calculations of metal solubilities and mineral stabilities for 10 and 25 eq. wt. % NaCl sedimentary brines at 150°C. At constant temperatures, higher salinity brines are (not surprisingly) concluded to be more effective at transporting Pb and Zn as chloride complexes. However, higher salinities have little effect on Fe solubilities, because even at high salinities, a significant component of Fe is transported as the bare ion (Fe^{+2}). Compared to 10 eq. wt. % brines, oxidised brines with salinities around 25 eq. wt. % NaCl and in equilibrium with siderite are capable of transporting sufficient Pb and Zn (1-100 ppm) to form a McArthur-style SEDEX deposit. They are not, however, capable of transporting enough Fe to account for the large pyrite accumulations in the Paleoproterozoic SEDEX deposits.

Introduction

A series of reports have now been presented that discussed metal solubilities and mineral stabilities for sedimentary brines at 150° and 250°C (Cooke, 1994; Cooke et al., 1994; Cooke et al., 1995; Cooke and Large, 1996). In each report, the effects of pH and f_{O2} variations on metal transport and mineral stabilities were discussed in detail for 150° and 250°C brines. All other variables (salinity, ΣS, ΣC) were held constant, to minimise the complexity of the discussions.

With regards to salinity, our assumption of 10 eq. wt. % NaCl for the mineralising brines is probably a reasonable assumption at 250°C, and is consistent with fluid inclusion studies of the Jason deposit in the Selwyn Basin (Gardner and Hutcheon, 1985). However, because of strong temperature controls on base metal solubilities as chloride complexes (e.g. Cooke and Large, 1994), our salinity estimate of 10 eq. wt. % is probably too low for 150°C brines. For example, MVT deposits form at 75-200°C and at salinities of 10-30 eq. wt. % NaCl (Leach and Sangster, 1993). The Silvermines Irish-style Pb-Zn deposit formed from 140-220°C fluids with salinities between 8 and 28 eq. wt. % NaCl (Samson and Russell, 1987). Furthermore, it seems likely that salt should have been leached from evaporites in the McArthur Group when brines migrated through them.

In this report, the results of thermodynamic calculations for two brine compositions (10 and 25 eq. wt. % NaCl) are compared. Both brines have temperatures of 150°C, ΣS contents of 0.001 molal and ΣC contents of 0.256 molal. Metal solubilities and mineral stabilities are plotted with respect to f_{O2} and pH variations on a series of activity diagrams (Figures 1 to 5). The results of these calculations are used to comment on the effects of salinity variations on selected aqueous species, mineral stabilities and metal solubilities, and on implications for SEDEX genesis.

Sulfur and carbon speciation

Although the molality of sulfur and carbon has been kept constant in both brines, the percentage abundances of these elements have decreased in the 25 eq. wt. % NaCl brine compared to the 10 wt % brine, because the concentrations of Na, Cl, K and Ca have increased substantially. For example, a concentration of 0.256 molal H_2CO_3 corresponds to 1.4 wt. % H_2CO_3 in the 10 eq. wt. % brine, and 1.2 wt. % in the 25 eq. wt. % brine. Similarly, 0.001 molal SO_4^{-2} corresponds to 85.0 ppm SO_4^{-2} in the 10 eq. wt. % brine, and 70.5 ppm in the 25 eq. wt. % brine.

Variations in the percentage abundance of ΣS and ΣC in the two brines has little effects on the predominance field boundaries. By comparing Figures 1A and B, it can be seen that increasing the salinity from 10 to 25 eq. wt. % NaCl has minimal effect on the positions of the predominance field boundaries for the aqueous carbon and sulfur species. The maximum variation is ≈ 0.1 pH units.

Iron oxides and sulfides

As for the S and C species, changing the salinity from 10 to 25 eq. wt. % NaCl has little effect on the stability fields for hematite, pyrite, magnetite and pyrrhotite (compare Figures 1A and B). The maximum variation is ≈ 0.1 pH units at alkaline pH values, and relates to slight variations in ionic strength, probably associated with carbon speciation behaviour, which affects the abundance of singly and doubly charged species in high pH solutions.

Siderite

The stability field for siderite is approximately 0.4 pH units larger for the 25 eq. wt. % NaCl brine than for the 10 % brine (Figures 1A and B). Siderite is therefore stabilised by higher salinities at 150°C, although the reason for this is not obvious. It may relate to variations in calculated activity coefficients due to minor changes in the relative abundance of singly- and doubly-charged carbon species (HCO_3^- vs. CO_3^{-2}).

Barite

Barite is highly soluble in reduced fluids, and is insoluble in acid solutions. Changing the salinity of the brine had little effect on barite solubilities at reduced conditions (H_2S-predominant, because of the strong redox controls near the H_2S-SO_4^{-2} predominance field boundary (the barite 'solubility cliff'; Figure 2). For oxidised conditions, barite solubility contours shifted approximately 0.4 pH units to the left (i.e. barite is insoluble at more acidic conditions; compare Figures 2A and B).

Pb and Zn solubilities

Metals that are transported as chloride complexes should be strongly affected by increasing salinity. By comparing Figures 3A and B, it can be seen that Pb and Zn become more soluble with increasing salinity. Under reduced (H_2S-predominant) conditions, the solubility contours for Pb and Zn shifted approximately 1 pH unit to the right when the salinity was increased to 25 eq. wt. % NaCl. Similarly, in oxidised fluids, Pb and Zn solubility contours shifted down by approximately 1 log f_{O2} unit (compare Figure 3A to 3B). This means that 25 eq. wt. % NaCl brines can transport Pb and Zn over a wider range of f_{O2}-pH conditions than 10 eq. wt. % brines.

Fe solubilities

Although Fe, like Pb and Zn, can be transported as chloride complexes in sedimentary brines, the effect of a salinity increase from 10 to 25 eq. wt % NaCl was predicted to much less pronounced (≈ 0.1 pH units for Fe compared to 1 pH unit for Pb and Zn; compare Figures 3A, 3B, 4A and 4B). Distribution of species calculations have shown that Fe is transported mostly as Fe^{+2}, with a lesser amount transported as $FeCl^+$ and a minor amount as $FeCl_{2\,(aq)}$ in the 25 eq. wt. % brine at 150°C. The bare ion (Fe^{+2}) is predicted to be much more stable than its Pb and Zn counterparts, and the amount of Fe transport achieved by the bare ion (Fe^{+2}) will not be enhanced by salinity increase, as can be seen from reaction 1:

$$FeCl_{2\,(aq)} + 2\,H_2S_{(aq)} + 0.5\,O_{2\,(g)} \Leftrightarrow FeS_{2\,(s)} + 2\,H^+ + 2\,Cl^- + H_2O \qquad (1)$$

The minor improvement in Fe transport is due to the predicted increase in abundance of $FeCl^+$ with increasing salinity (reaction 2) . The smaller increase in Fe abundance compared to Pb and Zn also relates

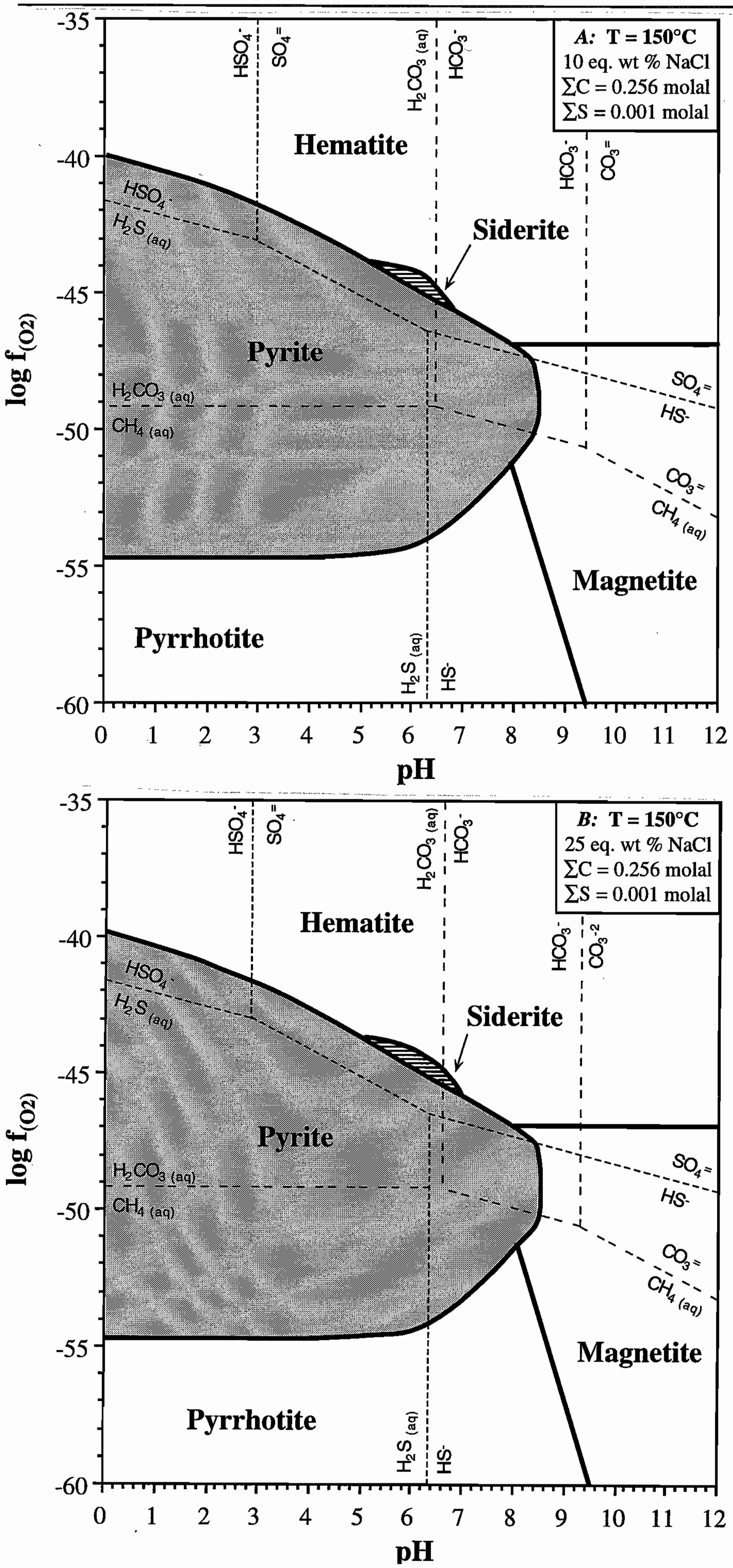

Figure 1: Log f_{O3}-pH diagram showing the stability fields of the common Fe-O-S minerals (hematite, magnetite, pyrite, pyrrhotite) and siderite, and the predominance boundaries between oxidised and reduced sulfur and carbon species at 150°C. ***A:*** *salinity = 10 eq. wt. % NaCl.* ***B:*** *salinity = 25 eq. wt. % NaCl solution. ΣS = 0.001 molal. ΣC = 0.256 molal.*

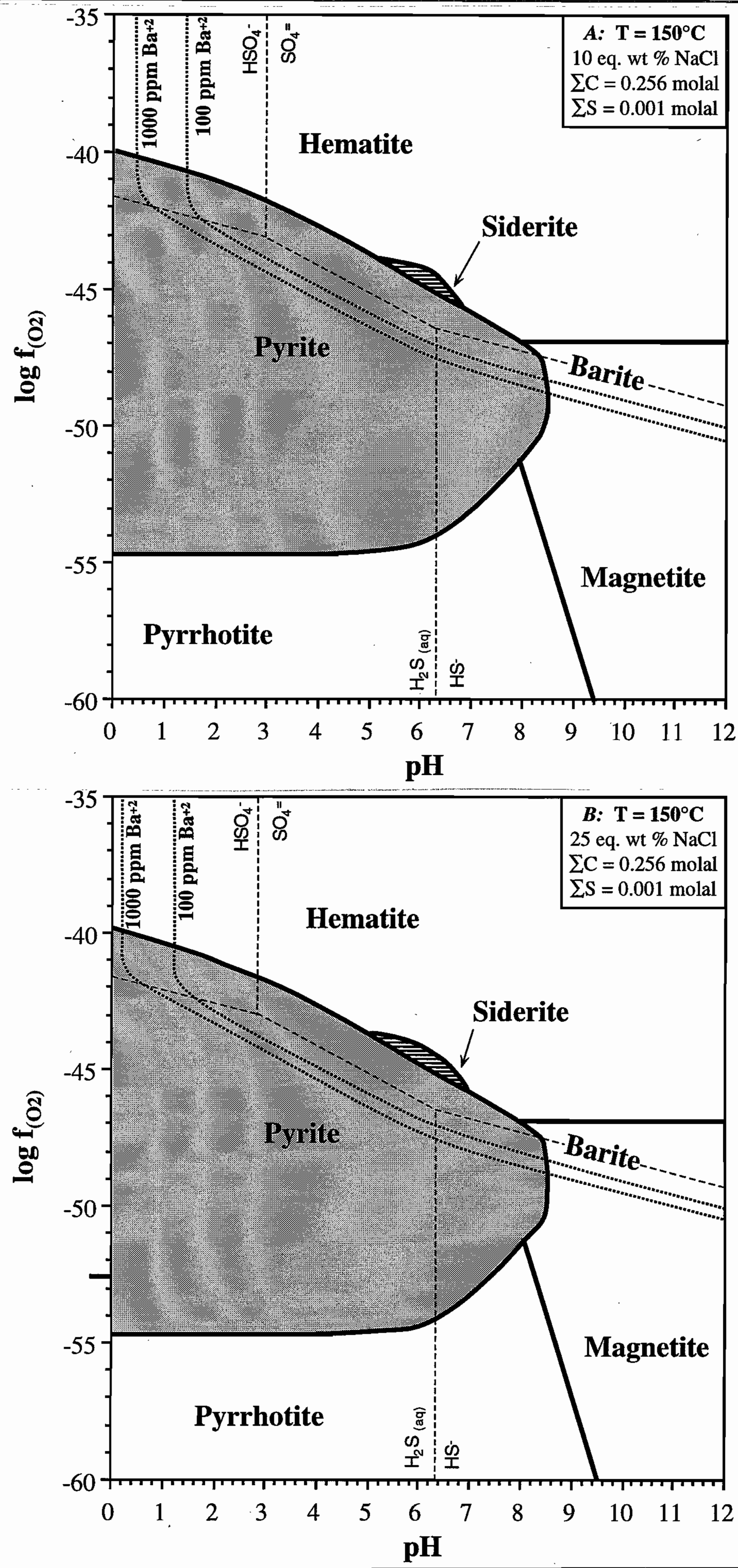

Figure 2: Log f_{O3}-pH diagram showing the stability fields of the common Fe-O-S minerals (hematite, magnetite, pyrite, pyrrhotite) and siderite, the predominance boundaries between oxidised and reduced sulfur species, and Ba solubility contours (100 and 1000 ppm) at 150°C. **A:** *salinity = 10 eq. wt. % NaCl.* **B:** *salinity = 25 eq. wt. % NaCl solution. ΣS = 0.001 molal. ΣC = 0.256 molal.*

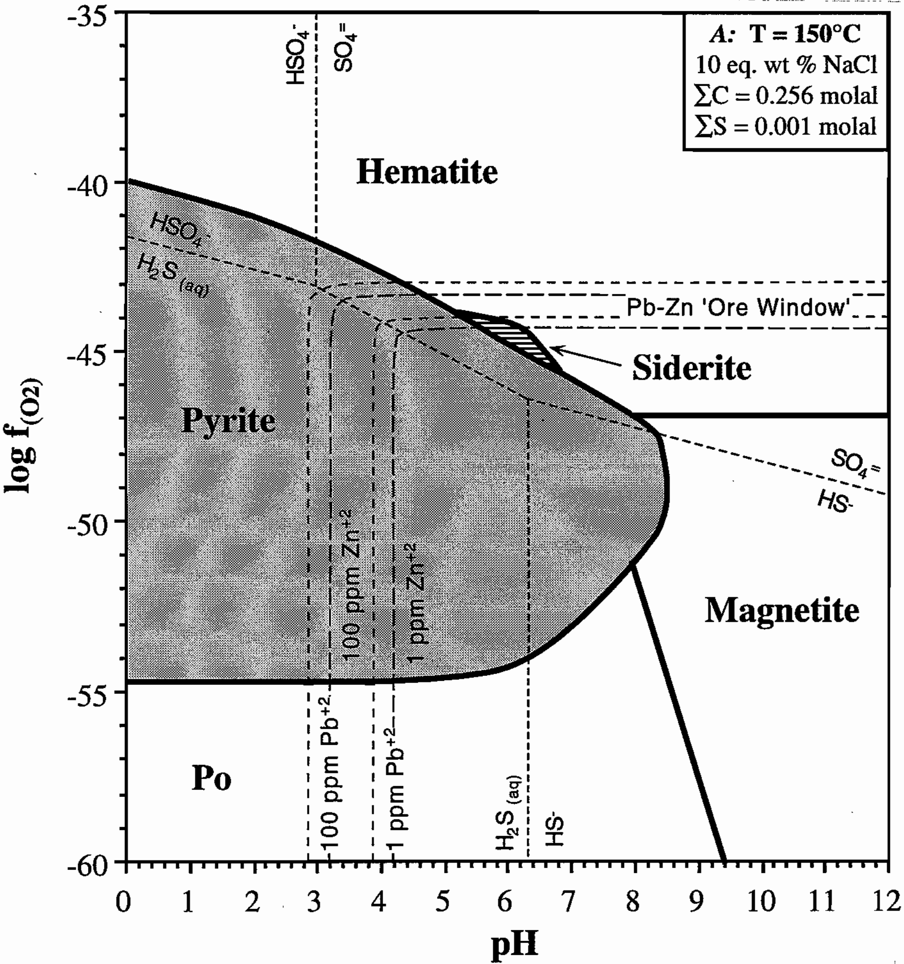

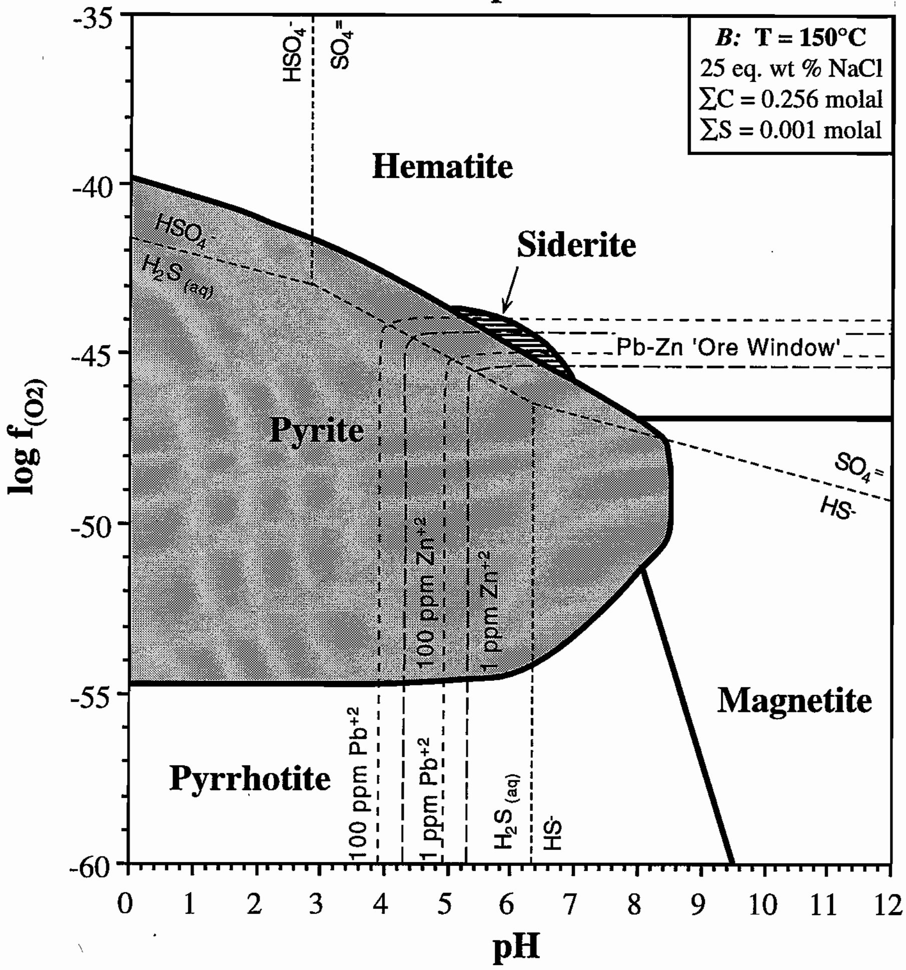

Figure 3: Log f_{O2}-pH diagram showing the stability fields of the common Fe-O-S minerals (hematite, magnetite, pyrite, pyrrhotite) and siderite, the predominance boundaries between oxidised and reduced sulfur species, and Pb and Zn solubility contours (1 and 100 ppm) at 150°C. **A:** *salinity = 10 eq. wt. % NaCl.* **B:** *salinity = 25 eq. wt. % NaCl solution. ΣS = 0.001 molal. ΣC = 0.256 molal.*

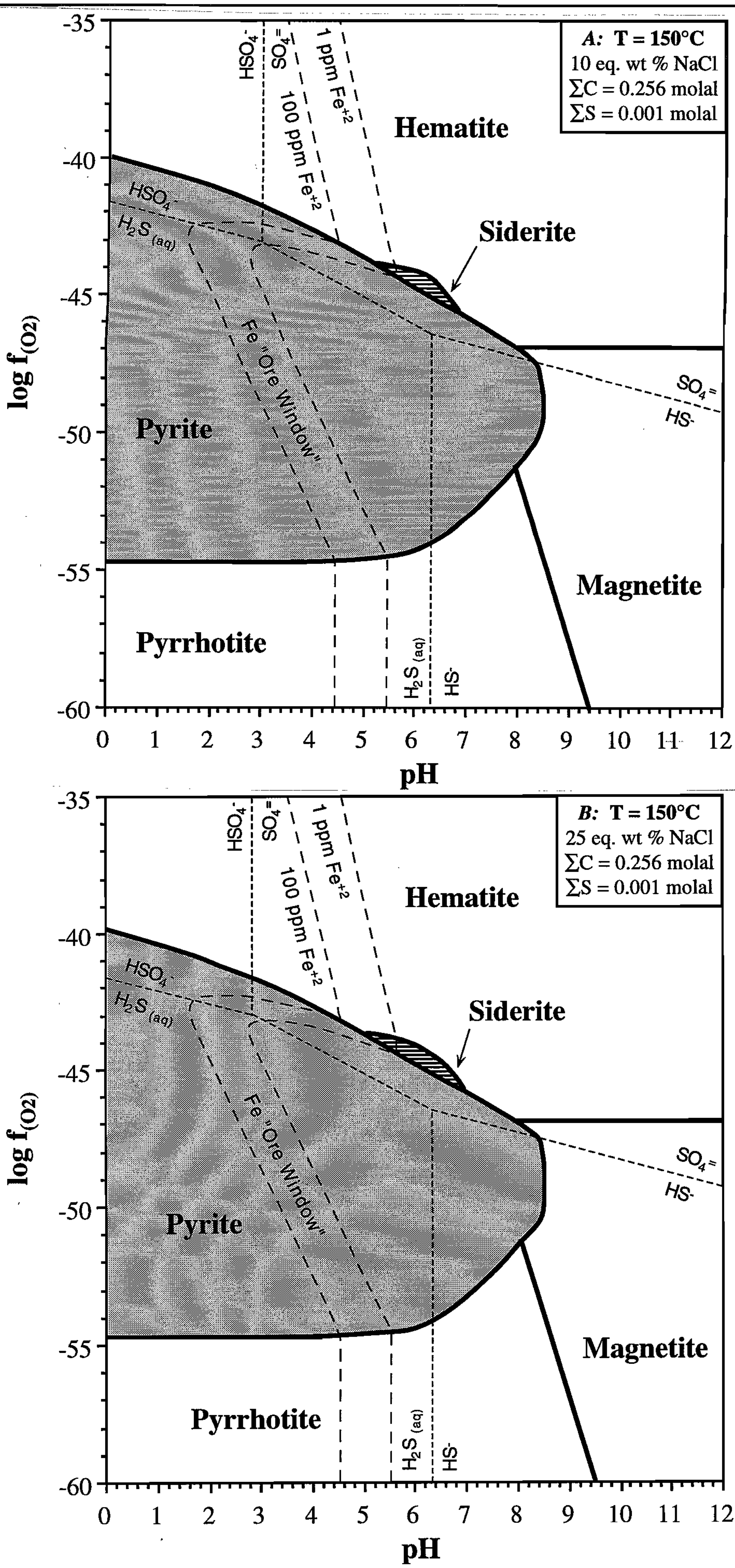

Figure 4: Log f_{O3}-pH diagram showing the stability fields of the common Fe-O-S minerals (hematite, magnetite, pyrite, pyrrhotite) and siderite, the predominance boundaries between oxidised and reduced sulfur species, and Fe solubility contours (1 and 100 ppm) at 150°C. ***A:*** *salinity = 10 eq. wt. % NaCl.* ***B:*** *salinity = 25 eq. wt. % NaCl solution. ΣS = 0.001 molal. ΣC = 0.256 molal.*

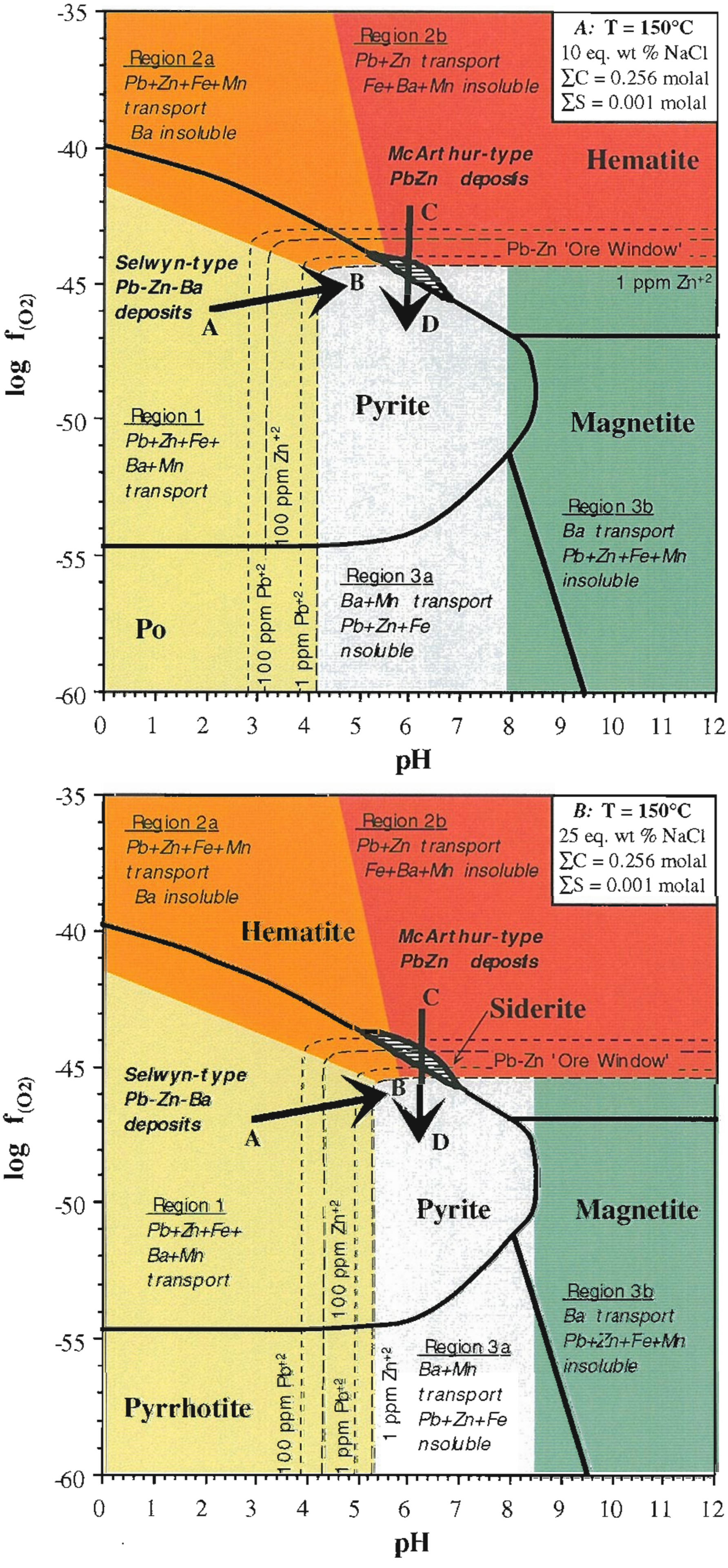

Figure 5: Log f_{O3}-pH diagram showing the stability fields of the common Fe-O-S minerals (hematite, magnetite, pyrite, pyrrhotite) and siderite, Pb-Zn solubility contours (1 and 100 ppm) and the major regions for base metal transport in sedimentary brines at 150°C. ***A:*** *salinity = 10 eq. wt. % NaCl.* ***B:*** *salinity = 25 eq. wt. % NaCl solution. McArthur-type SEDEX deposits are believed to be precipitated from brines with compositions in region 2b. Selwyn-type SEDEX deposits are believed to form from brines with compositions in region 1. Arrows A-B and C-D illustrate possible depositional trajectories for Selwyn- and McArthur-type fluids respectively. ΣS = 0.001 molal. ΣC = 0.256 molal.*

partly to the stoichiometry of the metal chloride complexes. At 150°C, Pb and Zn are transported predominantly as $PbCl_4^{-2}$ and $ZnCl_4^{-2}$ in the 25 eq. wt. % NaCl brine. In contrast, Fe is transported as Fe^{+2} and $FeCl^+$. The higher abundance of chloride in the Pb and Zn species means that they respond more dramatically to salinity increases, as can be seen in reactions 2 and 3:

$$FeCl^+ + 2\ H_2S_{(aq)} + 0.5\ O_{2\,(g)} \Leftrightarrow FeS_{2\,(s)} + 2\ H^+ + Cl^- + H_2O \qquad (2)$$

$$ZnCl_4^{-2} + H_2S_{(aq)} \Leftrightarrow ZnS_{(s)} + 2\ H^+ + 4\ Cl^- \qquad (3)$$

Discussion

A 25 eq. wt. % NaCl brine can transport Pb and Zn over a wider range of f_{O2}-pH conditions than a 10 eq. wt. % NaCl brine at 150°C. With regards to the model proposed by Cooke et al. (1995) for two classes of sediment-hosted Pb-Zn deposits, the Pb-Zn 'ore-forming window' (1-100 ppm) passes completely through the siderite field for a 25 wt. % brine (Fig. 5B), whereas it only just intersected the top corner of the siderite field at 10 wt % (Fig. 5A). This means that an oxidised, near-neutral brine in equilibrium with siderite at a salinity of ≈ 25 wt. % (region 2B on Figure 5B) is capable of carrying enough Pb and Zn to form a McArthur-type SEDEX deposit. However, even at these high salinities, it is not capable of carrying sufficient Fe to form a large pyrite accumulation.

A salinity of 25 eq. wt. % NaCl is also more favourable for Pb-Zn transport in a Selwyn-type fluid at 150°C, because the pH required to mobilise Pb and Zn is around one unit less acid than for 10 eq. wt. % NaCl (eg. sericite-stable rather than kaolinite-stable). The Selwyn-type fluid is still, however, too acid to be in equilibrium with carbonate, and could not transport Pb and Zn over long distances along or across stratigraphy in a carbonate-evaporite basin.

Conclusions

Higher salinities are more favourable for Pb and Zn (but not Fe) transport in 150°C sedimentary brines. A salinity of 25 eq. wt. % NaCl is probably more geologically realistic than 10 % for metalliferous brines in the McArthur and other Paleoproterozoic basins. Consequently, future reports in this series will focus on 25 eq. wt. % NaCl brines, as they are considered to be better approximations for the solutions responsible for McArthur-type SEDEX deposit formation.

References

Cooke, D.R., 1994. Conditions of formation for siderite and barite from sedimentary brines - implications for the formation of sediment-hosted base metal deposits AMIRA/ARC Project P.384, Report No. 7, 149-158.

Cooke, D.R., and Large, R.R., 1994. Geochemical modelling of hydrothermal systems: implications for ore genesis and predictions for mineral exploration. Australian Mineral Foundation: Australian Research on Ore Genesis Conference, Adelaide (abst.)

Cooke, D.R., and Large, R.R., 1996. Manganese transport in sedimentary brines - chemical controls on McArthur-type and Broken Hill-type sediment-hosted Pb-Zn deposits. AMIRA/ARC Project P.384a, Report No. 2.

Cooke, D.R., Large, R.R., and McGoldrick, P.J., 1994. Progress report: conditions of formation for siderite and ferroan carbonate - implications for the formation of sediment-hosted base metal deposits. AMIRA/ARC Project P.384, Report No. 5, 55-64.

Cooke, D.R., Large, R.R., McGoldrick, P.J., and Bull, S.W., 1995. Two classes of sediment-hosted Pb-Zn deposits. AMIRA/ARC p.384, Final Report, 345-370.

Gardner, H.D., and Hutcheon, I., 1985. Geochemistry, mineralogy and geology of the Jason Pb-Zn deposits, Macmillan Pass, Yukon, Canada. Econ. Geol., 80, pp. 1257-1276.

Leach, D.L., and Sangster, D.F., 1987. Mississippi Valley-type lead-zinc deposits. *in* Kirkham, R.V., Sinclair, W.D., Thorpe, R.I. and Duke, J.M., (Eds.) Mineral Deposit Modelling. Geol. Assoc. Canada Spec. Paper 40., p. 289-314

Samson, I.M, and Russell, M.J., 1987. Genesis of the Silvermines zinc-lead-barite deposit, Ireland: fluid inclusion and stable isotope evidence. Econ. Geol., 82, pp. 371-394.

Europium transport in sedimentary brines — Physicochemical controls in the ore-forming environment of McArthur- and Broken Hill-type sediment-hosted Pb-Zn deposits

Stephen B. Bodon and David R. Cooke
Centre for Ore Deposit Research, University of Tasmania

Summary

Positive europium anomalies on chondrite normalised rare earth element (REE) plots, are characteristic of hydrothermal precipitates in modern day sea-floor sulphide deposits. They are also characteristic in Broken Hill-type and VHMS deposits. As a result of this feature, positive europium anomalies have been used in the exploration industry to characterise potential ore-forming fluids, as well as some physicochemical conditions of the fluid (c.f. Sverjensky, 1984). To appreciate the potential of Eu for exploration and ore genesis applications, it necessary to understand the behaviour of Eu in hydrothermal solutions.

For 25 eq. wt% NaCl brines that contain ΣC=0.256 molal and ΣS=0.001 molal, europium is predominantly transported as $EuCl_4^{-2}$ (Eu^{+2} species) under most ore-forming conditions. Hydrothermal precipitates in the "SEDEX" (both McArthur and Selwyn-types) and BHT environments should therefore, display positive Eu anomalies. Eu speciation is not sensitive to fluctuations in fO_2 over the common range of hydrothermal ore-forming conditions, and therefore, the presence of positive Eu anomalies in hydrothermal precipitates is not a good indicator of oxidation state. Further work is required to assess the effects of changes in ΣS, ΣC, temperature and salinity on Eu speciation in both the source region for Eu and the ore-forming environment.

Introduction

The application of rare earth-element systematics as geochemical indicators to solve petrogenetic problems in igneous petrology and sedimentology is well documented (e.g. Haskin, 1984; McKay, 1989; McDaniel et al., 1994). However, the application of rare earth elements to ore genesis studies is becoming increasingly popular as more is learnt about their relative mobility in hydrothermal fluids. The results of such research have provided the foundation for constraining the sources and compositions of hydrothermal fluids, and some physicochemical conditions of ore formation when used in conjunction with isotopic data, fluid inclusions, mineral stabilities, etc. (e.g. Baker and Hellingwerf, 1988; Lottermoser, 1989 and 1992; Schandl and Gorton, 1991; Vander Auwera and André, 1991; Parr, 1992; Lapointe and Chown, 1993; McDaniel et al., 1994; Bierlein, 1995). However, interpretations are by no means simple, as the relative mobility of REE in a hydrothermal fluid is influenced by water/rock interaction, physicochemical properties of the fluid, temperature and pressure (Bau, 1991; Lottermoser, 1992). In addition, the influence of post-depositional processes such as diagenesis, metamorphism and hydrothermal alteration on REE mobility is debatable (MacLean, 1988; Whitford et al., 1988; Schandl and Gorton, 1991; McLennan and Taylor, 1991).

A feature of the mineralisation in Broken Hill-type and volcanic associated massive sulphide deposits is the existence of positive europium anomalies ($Eu^* = Eu_{chon}/\sqrt{Sm_{chon} \times Gd_{chon}}$) on chondrite-normalised REE plots. These are produced by fractionation of Eu^{+2} over Eu^{+3} in the source reservoir of the hydrothermal fluid due to water/rock interaction, and are controlled by the fluid composition and physicochemical conditions. Sverjensky (1984) demonstrated that this fractionation is strongly temperature dependent and, to a lesser degree, fO_2 and pH dependent. Aqueous Eu^{+2} is claimed to be more stable in reduced hydrothermal fluids at temperatures >250°C, whereas Eu^{+3} requires more oxidised conditions and temperatures <250°C (Sverjensky, 1984). This behaviour enables prediction of temperature, fO_2 and pH conditions at the site of deposition and leads to the generalised interpretation that positive Eu anomalies (Eu^{+2}) may provide a "fingerprinting" tool for the characterisation of potential ore-bearing hydrothermal fluids. The aim of this report is to calculate the aqueous speciation of Eu for a generalised high salinity brine indicative of sediment hosted Pb-Zn deposits, and assess the plausibility that positive Eu anomalies at the sites of ore deposition reflect a "reduced" brine composition.

Previous work

Studies have shown that primary REE signatures of rocks remain unchanged during post-depositional metamorphism and hydrothermal alteration unless water/rock ratios are extremely high, e.g. $>10^6$ (Lesher et al., 1986; Michard and Albarède, 1986; Michard, 1989; Bau, 1991; Parr, 1992; Bierlein, 1995). Such a finding is particularly attractive when working in metamorphic terrains, as it leaves scope for the preservation of primary REE signatures in the rocks even if they have been metasomatised. Other studies, however, indicate compositional evidence for REE mobility during metamorphism and hydrothermal alteration from a variety of geological settings and rock types (Campbell et al., 1984; Lottermoser, 1990; McLennan and Taylor, 1991; Wood and Williams-Jones, 1994; Banks et al., 1994; Klinkhammer et al., 1994; Bingen et al., 1996; Lewis et al., 1997). From experimental measurements of the complexation constants of REE with inorganic ligands at 25°C and 1 bar, there is a strong tendency for the REE to form aqueous complexes at room temperature (Cantrell and Byrne, 1987; Lee and Byrne, 1992, 1993). Lottermoser (1992) suggests that REE mobility is favoured by large fluid residence times during fluid/rock interaction and abundance of REE complexing ligands in the hydrothermal solutions.

Given the potential for REE mobility during hydrothermal alteration, a distinction must be drawn between the source site of the REE and the depositional site. Firstly, the hydrothermal fluid must liberate the REE from a source reservoir, and secondly the REE complexes must be destabilised in the depositional site by a sharp change in pH, temperature, or fO_2 (more likely combinations of these). Eu^{+2} is preferentially partitioned into plagioclase (especially albite). Breakdown of plagioclase by the hydrothermal fluid (e.g. leaching of feldspathic volcaniclastic rocks) liberates Eu^{+2} which is incorporated into the hydrothermal fluid and transported to the ore-forming environment (Michard and Albarède, 1986; Klinkhammer et al., 1994; Blundy and Wood, 1991). The REE signature of the fluid would therefore be proportional to the amount of Eu^{+2} (i.e. plagioclase) in the source rock, as well as being a function of the degree of alteration. The physicochemical characteristics of the scavenging fluid, abundance of plagioclase and degree of hydrothermal alteration (i.e. degree of plagioclase breakdown) are therefore, major controls on REE systematics in the hydrothermal fluid at the source region. In addition, variations in Eu signatures between different fluids may result from compositional differences in the plagioclase undergoing alteration (Klinkhammer et al., 1994).

The ability for the hydrothermal precipitates to reflect the REE composition of the fluid is questionable. Research suggests that the REE pattern of a precipitated mineral will be a function of the crystallographic ability of the particular mineral to accommodate the REE (Morgan and Wandless, 1980; Alderton et al., 1980). Nonetheless, while this is true for igneous processes and some simple hydrothermal phases regardless of fluid composition, other studies indicate a clear independence of mineralogy (Baker and Hellingwerf, 1988; Lottermoser, 1989; Parr, 1992; Bierlein, 1995). Adsorption of REE onto the surfaces of clays and/or Fe-hydroxides is another mechanism in which REE maybe deposited (c.f. Klinkhammer et al., 1994).

Europium in hydrothermal solutions

Eu occurs naturally in two oxidation states (divalent - Eu^{+2} and trivalent - Eu^{+3}). Thermodynamic data at elevated pressures and temperatures is available for the following Eu^{+2}- and Eu^{+3}-bearing aqueous species (Haas et al., 1995):

Eu^{+3}

- Europium ion: Eu^{+3}
- Chloride: $EuCl^{+2}$, $EuCl_2^+$, $EuCl_{3(aq)}$, $EuCl_4^-$
- Fluoride: EuF^{+2}, EuF_2^+, $EuF_{3(aq)}$, EuF_4^-
- Hydroxide: $EuOH^{+2}$, $EuO_2H_{(aq)}$
- Oxalate: EuO^+, EuO_2^-
- Nitrate: $EuNO_3^{+2}$
- Carbonate: $EuHCO_3^{+2}$, $EuCO_3^+$
- Phosphate: $EuH_2PO_4^{+2}$
- Sulphate: $EuSO_4^+$

Eu^{+2}

- Europium ion: Eu^{+2}
- Chloride: $EuCl^+$, $EuCl_{2(aq)}$, $EuCl_3^-$, $EuCl_4^{-2}$
- Fluoride: EuF^+, $EuF_{2(aq)}$, EuF_3^-, EuF_4^{-2}

Eu speciation calculations excluded the fluoride, nitrate and phosphate complexes to simply the system on a first pass basis. These complexes (especially fluoride and phosphate) probably play a significant role in Eu speciation in BHT systems due to the relative abundance of fluorite and fluor-apatite associated with sulphides (e.g. Cannington). The importance of lanthanum and lutetium fluoride complexes in simplified geothermal fluids at various pressures and temperatures is well illustrated in the speciation calculations of Haas et al. (1995). These complexes will be included in future calculations as the research progresses.

For 25 eq. wt% NaCl brines that contain $\Sigma C=0.256$ molal and $\Sigma S=0.001$ molal, distribution of Eu species calculations have shown that $EuCl^{+2}$, $EuCl_4^{-2}$ and EuO_2^- predominate at 150°C (Fig. 1). EuCl+2 predominates under extremely acidic conditions (pH<2), whereas EuO_2^- predominates under more alkaline conditions (pH>8). Therefore, trivalent Eu complexes only predominate at either extremely acidic conditions ($EuCl^{+2}$), or alkaline conditions (EuO_2^-). By far the most important complex for Eu transport at the calculated conditions is $EuCl_4^{-2}$ (Eu^{+2} species) which spans the majority of the Pb-Zn "ore window" (both the reduced acid Selwyn-type and the oxidised McArthur-type fields), as well as the siderite, kaolinite, muscovite, K-feldspar stability fields in Figure 1.

Implications for sediment-hosted Pb-Zn mineralisation

Based on our calculations, the predominant Eu aqueous species in SEDEX and Broken Hill-type fluids (given the conditions in Figure 1) should be divalent Eu. Precipitates from this fluid should yield positive Eu anomalies assuming that they preserve the REE signature of the hydrothermal fluid. While we are unaware of the REE signatures of SEDEX deposits, positive Eu anomalies characterise mineralisation at Broken Hill and the Pinnacles (Lottermoser, 1989; Parr, 1992). From Figure 1, pH clearly controls the predominance of Eu^{+2} and Eu^{+3} rather than oxygen fugacity (fO_2).

$$EuCl^{+2} + 3Cl^- + {}^1/_2H_2O \Longleftrightarrow EuCl_4^{-2} + H^+ + {}^1/_4O_{2(g)}$$

$$EuCl_4^{-2} + {}^3/_2H_2O + {}^1/_4O_{2(g)} \Longleftrightarrow EuO_2^- + 4Cl^- + 3H^+$$

These relationships suggest that a positive Eu anomaly relates to the pH of the hydrothermal fluid and not the oxidation state. Hence, the assumption that a positive Eu anomaly reflects reducing conditions in the ore-forming environment is incorrect. At 150°C and 25 eq. wt% NaCl, if the pH of the hydrothermal fluid is somewhere between 0-8 in the source reservoir and the transporting fluid, then a positive Eu anomaly is predicted in the hydrothermal precipitates in the ore-forming environment (based on the pretext that the precipitates reflect the REE signature of the hydrothermal fluid). Therefore, a whole-rock REE analysis of a single mineralised sample will yield more information about the processes involved in the source region of the hydrothermal fluid rather than the actual ore-forming environment. Measurement of physicochemical changes in the ore-forming environment using whole-rock REE systematics, requires recognition of paragenetically controlled REE zonation patterns. Further work is required to understand the

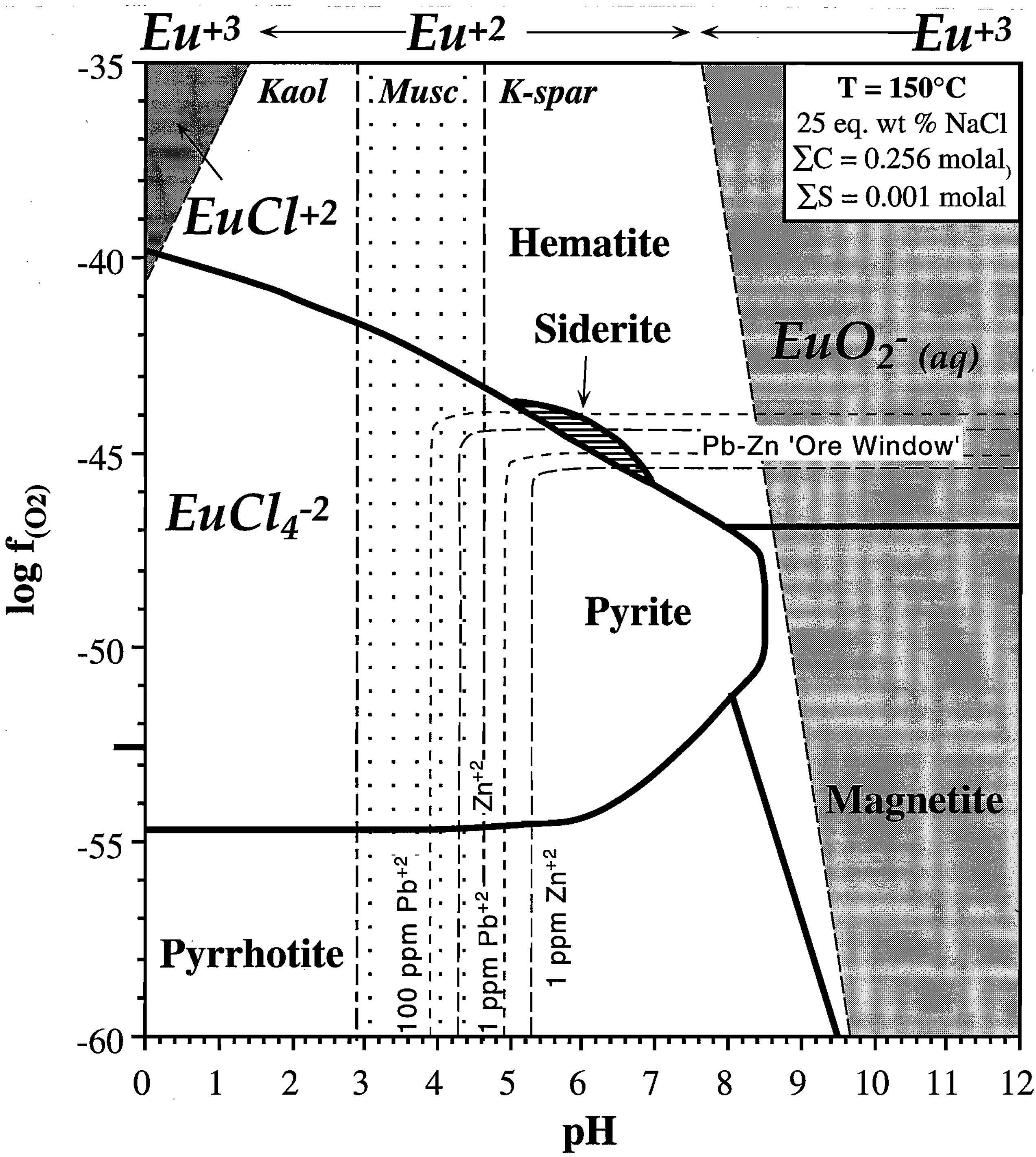

Figure 1. Log fO_2-pH diagram at 150°C showing the predominance fields for aqueous Eu species, together with the stability fields for pyrite, pyrrhotite, magnetite, hematite, siderite, kaolinite, muscovite and K-feldspar. This diagram has been calculated for a 25 eq. wt% NaCl brine that contains 0.001 molal ΣS, 0.256 molal ΣC (≈ 1 wt% $CO_{2(aq)}$).

how changes in ΣS, ΣC, salinity and temperature influences Eu speciation in hydrothermal fluids in the ore environment.

References

Alderton, D. H. M., Pearce, J. A., and Potts, P. J., 1980, Rare earth element mobility during granite alteration: evidence from southeast England: Earth and Planetary Science Letters, v. 49, p. 149-165.

Baker, J. H., and Hellingwerf, R. H., 1988, Rare earth element geochemistry of W-Mo-(Au) skarns and granites from western Berslagen, central Sweden: Mineralogy and Petrology, v. 39, p. 231-244.

Banks, D. A., Yardley, B. W. D., Campbell, A. R., and Jarvis, K. E., 1994, REE composition of an aqueous magmatic fluid: A fluid inclusion study from the Capitan pluton, New Mexico: Chemical Geology, v. 113, p. 259-272.

Bau, M., 1991, Rare-earth element mobility during hydrothermal and metamorphic fluid-rock interaction and the significance of the oxidation state of europium: Chemical Geology, v. 93, p. 219-230.

Bierlein, F. P., 1995, Rare-earth element geochemistry of clastic and chemical metasedimentary rocks associated with hydrothermal sulphide mineralisation in the Olary Block, South Australia: Chemical Geology, v. 122, p. 77-98.

Bingen, B., Demaiffe, D., and Hertogen, J., 1996, Redistribution of rare earth elements, thorium, uranium over accessory minerals in the course of amphibolite to granulite facies metamorphism: The role of apatite and monazite in orthogneisses from southwestern Norway: Geochimica et Cosmochimica Acta, v. 60, p. 1341-1354.

Blundy, J. D., and Wood, B. J., 1991, Crystal-chemical controls on the partitioning of Sr and Ba between plagioclase feldspar, silicate melts, and hydrothermal solutions: Geochimica et Cosmochimica Acta, v. 55, p. 193-209.

Campbell, I. H., Lesher, C. M., Coad, P., Franklin, J. M., Gorton, M. P., and Thurston, P. C., 1984, Rare-earth element mobility in alteration pipes below massive Cu-Zn-sulfide deposits: Chemical Geology, v. 45, p. 181-202.

Cantrell, K. J., and Byrne, R. H., 1987, Rare earth complexation by carbonate and oxalate ions: Geochimica et Cosmochimica Acta, v. 51, p. 597-605.

Haas, J. R., Shock, E. L., and Sassani, D. C., 1995, Rare earth elements in hydrothermal systems: Estimates of standard partial molal thermodynamic properties of aqueous complexes of the rare earth elements at high pressures and temperatures: Geochimica et Cosmochimica Acta, v. 59, p. 4329-4350.

Haskin, L. A., 1984, Petrogenetic Modelling - Use of rare earth elements: in P. Henderson (ed.), Rare Earth Element Geochemistry. Developments in Geochemistry: Elsevier, Amsterdam, v. 2, p. 115-152.

Klinkhammer, G. P., Elderfield, H., Edmond, J. M., and Mitra, A., 1994, Geochemical implications of rare earth element patterns in hydrothermal fluids from mid-ocean ridges: Geochimica et Cosmochimica Acta, v. 58, p. 5105-5113.

Lapointe, B., and Chown, E. H., 1993, Gold-bearing iron-formation in a granulite terrane of the Canadian Shield: a possible deep-level expression of an Archean gold-mineralizing system: Mineralium Deposita, v. 28, p. 191-197.

Lee, J. H., and Byrne, R. H., 1992, Examination of comparative rare earth element complexation behavior using linear free-energy relationships: Geochimica et Cosmochimica Acta, v. 56, p. 1127-1137.

Lee, J. H., and Byrne, R. H., 1993, Complexation of trivalent rare earth elements (Ce, Eu, Gd, Tb, Yb) by carbonate ions: Geochimica et Cosmochimica Acta, v. 57, p. 295-302.

Lesher, C. M., Gibson, H. L., and Campbell, I. H., 1986, Composition-volume changes during hydrothermal alteration of andesite at Buttercup Hill, Noranda District, Quebec: Geochimica et Cosmochimica Acta, v. 50, p. 2693-2705.

Lewis, A. J., Palmer, M. R., Sturchio, N. C., and Kemp, A. J., 1997, The rare earth element geochemistry of acid-sulphate and acid-sulphate-chloride geothermal systems from Yellowstone National Park, Wyoming, USA: Geochimica et Cosmochimica Acta, v. 61, p. 695-706.

Lottermoser, B. G., 1989, Rare earth element study of exhalites within the Willyama Supergroup, Broken Hill Block, Australia: Mineralium Deposita, v. 24, p. 92-99.

Lottermoser, B. G., 1990, Rare-earth element and heavy-metal behavior associated with the epithermal gold deposit on Lihir Island, Papua New Guinea: Journal of Volcanological and Geothermal Research, v. 40, p. 269-289.

Lottermoser, B. G., 1992, Rare earth elements and hydrothermal ore formation processes: Ore Geology Reviews, v. 7, p. 25-41.

MacLean, W. H., 1988, Rare earth element mobility at constant inter-REE ratios in the alteration zone at the Phelps Dodge massive sulphide deposit, Matagami, Quebec: Mineralium Deposita, v. 23, p. 231-238.

McDaniel, D. K., Hemming, S. R., McLennan, S. M., and Hanson, G. N., 1994, Resetting of neodymium isotopes and redistribution of REEs during sedimentary processes: The Early Proterozoic Chelmsford Formation, Sudbury Basin, Ontario, Canada: Geochimica et Cosmochimica Acta, v. 58, p. 931-941.

McKay, G. A., 1989, Partitioning of rare earth elements between major silicate minerals and basaltic melts: in B.R. Lipin and G.A. McKay (eds.), Geochemistry and Mineralogy of Rare Earth Elements, Mineralogical Society of America, Reviews in Mineralogy: , v. 21, p. 45-74.

McLennan, S. M., and Taylor, S. R., 1991, Sedimentary rocks and crustal evolution: tectonic setting and secular trends: Journal of Geology, v. 99, p. 1-21.

Michard, A., 1989, Rare earth element systematics in hydrothermal fluids: Geochimica et Cosmochimica Acta, v. 53, p. 745-750.

Michard, A., and Albarède, F., 1986, The REE content of some hydrothermal fluids: Chemical Geology, v. 55, p. 51-60.

Morgan, J. W., and Wandless, G. A., 1980, Rare earth element distribution in some hydrothermal minerals: evidence for crystallographic control: Geochimica et Cosmochimica Acta, v. 44, p. 973-980.

Parr, J. M., 1992, Rare-earth element distribution in exhalites associated with Broken Hill-type mineralisation at the Pinnacles deposit, New South Wales, Australia: Chemical Geology, v. 100, p. 73-91.

Schandl, E. S., and Gorton, M. P., 1991, Postore mobilization of rare earth elements at Kidd Creek and other Archean massive sulfide deposits: Economic Geology, v. 86, p. 1546-1553.

Sverjensky, D. A., 1984, Europium redox equilibria in aqueous solution: Earth and Planetary Science Letters, v. 67, p. 70-78.

Vander Auwera, J., and Andre, L., 1991, Trace elements (REE) and isotopes (O, C, Sr) to characterize the metasomatic fluid sources: evidence from the skarn deposit (Fe, W, Cu) of Traversella (Ivrea, Italy): Contributions to Mineralogy and Petrology, v. 106, p. 325-339.

Whitford, D. J., Korsch, M. J., Porritt, P. M., and Craven, S. J., 1988, Rare earth element mobility around the volcanogenic polymetallic massive sulfide deposit at Que River, Tasmania, Australia: Chemical Geology, v. 68, p. 105-119.

Wood, S. A., and Williams-Jones, A. E., 1994, The aqueous geochemistry of the rare-earth elements and yttrium 4.

Monazite solubility and REE mobility in exhalative massive sulfide-depositing environments: Chemical Geology, v. 115, p. 47-60.

The solubility of gold in 150°C saline brines – implications for the gold tenor of SEDEX ores

David R. Cooke and Peter McGoldrick
CODES Special Research Centre

Summary

Gold does not occur in anomalous concentrations in McArthur-type SEDEX deposits (e.g. Mount Isa, HYC; McGoldrick et al., 1996). Our calculations show that Au will only be transported in insignificant amounts (<< 0.1 ppb) within 150°C, saline, oxidised (siderite–hematite–carbonate–stable), near-neutral pH brines. In contrast, Selwyn-type SEDEX deposits that precipitate from reduced, acid, H_2S-bearing brines (pyrite–sericite-stable) should contain anomalous gold, because > 0.1 ppb can be transported in these brines as AuHS. There is potential for ore-grade gold in Selwyn-type deposits, provided that the fluids contained sufficient H_2S for Au transport, and that an effective Au depositional mechanism (H_2S loss, oxidation or reduction) operated at the trap site.

Introduction

McGoldrick et al. (1996) analysed the gold content of the Mount Isa, Lady Loretta, and HYC Paleoproterozoic SEDEX deposits. Their results, which are summarised in Table 1, indicate that McArthur-type SEDEX deposits are characterised by a remarkably low gold tenor with respect to the average crustal abundance of gold in unmineralised clastic rocks (1–5 ppb; Glasson and Keays, 1978; Crocket and Kuo, 1979) and carbonates and associated evaporites (1.9 ppb; Crocket, 1991).

McGoldrick et al. (1996) explained the low gold content in McArthur-type SEDEX deposits as the result of one of two possibilities:

- Gold became saturated in the mineralising brines at low gold concentrations (<< 1 ppb), preventing the transport of significant quantities of gold.
- Gold was transported, but not precipitated at the trap site, either due to precipitation in the feeder system, or passage of gold through the depositional environment without gold precipitation occurring.

McGoldrick et al (1996) favoured the first hypothesis, because the second is considered geologically and geochemically unlikely. A third possibility exists: the fluids could have been capable of transporting gold, but were undersaturated due to low gold contents and/or inefficient leaching in the source regime, thus preventing gold saturation within the brines at the trap site. This hypothesis seems unlikely, given that the average gold contents of clastic rocks and carbonates listed above are comparable to most other crustal lithologies (Crocket, 1991); i.e. the clastic and carbonate lithologies of the Paleoproterozoic basins are unlikely to be anomalously depleted in gold.

Table 1: Gold content of ores and host lithologies from the Mt. Isa, Lady Loretta and HYC SEDEX deposits (summarised from McGoldrick et al., 1996).

	Average gold content (ppb)		
Lithology	Mt. Isa	Lady Loretta	HYC
Zn–Pb–Ag ores	2.0	2.2	5.1
Pyritic shales and siltstones	2.1	0.9	6.2
Barren shales and siltstones	0.6	0.4	1.7

In this report, gold speciation and solubilities are discussed in terms of redox and pH variations for a 25 eq. wt. % NaCl brine at 150°C ($\Sigma S = 0.001$ molal; $\Sigma C = 0.256$ molal). Metal solubilities and mineral stabilities are plotted with respect to f_{O2} and pH variations on a series of activity diagrams (Figs 1 to 3). The results of these calculations are used to comment on the effects of salinity variations on selected aqueous species, mineral stabilities and metal solubilities, and on implications for SEDEX deposits.

Gold speciation

The two ligands that are involved in Au transport in most hydrothermal environments are chloride (Cl^-) and bisulfide ions (HS^-). High temperature thermodynamic data are available for the species $AuCl_2^-$, $Au(HS)_2^-$ and AuHS. Other important Au complexes may also exist (e.g. telluride or cyanide species), but no thermodynamic data are available for them. Significant quantities of Au can be transported as bisulfide complexes (e.g. low sulfidation epithermal Au, Archean shear zone-hosted Au, Pb–Zn–Ag–Au VHMS deposits, etc.) and as chloride complexes (porphyry Cu–Au, high sulfidation epithermal Au, etc.). Consequently, gold can form in a greater diversity of geological environments than metals which are only transported as chloride complexes (eg. Pb, Zn, etc.).

Figure 1 illustrates the predominance fields for $AuCl_2^-$, $Au(HS)_2^-$ and AuHS, together with the stability fields for pyrite, hematite, magnetite, pyrrhotite, siderite, kaolinite, muscovite and K-feldspar at 150°C and 25 eq. wt. % NaCl as a function of $\log f_{O2}$ and pH variations. Au speciation is strongly dependent on the ΣS concentration of the fluid, with AuHS stabilised at lower ΣS concentrations than $Au(HS)_2^-$, and gold bisulfide complexes stabilised at high ΣS concentrations. Choosing a ΣS concentration lower than 0.001 molal would have resulted in a larger $AuCl_2^-$ field, and the switchover from AuHS to $Au(HS)_2^-$ would occur at higher pH values on Figure 1.

In reduced (H_2S-predominant), acid fluids (pH < 3.9; kaolinite–muscovite-stable) gold is transported principally as AuHS (Fig. 1). For reduced fluids at higher pH values (muscovite–K-feldspar stable), $Au(HS)_2^-$ is the predominant Au-bearing species (Fig. 1). $AuCl_2^-$ is the major gold-transporting complex for oxidised (hematite-stable) brines (Fig. 1).

Gold solubilities

Figure 2 shows calculated gold solubility contours (0.1 to 100 ppb) at 150°C and 25 eq. wt. % NaCl, together with the predominance fields for Au-complexes, and the stability fields for pyrite, hematite, magnetite, pyrrhotite and siderite. Two solubility maxima occur on this diagram. The first, with Au solubilities in excess of 100 ppb, occurs in the top left hand corner of Figure 2, and is associated with hematite–kaolinite stable fluids that transport gold as $AuCl_2^-$ (e.g. high sulfidation epithermal fluids). The second, with Au solubilities in excess of 10 ppb, occurs at the H_2S–HS^-–SO_4^{-2} triple point in the pyrite–K-feldspar–carbonate field (e.g. low sulfidation epithermal fluids). Note the steep gradient between Au solubility contours above the second solubility maxima (Fig. 2). This 'solubility cliff' relates to the transition from reduced sulfur (e.g. H_2S) to oxidised sulfur (SO_4^{-2}) predominance. Consequently, sulfate-bearing, near-neutral to alkaline brines have the lowest gold-transporting capacity of any brine composition portrayed on Figure 2. Acid, oxidised or H_2S-rich reduced, near-neutral fluids are best equipped to transport high concentrations of gold in solution.

Discussion

Figure 3 shows calculated gold solubility contours (0.1 to 100 ppb) at 150°C and 25 eq. wt. % NaCl, together with the stability fields for the Fe–O–S minerals and siderite, and the various sedimentary brine types defined by Cooke et al. (1995) and Cooke (1997). McArthur-type deposits are inferred to be precipitated from siderite–hematite–carbonate stable near-neutral brines (region 2b on Fig. 3). These brines are excellent Pb and Zn transporting solutions, but are incapable of transporting Au, thus explaining the lack of Au anomalism noted in the Pb–Zn–Ag ores at Mount Isa, Lady Loretta and HYC by McGoldrick et al (1996; Table 1). These brines are also incapable of carrying Ba (consistent with the absence of barite in most McArthur-type deposits) and Fe and Mn, which has lead to the two-fluid models proposed for HYC and Lady Loretta by Large et al. (1995) and McGoldrick et al. (1995) respectively.

Selwyn-type SEDEX deposits are believed to form from reduced, acid fluids (region 1 on Figure 3). Although these fluids do not correspond with either of the gold solubility maxima, they are capable of transporting reasonable amounts of Au (0.1 to ≈ 4 ppb) at 150°C, and will be capable of carrying higher Au concentrations at higher temperatures and/or ΣS concentrations. We therefore predict that Selwyn-type SEDEX deposits should contain anomalous gold compared to their unmineralised host rocks. Furthermore, given sufficiently high ΣS concentrations and an effective Au depositional mechanism, Selwyn-type deposits could contains areas of economic Au grades. Au will most likely be transported as AuHS in Selwyn-type fluids (compare Figs 2 and 3). Sulfur loss, reduction and/or oxidation to sulfate-stable conditions will be the principal causes of Au deposition for Selwyn-type deposits; pH changes will not be important:

$$AuHS_{(aq)} + 0.5\ H_2O_{(aq)} = Au^0_{(s)} + H_2S_{(aq)} + 0.25\ O_{2\ (g)}$$

References

Cooke, D.R., 1997. Salinity controls on mineral stabilities and metal solubilities in 150°C sedimentary brines. AMIRA/ARC p.384a, Report No. 3 (this report).

Cooke, D.R., Large, R.R., McGoldrick, P.J., and Bull, S.W., 1995. Two classes of sediment-hosted Pb-Zn deposits. AMIRA/ARC p.384, Final Report, 345-370.

Crocket, J.H., and Kuo, H.Y., 1979. Sources for gold, palladium and iridium in deep-sea sediments. Geochim. et. Cosmochim. Acta, 43, p. 831-845.

Crocket, J.H., 1991. Distribution of gold in the Earth's crust. *in* R.P. Forster (Ed.) Gold metallogeny and exploration. Blackie and Son Ltd., London, 1-36.

Glasson, M.J., and Keays, R.R., 1978. Gold mobilisation during cleavage development in sedimentary rocks from the auriferous slate belt of Central Victoria: some important boundary conditions. Econ. Geol., 73, 496-511.

Large, R.R., Bull, S.W., Cooke, D.R., and McGoldrick, P.J., 1995. Review of genetic models at HYC: constraints from new sedimentology, alteration halo studies and fluid chemical modelling. AMIRA/ARC p.384, Final Report, 371-408.

McGoldrick, P.J., Dunster, J., and Aheimer, M., 1995. The Lady Loretta zinc-lead-silver deposit: primary dispersion halos, sedimentology, ore textures, stable isotopes, and metal distributions - towards a genetic model. AMIRA/ARC p.384, Final Report, 409-446.

McGoldrick, P., Keays, R., Smith, R., McOrist, G. and Fardy, J., 1996. Gold in Australian late Paleoproterozoic stratiform sediment-hosted zinc-lead-silver deposits. Geol. Soc. Aust. Abstracts, 41, p. 287.

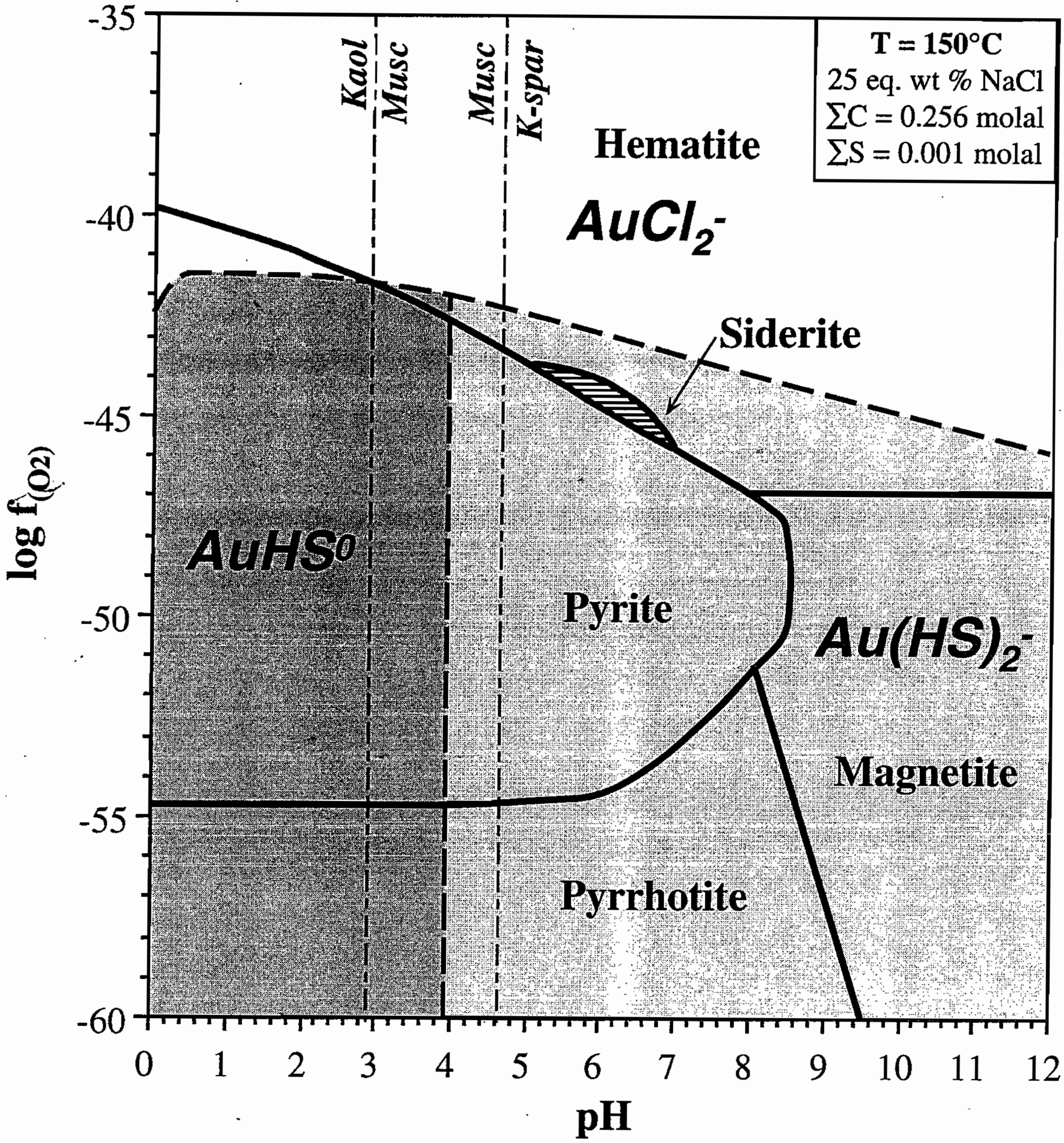

Figure 1: Log f_{O3}–pH diagram at 150°C showing the stability fields of the common Fe–O–S minerals, siderite, kaolinite, muscovite and K-feldspar, and the predominance fields for $AuCl_2^-$, $Au(HS)_2^-$ and AuHS. This diagram was drawn for a 25 eq. wt. % NaCl brine with $\Sigma S = 0.001$ molal and $\Sigma C = 0.256$ molal.

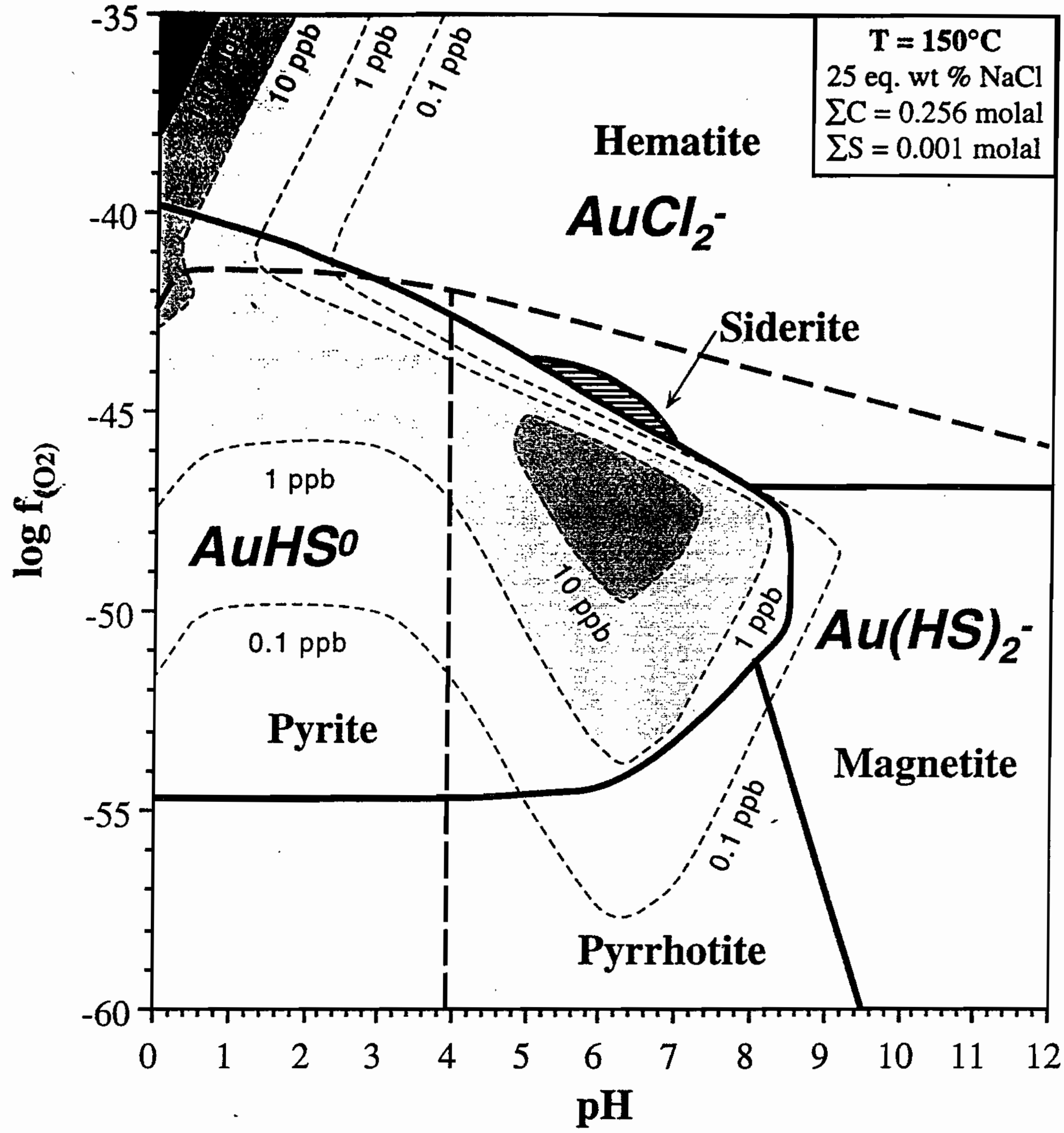

Figure 2: Log f_{O2}–pH diagram at 150°C showing the stability fields of the common Fe–O–S minerals and siderite, the predominance fields for $AuCl_2^-$, $Au(HS)_2^-$ and AuHS, and Au solubility contours. This diagram was drawn for a 25 eq. wt. % NaCl brine with ΣS = 0.001 molal and ΣC = 0.256 molal.

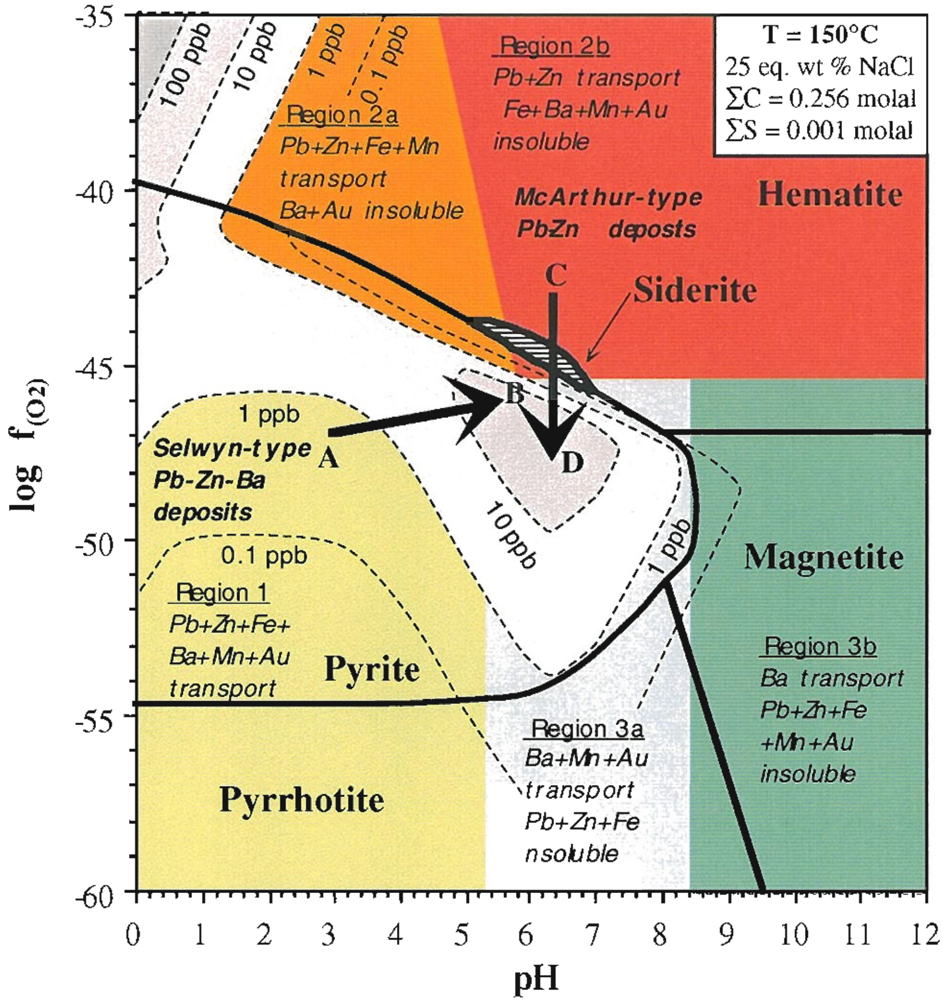

Figure 3: Log f_{O_2}–pH diagram at 150°C showing the stability fields of the common Fe–O–S minerals and siderite, the predominance fields for $AuCl_2^-$, $Au(HS)_2^-$ and AuHS, and Au solubility contours. This diagram was drawn for a 25 eq. wt. % NaCl brine with $\Sigma S = 0.001$ molal and $\Sigma C = 0.256$ molal. The coloured fields portray various sedimentary brine compositions defined by Cooke et al. (1995) and Cooke (1997). McArthur-type SEDEX deposits are believed to be precipitated from brines with compositions in region 2b. Selwyn-type deposits are believed to form from brines with compositions in region 1. Arrows A–B and C–D illustrate possible depositional trajectories for Selwyn- and McArthur-type fluids respectively.

Regional geophysics — Preliminary study and comments, Camooweal and Dobbyn

by David Leaman
CODES Special research Centre, Geology Department, University of Tasmania.

Summary

Regional interpretation of geophysical data has been largely restricted to the Dobbyn region pending completion of thesis studies in the Camooweal-Lady Loretta region. Sufficient analysis has now been completed, however, to show that structures and sequences within the Camooweal sheet are generally consistent with those previously described for the Mt Drummond and Lawn Hill areas. These structures and sequences are distinctive and unlike those exposed in the Dobbyn and Cloncurry regions.

This report presents a summary of preliminary findings only.

Previous work had suggested that the major mafic sequence interpreted across the region may be a correlate or extension of the Eastern Creek Volcanics and this appears to be confirmed. Felsic sequences were tied to exposure in the Scrutton Ranges or the Murphy Inlier and were generally assumed to be equivalent elsewhere. This work suggests that many parts of these may be extensions of the Leichhardt Metamorphics or Argylla Formation. The disposition of sequences, and their implied repetition on a regional scale, suggests gross east-facing over-thrusting has occurred within the eastern succession and that some younger west-facing thrusts may be present where the eastern and western sequences abut. The western sequence appears to have experienced less deformation on the basis of implied structural style and gross relationships.

Insufficient analysis has been completed to enable proper association of mineralisation to primary structures but it seems likely that most mineralisation in the eastern sequence may be linked to complex alteration zones which disrupt thick sequences and, in the western sequence, to significant distortions or breaks in structural continuity. Lady Loretta may be correlated with such a feature which has been concealed by the younger cover sequences.

Introduction

This brief report outlines the status of current progress of regional interpretation within the area covered by the Camooweal-Dobbyn-Cloncurry-Mount Isa 1:250 000 geological map sheets. The comments given here deal particularly with the Camooweal and Dobbyn sheet areas.

Sufficient analysis has now been completed in this difficult and complex geological environment to enable some important inferences to be made about structural regimes and bulk correlations — including some from exposure to concealed units defined by previous work in areas to the north.

Due to thesis obligations (e.g. Duffett, 1996) this review, as a continuation of previous regional studies, was first delayed and then deflected around the Camooweal sheet. This has meant a less than ideal approach from the previous data base and an involvement in the complex features of the exposed eastern sequence. This has caused further delay since the geophysical character of the eastern sequence is distinctive and its exposure forces distractive review of, apparently important, details. Fewer profiles have been examined (than is considered adequate for definition appropriate to the region or consistent with previous work) as a result and the results should only be considered indicative and preliminary at the present time. Many details remain for evaluation and this study seeks only to define first order or regional elements and relationships.

The premises upon which this interpretation has been founded have been outlined in previous reports and will not be described in detail here. They include

(a) a coarse sampling of regional gravity and magnetic data which is consistent with the definition of both the data bases and the requirements of the interpretation,
(b) use of rock properties which lie within observed ranges and which are credible estimates of fresh material,
(c) a methodology which is essentially two dimensional but which applies consistent criteria, base shift and source categorisation.

The work reported here, and which is continuing, will supersede that provided by Duffett (1996) and will extend the previous McArthur basin assessment to Mount Isa.

Comments on Duffett (1996)

1. Duffett (1996) noted that some conflicts appeared to exist between his work and earlier interpretations for this project. Such conflicts do exist but it is possible to demonstrate sequence and structural alternatives not considered by Duffett which are consistent with prior work and which resolve all the ambiguities raised by him (see below).
2. Duffett (1996) also comments that some data misfits may occur between map sheets and surveys. This is almost certainly the case. It is not possible to precisely define the amount of offset in each case due to the unfortunate conjunction between map or survey limit and major geological boundaries - especially that between the eastern and western sequences. Gravity data are not affected but it is not possible to match magnetic anomalies or field values around the edges of the surveys for the Camooweal, Dobbyn, Mount Isa and Cloncurry sheets without a mismatch of between 50 and 150 nT. This may be assigned to either contouring limitations and character at map edges or to base offsets fundamental to the surveys themselves. Since this latter data is still almost never acquired, noted or recorded it is likely that this is the origin of the problem in this older data.
3. Apart from the work of Duffett (1996) no previous study can be considered to be of relevant depth or comparability. Qualitative indications, which have formed the basis for most comment about this part of Australia (see Duffett, 1996 for references), are not necessarily valid due to the many interfering variables involved.
4. Rock property assumptions and evaluations are critical to all interpretations. Some property assumptions used for earlier phases of this project have been challenged but comparison of Duffett's Figures 7 and 8 (and all values supported by fresh samples, not surface affected, altered or weathered) indicates that the gross assumptions applied for previous work have not only been reasonable but possibly conservative. Mine studies near Mount Isa have been distorted by the local data base which is largely derived from mineralised or altered samples - especially of the volcanics. These values should not be used in any assessment of regional properties. Nor should any artificial correlations influence judgments about properties. Previous work has defined deeper units which are denser than background and also modestly magnetic and these have been termed 'felsics'. The correlation has depended upon association with exposures within the Scrutton Ranges and near the Murphy Inlier even though there may be considerable variation within the exposed rocks. The present work suggests that a further sequence may account for some of the deeper, moderately magnetised units (below).
5. The initial Camooweal interpretation provided by Duffett (1996) involves neutral base shifts, omission of some units (e.g. felsics, Leichhardts/Argyllas) on the basis of poor resolution, and possible crustal thickness changes. Some features were not explained using the materials thought to be at hand (e.g. line 091).

Interpretation

Most recent review has been focussed on the rocks of the Dobbyn and north Cloncurry regions with some longer regional extensions into the Camooweal region in order to avoid conflicts with other workers (notably Duffett). Only four profiles are presented here. These are samples which suggest the nature of structuring within the eastern sequence of the Dobbyn region and of the relationship between the eastern and western sequences between 19° and 20° south latitude. Two profiles provide a complete cross section of both the Camooweal and Dobbyn map sheets and one provides a direct tie to previous analysis reported for this project.

Line A: (Line 144). Figure 1. At 19° South.

The western half of the model can be compared directly with previous work (the eastern half of line 101) and shown to be fully compatible and consistent in structural style and thickness pattern for the sources resolved. Minor depth changes have been enforced due to implications and effects derived from the units of the eastern succession. The direct linkage from previous interpretations to the northern part of the Camooweal region and to the western part of the Dobbyn region implies that much (perhaps most) of the material previously described as felsics may be correlated with, or actually be, extensions of the Leichhardt Metamorphics or the Argylla Formation. Although these suites do have different properties they are not easily resolved at this scale or level of analysis.

The model does show, however, that no special pleading is required to generate a reasonable solution. Satisfactory gravity and magnetic balances are possible within the constraints of probable rock property ranges and that there is scope for further adjustment without forcing either observed data set (see general concluding comments below).

Line B: (part of line 143). Figure 2. At 19.25° South.

This profile provides some detail within the Dobbyn region and illustrates some of the possible internal character and relationships. Some magnetic properties, consistent with limited drilling and sampling beneath the Cretaceous to Recent cover, are extreme. The solution shown in Figure 2 implies detachment of the Naraku Granite but other options are feasible within the base shift allowance indicated in the data sets. Inclusion of additional units, such as the Myally Formation, at the western end within the folds mapped would improve the gravity fit.

Line C: (Line 142). Figure 3. At 19.5° South.

This model presents a further regional cross section of both the Camooweal and Dobbyn regions. Much of the western half of this section may be directly compared with line 091 of Duffett (1996). It is essentially parallel to line 091 and only a few kilometres south of it. Most anomaly forms can be recognised on each profile.

Duffett (1996) provided two alternative models for line 091 and suggested that they were either not compatible with realistic properties or not consistent with previous concepts and patterns. The problem was not resolved.

Figure 3 provides an additional solution which is both consistent with previous basin studies (compare Figure 1) and satisfies both gravity and magnetic fields without strain on property or unit relationship assumptions. The model demonstrates that it is possible to satisfy the magnetic field in the western half of the Camooweal sheet using a relatively small volume of material with properties consistent with those of the Eastern Creek Volcanics and, further, that this material can be traced across section to outcrop of these rocks. What has not yet been established beyond reasonable doubt is the depth to the upper surface of these rocks. The model suggests an upper surface depth of about 1000 m and a variable thickness not exceeding 1400 m. These values could be consistent with the findings of well Morestone #1 and the limit reflections considered to be derived from depths of no more than 3000 m (see Duffett, 1996). The change in reflection character could be consistent with a thick, homogeneous underlying unit (perhaps a correlate of the Mt Guide Quartzite) or granite. The model allows either of these possibilities.

The principal problem with the present model is its simplicity. Some other alternatives do exist for possible negative (density) contrasts and these might displace some of the granitoids currently defined by the model. Inclusion of McNamara Group, Myally Sub Group and Leander/Mt Guide Quartzite would add a significant degree of freedom to the gravity interpretation and generate much more comfortable fits. The magnetic interpretation, which is critical to

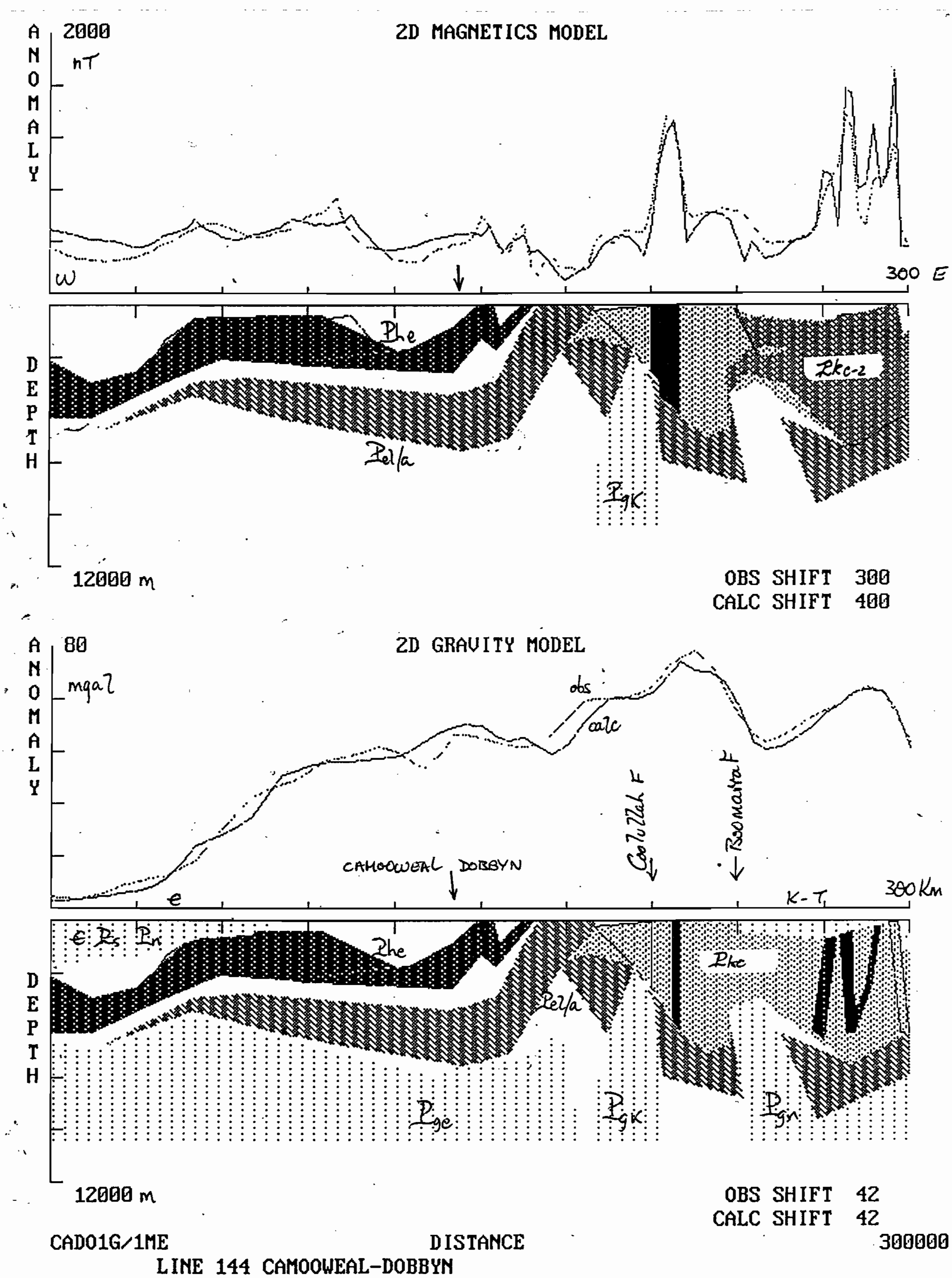

Fig 1. Line A (144) at 19° south.
Proterozoic symbols: kc Corella Fm and variations labelled 1 and 2; hm Myally Sub Gp; he Eastern Creek Volcanics; el/a Leichhardt Metamorphics/Argylla Fm; ge, gk, gn - Ewen, Kalkadoon, Naraku Granites; s, m - Sth Nicholson, McNamara Gps; E-K-T, Cambrian-Cretaceous-Tertiary cover. Not all variations within kc, el/a are labelled in these diagrams. Background in all sections (no pattern) indicates a bulk density of about 2.74 t/cu m and a susceptibility of 0.0.

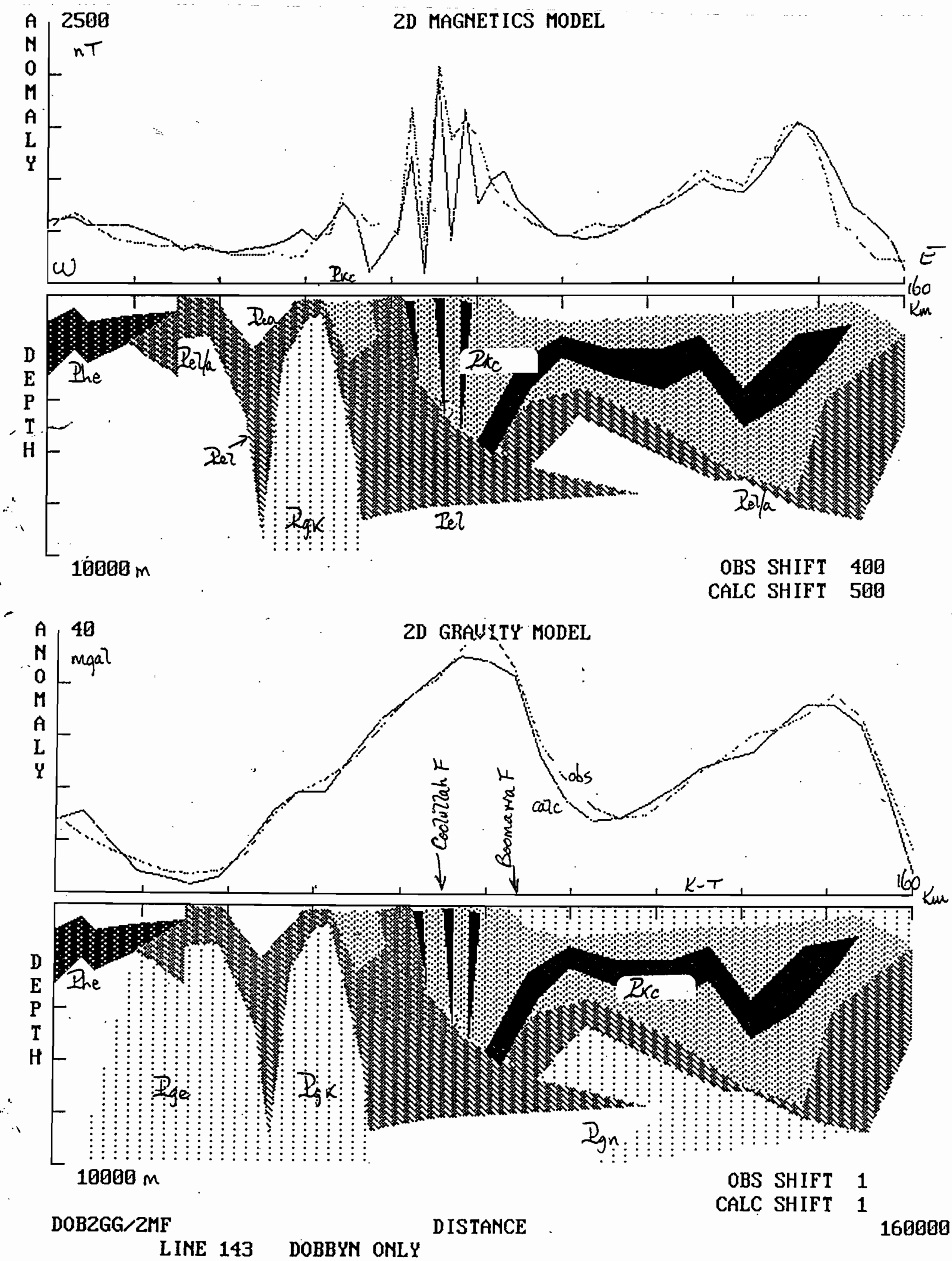

Fig 2. Line B (143 part) at 19.25° south.
Symbols as for Fig 1. Note implied east-facing detachment which is distinct from surface fault indications.

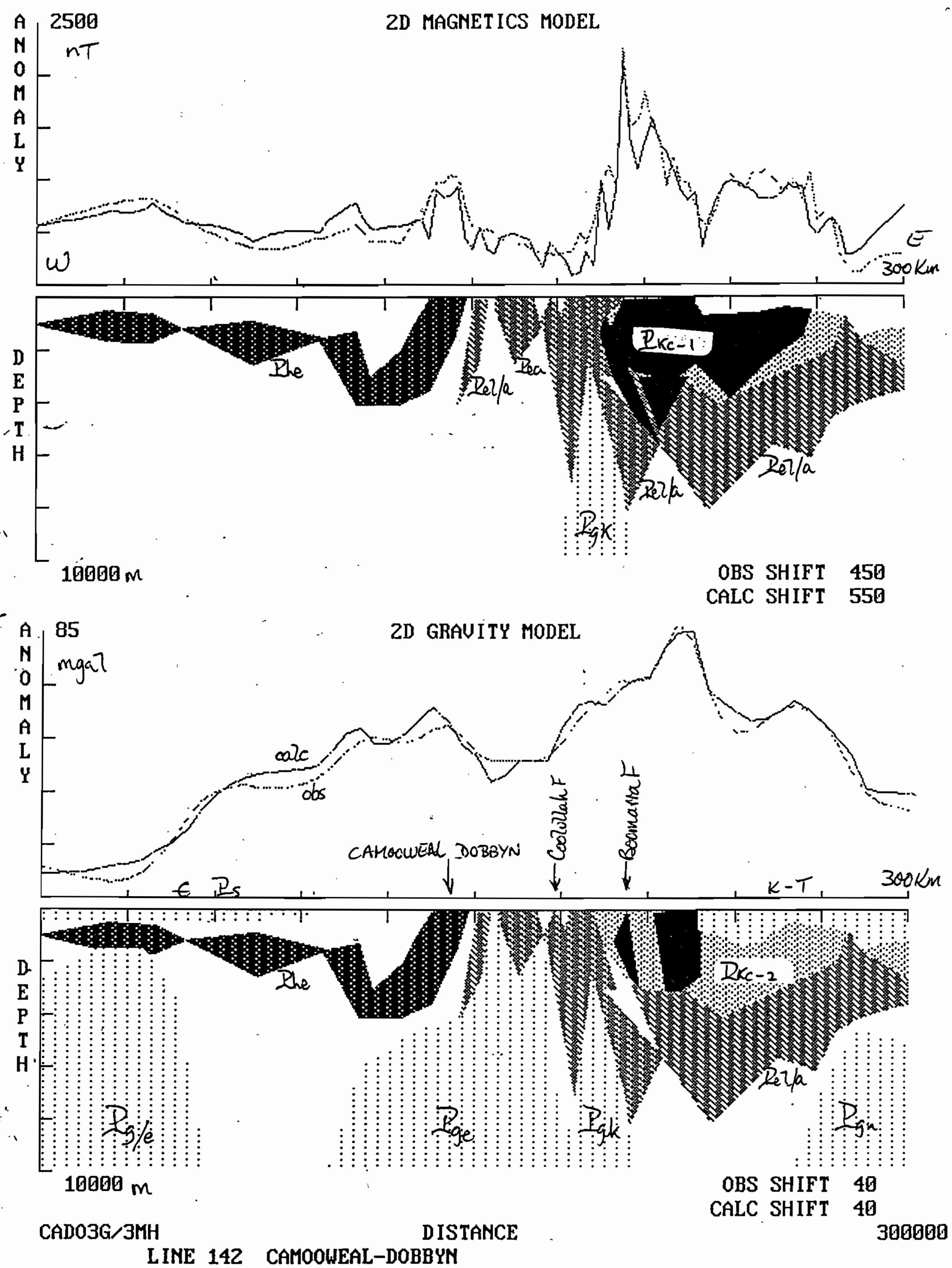

Fig 3. Line C (142) at 19.5° south.
Symbols as for Fig. 1..

the definition of relatively shallow structure, would be unaltered. This freedom shows that the problem described by Duffett does not exist. Inclusion of a variable such as crustal thickness is possible but certainly not necessary. It these sources of variation are accepted then it is possible to modify the depth of the volcanics near the western end of the model and to vary their thickness as well.

The disposition of units within the geological section and extraction of a valid geophysical solution cannot be completed until more profiles have been analysed and tied to relevant exposures within the Mount Isa area. Comparable issues were described and resolved for the area near Mt Young where these involved the Yiyintyi Sandstone (Leaman, 1992).

The model does not sample the structures and mineralisation of the Lady Loretta area but the large fold and change in character near 110 km is along strike. The Mammoth mineralisation may be related to structures on the eastern limb of this major deformation. More work is required before any detailed relationships can be suggested.

Line D. (Part of Line 141). 19.75° South. Figure 4

This model provides further details about possible relationships within the Dobbyn region. The solution provided does indicate that the eastern succession is dislocated and detached.

Although the models presented are samples and far from complete they do allow some important conclusions to be drawn.

(a) The eastern sequence is very much denser and much more magnetic overall than the western sequence. It may also be much thicker as a package.
(b) The granite content of the two terranes is also very different. Only the Naraku Batholith is a significant body in the eastern region wherease granites may form a large part of the basement in the western region.
(c) Mass differences between eastern and western areas can be explained in terms of rocks known to occupy the upper crust and do not need to be explained by changes in crustal thickness. It is difficult to find evidence for these in extant seismic data (e.g. Duffett, 1996, Fig . 5).
(d) Large portions of the eastern sequence may be stacked and repeated by east-facing thrusts.
(e) Very few zones can be defined which are magnetically anomalous within the eastern sequence since so much material is abnormal. Those zones which can be recognised are very localised, and have sub vertical easterly dips.
(f) The western sequence is more gently folded but may include west-facing thrusts in the region where the sequences abut. It is possible that these are younger structures given the implied relationships.

Other comments

In the three to five years since earlier work on regional interpretation was reported for this project others have had opportunity to review, check model or appraise the solutions offered. Although there has been negligible feedback some critical comments have been made. Most of these comments are grounded in a misunderstanding of the aims and assumptions of the original work.

Those critical of the basin scale modelling undertaken for this project should

(a) present quantitative sets of models and solutions to demonstrate that concepts and solutions have been omitted or overlooked. These alternatives must comply with the evaluation criteria defined by Leaman (1994) at very least.
(b) understand that the models provided were primary, indicative and regional and generated in the belief that they would be reworked, normalised and reviewed at a later stage in the project. It was originally thought that the study would be restricted to the "Batten Trough" area. Instead, the set was expanded to cover most of the southern part of the basin rather than be reviewed and revised. Surprisingly, however, the growing set of models has been found to be consistent (with minor discrepancies) and to satisfy near outcrop or outcrop constaints where these exist. This suggests either that the entire model set is suspect or that it is grossly valid.
(c) appreciate that the models are regional and were never intended to provide detailed descriptions of any area. The original intention was to use

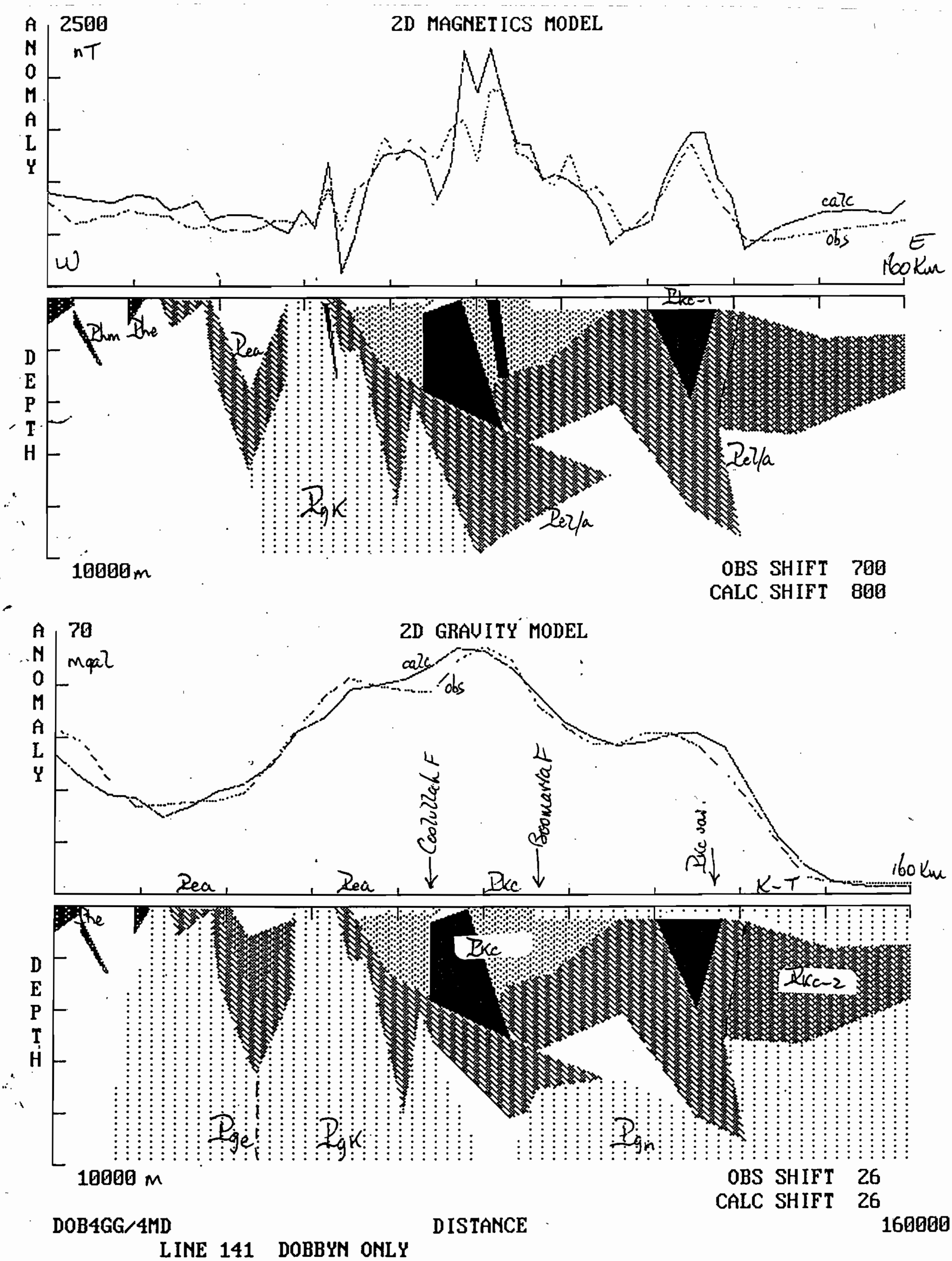

Fig 4. Line D (141) at 19.75° south.
Symbols as for Fig 1. Major east-facing detachment indicated with a much thinner and simpler Corella sequence beneath cover. Differences in Corella Formation rocks reflect changes in magnetic properties rather than density variations but some combinations of changes are involved.

them to provide a regional setting for smaller, detailed assessments. (These have not been requested.) Consequently, no fine details have ever been included in the models and structural styles and relationships have been reviewed at basin scale. Data fits have been made on this basis and observed data has been sampled relatively coarsely (usually consistent with the quality and nature of the available regional data sets).

(d) ensure that any comparison of old and re-calculated models or profiles be valid. This means that observed field and model detail should be consistent. Chalk should be compared with chalk. In addition valid comparisons and judgments require that profiles be in the same place, and that similar properties, surface weathering or depth assumptions, and base levels have been included.

(e) appreciate that discrepancies may well exist in various magnetic solutions if much higher frequency sampling is employed either in the observed profile or under calculation. Many of the magnetic data sets made available as a basis for the original work certainly did not justify sampling at intervals less than one to three kilometres when not actually aligned along a flight path. In any case, high frequency components can be positive distractions when data is reviewed as part of regional basin analysis. All gross, deep or regional forms generating longer wavelengths have been fully compensated in the models.

(f) report their contradictory findings for discussion so that all may benefit from both the original work and the implications of any changes. If this cannot be done then the criticism should be muted since no viable response or discourse is possible.

References

Duffett, M., 1996. Regional geophysics - Camooweal map sheet. AMIRA/ARC project P384A, Report 2, Oct.

Leaman, D.E., 1992. Regional geophysics - basin architecture. AMIRA/ARC project P384, Report 1, Nov.

Leaman, D.E., 1994. Criteria for evaluation of potential field interpretations. First Break, 12 (4), 181-191.

Appendix

GOLD IN AUSTRALIAN LATE PALAEOPROTEROZOIC STRATIFORM SEDIMENT-HOSTED ZINC-LEAD-SILVER DEPOSITS

Peter McGoldrick[1], Reid Keays[2], Rob Smith[3], Gordon McOrist[4] and John Fardy[4]
[1]CODES/Geology, University of Tasmania, PO Box 252C, Hobart, Tas., 7001
[2]Faculty of Science and Engineering, Laurentian University, Ramsey Lake Rd, Sudbury, Ontario, [illegible] Canada
[3]Western Mining Corporation Ltd., Olympic Dam Operations, PO Box 150, Roxby Downs, S.A., 5725
[4]ANSTO, Environmental Science Program, Lucas Heights Research Labs, New Illawarra Rd, Lucas Heights, NSW, 2234

The gold contents of ores, pyritic and barren host sediments, and some more distal barren host rocks from the stratiform sediment-hosted (SSH) deposits at Mount Isa, Lady Loretta and HYC deposits have been measured by radiochemical neutron activation analysis.

Zinc-lead-silver ores contain, on average, 2.0 parts per billion (ppb), 2.2 ppb and 5.1 ppb gold, at Mount Isa, Lady Loretta and HYC, respectively. Pyritic shales and siltstones contain 2.1 ppb, 0.9 ppb and 6.2 ppb gold, and barren (low sulfide) shales and siltstones contain 0.6 ppb, 0.4 ppb and 1.7 ppb gold. These are remarkably low gold levels, both in terms of absolute gold tenor and the proportion of gold compared to base metals in the ores. For instance, Shaw et al., (1976) estimated that "average continental crust" contains 1.8 ppb gold and 52000 ppb zinc (zinc:gold ratio of 29,000:1). Unmineralised fine grained clastic sedimentary rocks contain between 1 and 5 ppb gold (Glasson and Keays, 1978; Crocket and Kuo, 1979) and between 40,000 and 200,000 ppb zinc (zinc:gold ratios between 8000 and 200,000:1). By contrast, ores from the three stratiform sediment-hosted deposits have zinc:gold ratios are between 1 million and 50 million.

The low gold tenor in the SSH deposits can be explained in two ways. Either, the ore forming fluid carried very little gold (and had a base metal:gold ratio >> typical crustal ratios), or, the fluid did contain some gold but this gold was not precipitated at the site of base metal sulfide precipitation. The former explanation is preferred because in the latter case, special pleading is required to either, very efficiently remove gold from solution before the base metals, or, to keep the gold in solution during base metal sulfide precipitation. Neither scenario is considered geologically or geochemically likely.

A base metal sulfide ore-forming fluid containing very little gold that is at, or near, saturation in base metals and gold, has important implications for the physico-chemical character of the mineralising fluid in Australian SSH deposits. In order for saline hydrothermal fluids to have low gold solubilities they must be either cool and oxidised, or very reduced. Cool, oxidised saline fluids are excellent base metal solvents, whereas reduced fluids must be hot (>> 200°C) in order to carry base metals. There is no direct evidence (e.g. fluid inclusion data) for the temperature of formation of Australian Palaeoproterozoic SSH zinc-lead-silver deposits, but, the lack of obvious hydrothermal alteration or feeders to the deposits, and the shallow sedimentary setting of some deposits precludes high-temperature fluids. Hence, cool (<<200°C) and relatively oxidised ($SO_4^{2-} >> H_2S+HS^-$) are the likely mineralising fluid in the northern Australian deposits. This conclusion has important implications for the ore deposit models used in exploration for this important class of deposit.

REFERENCES

CROCKET, J. H., & KUO, H. Y. 1979. Sources for gold, palladuim and iridium in deep-sea sediments. *Geochimica et Cosmochimica Acta* **43**, 831-845.
GLASSON, M. J., & KEAYS, R. R. 1978. Gold mobilisation during cleavage development in sedimentary rocks from the auriferous slate belt of Central Victoria, Australia: Some important boundary conditions. *Economic Geology* **73**, 496-511.
SHAW, D. M., DOSTAL, J., & KEAYS, R. R. 1976. Additional estimates of continental surface Precambrian shield composition in Canada. *Geochimica et Cosmochimica Acta* **40**, 73-83.

Acknowledgements: This work was made possible through ARGC, ARC and AINSE grants to RRK over many years, and AINSE Grant 93/044 to PMcG. MIM Ltd and Pancontinental Mining provided access to the Mount Isa, HYC and Lady Loretta deposits.

GEOLOGICAL SOCIETY OF AUSTRALIA, ABSTRACTS No. 41
13th Australian Geological Convention, Canberra, February 1996

PROTEROZOIC STRATIFORM SEDIMENT-HOSTED ZN-PB-AG DEPOSITS

Peter McGoldrick and Ross Large
CODES SRC
University of Tasmania
PO Box 252-79 Hobart, Tas. 7001

IN PRESS

AGSO JOURNAL OF GEOLOGY & GEOPHYSICS 50TH ANNIVERSARY VOLUME

Exploration Model
Stratiform Sediment-hosted Zn-Pb Deposits

Examples: Mount Isa Pb-Zn-Ag, Hilton, George Fisher, Century, Lady Loretta, HYC, Dugald River (Sullivan, Red Dog, Selwyn Basin deposits, Rammelsberg, Meggen)

TARGET

- Large deposits are characteristic (average for Australian deposits is about 100 Mt at >> 10wt% Zn+Pb
- May contain structurally controlled higher grade zones (> 25wt% Zn equivalent)
- Zn/(Zn+Pb) ratios vary between about 40 to more than 90
- Often with high Ag credits (e.g. Mount Isa 150ppm, HYC 60ppm)

MINING AND TREATMENT

- Tabular form and uniform grades allow relatively easy assessment and mining
- Some fine grained ores create treatment difficulties
- Coarser (metamorphosed and/or recrystallised) ores are easier to treat
- Smelter penalties can be a problem due to high, but variable As, Sb, Bi, Cd, Hg, In and Tl
- Mn in soloid solution in sphalerite can cause treatment problems (e.g. Dugald River)

HYC GEOLOGY 182900N (from Hynman et al., 1995)

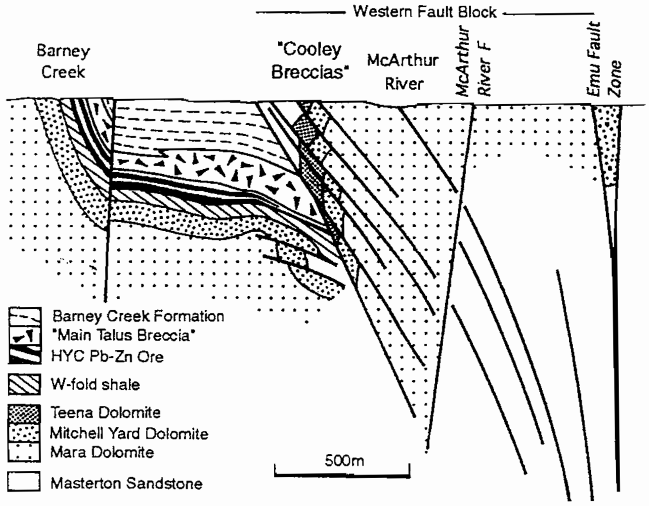

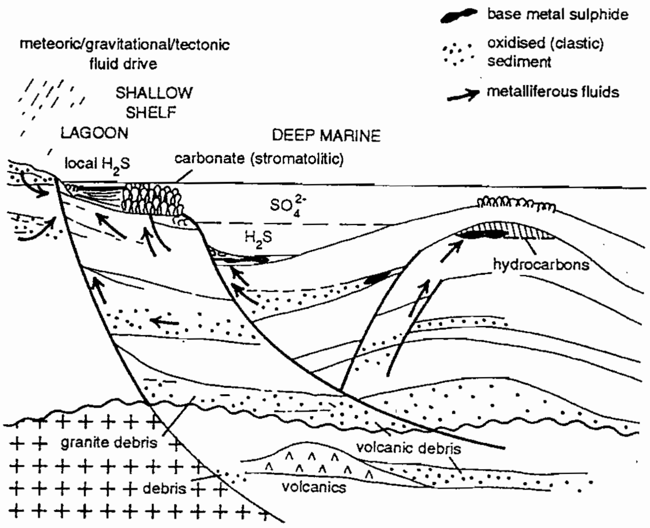

REGIONAL GEOLOGICAL CRITERIA

- Intracontinental rift or rifted margin (marine) basins
- Unmetamorphosed to greenschist-amphibolite transition
- Continental basalts and felsic volcanics and intrusives form an important part of the underlying (older) rift fill
- Diverse sedimentary host lithologies deposited in terrestrial, peritidal and deep marine settings; in part evaporitic; includes black, grey, brown and red rocks
- All major deposits lie within a few kilometres of major long-lived regional scale fault systems (e.g. Emu Fault, Mount Isa Fault, Termite Range Fault)
- Regional host sequence is often the latest sag phase fill of a series of rift-sag cycles
- Most (possibly all) Australian deposits are in rocks between 1660 and 1590 Ma old

MINERALISATION FEATURES

- Stratiform (stacked) lenses are common
- Individual lenses have a sheet-like aspect ratio
- Base metal sulfides are interbedded with, and form impregnations in clastic sedimentary layers
- Pyrite is abundant in most deposits, but in detail there is no simple relationship between pyrite and base metal sulfide abundance
- Pyrrhotite is only common in metasomatised/metamorphosed deposits (e.g. Mount Isa)
- Wide range of Zn/(Zn+Pb), but most deposits and most parts of individual deposits Zn>Pb
- Only minor Cu (500 to 5000 ppm)
- Weak (Cu) > Pb > Zn zonation in some deposits
- Barite is usually not present (Lady Loretta is an exception)

ALTERATION

- Footwall alteration ('feeder') pipes are not recognised in Australian deposits' but are known from overseas examples (e.g. Rammelsberg)
- Neomorphic Ca,Mg,Fe,Mn-carbonates are present in the host rocks (i.e. interore beds, hangingwall and footwall sediments)
- Fe and Mn content of the host carbonates increase toward ore lens in some cases (e.g. HYC - Lambert & Scott, 1973; Lady Loretta - McGoldrick et al., in prep.).
- Halo of sideritic carbonate may surround ore lenses (e.g. Lady Loretta and Century)
- In low metamorphic grade deposits, the organic matter associated with the ores is more thermally mature than organic matter in surrounding host rocks

SURFICIAL GEOCHEMICAL CRITERIA

- All Australian deposits (except George Fisher) crop out at the surface and (with the exception of Century) have (or had) prominent gossans
- Rock chip and soil samples from the vicinity of all deposits return anomalous base metal values
- Soil geochemistry (Pb, Zn) has assisted in targeting drilling

LOCAL GEOLOGICAL CRITERIA

- Host sediments and ores are essentially co-eval in most deposits i.e. syngenetic (exhalative) or early diagenetic timing for the introduction of base metal bearing fluids (Century may be an exception)
- Host rocks are carbonaceous and/or pyritic black and grey (dolomitic) siltstone, mudstone and shale, often with a significant clastic carbonate (dolomite) component i.e. the most 'reduced' parts of the local sequence
- Turbidite and/or tempestite facies are commonly present
- The water depths under which the sediments were deposited is different in different deposits (shallow/emergent to sub-photic zone and sub-storm wave base)
- Course grained debris flows (breccias) in some deposits indicate local syn-sedimentary faulting
- Fine grained tuffaceous component is the only indication of (distal) co-eval volcanic activity

DEPOSIT GEOCHEMICAL CRITERIA

- Host sequences are anomalous in Zn, Fe, Mn and Tl
- Fe and Mn content of carbonates in host sediments increases towards ore lenses in some cases (e.g. HYC — Lambert & Scott, 1973; Corbett et al., 1973)
- Ores contain high, but variable, Ag, As, Sb, Bi, Cd, Hg, In and Tl, but very low Au
- Se, low; S/Se ratios base metal sulfides and pyrite are high
- Sulfur isotope signatures of base metal sulfides and pyrite are heavy and highly variable within and between deposits
- Lead isotopes in the ores are (mostly) non-radiogenic and have model ages consistent with the ages of the host sequences

GEOPHYSICAL CRITERIA

- Processed regional potential field data can be used to define basement structures, basin margins, the nature and thickness of basin fill (depocentres) and other (?syn-sedimentary) structures
- Density contrast between ores and host rocks may be recognisable from detailed gravity surveys
- Ores are generally poor electrical conductors and non-magnetic (pyrrhotite-bearing ores are an exception)
- Airborne and ground electromagnetic surveys can locate carbonaceous and pyritic sedimentary host facies

FLUID CHEMISTRY AND SOURCE

- No direct evidence from fluid inclusions is available for the Australian deposits
- Indirect evidence from fluid modelling, Au geochemistry, O isotopes, and (possible) ore fluid aquifer characteristics indicates base metal transporting fluids were:
  - High salinity (5-25wt% NaCleq)
  - Low to moderate temperature (100 – 200°C)
  - Wealy oxidised ($SO_4^{2-} >> H_2S$)
- Base metal fluid source was basinal brines
- Thermochemical or biogenic
- Metal sulfide deposition was due to reduction of brine SO_4^{2-} and/or addition of biogenic H_2S

COMMENTS ON GENESIS

The older, conventional model for these deposits invokes an exhalative process and a syngenetic timing for their formation in which sulfides accumulated as (chemical) sedimentary layers at the sediment-water interface (Stanton, 1973). Mineralising fluids were thought to be relatively hot and reduced i.e. they carried all the ingredients required to precipitate pyrite and base metal sulfides contained in the orebodies (Russell et al., 1980). However, textural, sedimentological and isotopic evidence from some deposits (notably HYC — Williams, 1978a&b, Rye and Williams, 1981, Logan 1979, Eldridge et al., 1993; Hynman et al., 1996) was used to support a model in which base metal sulfide mineralisation formed within the unconsolidated sediments during diagenesis and in which significant amounts of pyrite forms independently of the base metal sulfides. The genetic model presented here has some elements of both earlier models, but an important difference is that cool, oxidised fluids are invoked as the likely base metal transporting fluids (McGoldrick & Keays, 1990; Cooke et al., in prep.).

Oxidised fluids moving through or out of the sediment pile will precipitate base metal sulfides if their dissolved sulfate undergoes reduction to sulfide, or if they encounter another source of reduced sulfur. This could happen in a variety of ways:

- exhalation into an anoxic and/or organic matter-rich water body (e.g. HYC, part of Lady Loretta)
- reaction between transient oxidised brines and organic matter or diagenetic Fe sulfides in porous sediments in the shallow sub-surface prior to significant burial (e.g. part of Lady Loretta)
- reaction between transient oxidised brines and organic matter accumulations (?petroleum) in the deep sub-surface (e.g. Century).

An alternative model, developed for the Mount Isa Zn-Pb-Ag deposits, suggests they formed by hydrothermal replacement of lithified and deformed pyritic sedimentary rocks (Grounjis and Schouten, 1937; Perkins, 1990; Laing, 1990; Myers et al., 1996). This model cannot be extended to less deformed and unmetamorphosed deposits elsewhere.

INTRODUCTION

Late Palaeoproterozoic rocks in north west Queensland and the Northern Territory (the 'Carpentarian Zinc Belt' of Sweet et al., 1993 – Fig. 1) host five world class stratiform sediment-hosted Zn-Pb-Ag orebodies (Mount Isa, Hilton, George Fisher, Century and HYC) and two smaller (but significant) deposits (Lady Loretta and Dugald River). The gossanous outcrop of the Mount Isa Zn-Pb-Ag lodes was found in 1923 by Campbell Miles, a prospector. However, since World War 2, geologically-based exploration by mining companies has resulted in a significant discovery in every decade except the 1970s. These were the Hilton deposit at MIMs' 'Northern Leases' in 1948, HYC in 1956, Lady Loretta in 1966, Hilton North (now renamed George Fisher) by MIM in the early 1980s, and Century in 1990. All these deposits had gossanous outcrop or, in the case of Century, a strong soil geochemical signature. No world class deposits are known from other Australian Proterozoic sedimentary basins.

Discoveries in the Carpentarian Zinc Belt during the last decade (e.g. Century, George Fisher and Grevillea) hold promise for new major deposits in this region and in similar Proterozoic sedimentary basins elsewhere. The following discussion emphasises geological and geochemical features relevant to understanding ore genesis and developing better exploration models.

MAIN FEATURES OF THE DEPOSITS

The important geological features of the Carpentarian Zinc Belt deposits are summarised on Table 1. The deposits comprise multiple or single lenses of laminated to massive sphalerite, galena, Ag-bearing sulphosalts and pyrite. In the larger deposits the mineralisation has sheet-like aspect ratios and consist of multiple stacked lenses with individual lenses up to several hundred metres in diameter and several tens of metres thick. At Mount Isa more than thirty Zn-Pb-Ag ore lenses are present in the upper 650 metres of the Urquhart Shale Member of the Mount Isa Group; at McArthur River the HYC mineralisation occurs as seven ore lenses in 80 metres of the Barney Creek Formation and at Century there are two mineralised zones in a forty metre thick sequence of Member 4 of the Lawn Hill Formation.

Geological setting

The immediate host lithologies to all the Carpentarian Zinc Belt deposits are fine grained carbonaceous (i.e. organic matter-rich) siltstones and shales, however, local and regional facies relationships for individual deposits indicates a wide variety of sedimentary settings. For instance, the Lady Loretta host sequence is thought to have been deposited in a shallow, evaporitic, restricted water body in a partly emergent carbonate shelf (Dunster, 1996; McGoldrick et al., 1996). By contrast, sedimentological and geochemical halo features in the Barney Creek Formation can be traced more than twenty kilometres from HYC and indicate a substantial water body existed at the time of mineralisation (Bull et al., 1996; Large et al., 1996). Furthermore, the Barney Creek Formation is thickest at HYC and the mineralised sequence was probably deposited in the most rapidly subsiding (and deepest?) part of an elongate graben adjacent to the Emu Fault Zone (Neudert and McGeough, 1996). Microfossils from the ore sequence indicate deposition below the photic zone (Oehler and Logan, 1977). At Mount Isa, Neudert (1983) interpreted the Urquhart Shale, a dolomitic, pyritic, carbonaceous siltstone, as a ('deeper-water') shelf-slope facies of a large perennial lake. In contrast, the Lawn Hill Formation, host to Century, is a siliciclastic-dominated sandstone-mudstone unit deposited in a mid to outer shelf or deeper (marine) setting (Andrews, 1996).

Sedimentary breccias at HYC (Walker et al., 1977) and Walford Creek (Rohrlach et al., 1996) indicate local syn-sedimentary faulting contemporaneous with deposition of the mineralised sequences. These faults may have been conduits for mineralising fluids (Williams, 1978a; Rohrlach et al., 1996). Other deposits (e.g. Mount Isa, Century) are close to major regional faults, but, the host rocks do not contain sedimentary facies consistent with nearby syn-sedimentary faulting. These regional structures may have exerted fundamental control on early basin architecture and later basin inversion, and hence have been important in controlling (or focusing) hydrothermal fluid flow.

Deformation and metamorphism

All the deposits have been deformed, but the intensity of deformation varies greatly between deposits. High metal grade zones in some deposits may be due to deformation effects. Syn-sedimentary deformation of unconsolidated ores is recognised at HYC (Hinman, 1995); and late brittle structures disrupt both HYC and Century (Coutts, 1996; Waltho and Andrew, 1993; Waltho et al., 1993). Although some galena and sphalerite at HYC and Century show indications of recrystallisation, much of the mineralisation preserves primary depositional textures (Broadbent and McKnight, 1993; Eldridge et al., 1993; Hinman, 1996; Large et al., 1996). In other deposit, fine grained pyrite retains primary textures but the base metal sulphides are mostly recrystallised. The Dugald River Main Lode, a shoot-like body of slate-sulphide breccias up to 30 metre thick, is interpreted to have formed during folding by remobilisation of lower grade mineralisation (Newbery et al., 1993). The highest grade parts of the Lady Loretta orebody are strongly deformed and form the 'keel' of a canoe-shaped orebody corresponding to the hinge of a local D_2 syncline (Hancock and Purvis, 1990; Aheimer, 1994). The highest grade parts of the Hilton orebodies are also display strong structural control (Valenta, 1994). The Mount Isa orebodies occur in the west limb of a regional upright D_2 anticline and galena-rich ores show spectacular smaller scale disharmonic folds. These folds are tectonic and formed in response to D_2 and D_3 deformation (McClay, 1979).

Century and HYC are essentially unmetamorphosed, although slightly higher organic matter maturity in the immediate vicinity of HYC suggests a local thermal perturbation (Crick, 1992). Although a spaced axial plane cleavage is present in more argillaceous host rocks at Lady Loretta, peak metamorphic conditions are not constrained, but was probably sub-greenschist grade. The host sequences at Mount Isa (and Hilton) are generally ascribed a lower greenschist metamorphic grade on the basis of mafic mineral assemblages in older metavolcanic rocks near the mine, and phyllosilicate minerals in the Urquhart Shale. However, the metavolcanics are in fault contact with the Urquhart Shale, and 'metamorphic' phyllosilicates in the mine may be products of mineralisation-related hydrothermal alteration (Finlow-Bates and Stumpfl, 1979). Some phyllosilicate-rich zones can be related with certainty to the silica-dolomite metasomatic process (Swager et al., 1987; Waring et al., this volume). The Dugald River deposit has been metamorphosed at upper greenschist to lower amphibolite grades (Newbery et al., 1993).

Timing of mineralisation

Timing of the formation of the base metal sulphides in Carpentarian Zinc Belt deposits has been a major point of contention. The Mount Isa lodes were originally interpreted as hydrothermal replacement deposits (Grondijis and Schouten, 1937; Blanchard and Hall, 1942), but with the acceptance of syngenetic concepts in the fifties and sixties Mount Isa (and HYC) were re-interpreted as syngenetic-exhalative deposits (Murray, 1961; Stanton, 1962; Croxford, 1962; Mathias and Clark, 1975). The first descriptions of the HYC mineralisation assumed a syngenetic-exhalative origin for the deposit (Croxford and Jephcott, 1972; Lambert, 1976). Later, Williams (1978a&b) used textural and geochemical evidence from HYC and nearby minor deposits (Ridge and Cooley) to suggest that the HYC mineralisation formed some unspecified distance (centimetres? decimetres? metres?) below the sediment-water interface, from fluids sourced from the direction of the Emu Fault Zone. He argued that the formation of the HYC stratiform mineralisation was an epigenetic process (using the definition of 'epigenetic' proposed by Tourtelot and Vine (1976)). Nevertheless, the timing of formation of base metal sulphides was broadly 'syn-sedimentary' (i.e. early to late sedimentary diagenesis before lithification and porosity occlusion). Detailed textural and structural studies by Hinman (1995,1996) demonstrate that the bulk of base metal mineralisation was present in the sequence before consolidation of the Barney Creek Formation muds, and he favours a replacement process occurring at a shallow depth below the basin floor to account for the base metal sulphide and pyrite textural relationships. Recent re-interpretation of these textures by Large et al.(1996) as a 'layer by layer' paragenesis suggests individual base metal sulphide -rich bands formed at the sediment-water interface, hence, mineralisation may again be termeded to be 'syngenetic-exhalative' in origin.

The Lady Loretta deposit is hosted by sediments deposited in a shallow to emergent restricted (lagoonal?) setting (Dunster, 1996) and mineralisation probably formed both in the water column and in the shallow sediment subsurface by replacement and porosity infilling (McGoldrick et al., 1996) . Sulphur isotopes data (Carr and Smith, 1977; McGoldrick, unpublished data) suggest that large amounts of reduced S was generated by biogenic and/or thermochemical sulphate reduction processes associated with oxidation of reactive carbonaceous matter. High organic C contents preserved in fine grained host rocks to the Lady Loretta deposit indicate sedimentary-diagenetic environment at contained abundant reactive carbonaceous matter.

By contrast, at the Century deposit Broadbent et al. (1996) describe metal zoning, distinctive ore textures, and an intimate association of base metal sulphides with degraded hydrocarbons that they argue indicates mineralisation formed in the deep subsurface during late diagenesis due to the interaction of separate sulphate- and base metal-bearing fluids. The hydrocarbons were thought to be generated *in situ* from organic matter deposited with the siltstones, and the mineralisation event coincided with the onset of basin inversion.

Neudert (1983, 1984) argued on sedimentological and textural grounds that the Mount Isa Zn-Pb-Ag ores formed below the sediment-water interface after early diagenesis of the Urquhart Shale. Evidence presented included the observation that siltstones with early carbonate cements are unmineralised, and base metal sulphides occur preferentially in coarser grained, current deposited, beds.

A radically different genetic model for Mount Isa Zn-Pb lodes extends Perkins (1984) syntectonic-model for the Mount Isa Cu deposits (Waring et al., this volume) to include the Zn-Pb-Ag ores. Perkins (1990, 1995), Laing (1990) and Myers et al., (1996) argue that the Zn-Pb-Ag deposits formed after the major D_2 upright folding of the Mount Isa Group, during the same fault-controlled metasomatic event(s) responsible for forming the 'silica-dolomite' hosts to the Cu mineralisation. The Mount Isa Cu and Zn-Pb-Ag lodes in their model are structurally controlled, co-genetic, syntectonic, zoned hydrothermal replacement deposits. If this interpretation is correct, then 'Mount Isa style' Zn-Pb-Ag mineralisation is a distinct deposit type and should not be grouped with the other Carpentarian Zinc Belt stratiform deposits.

This model has yet to gain wide acceptance and the abundant similarities between the deposits described here supports a common, syn-sedimentation to late diagenetic origin for all the deposits, rather than a separate genesis for Mount Isa, Hilton, and George Fisher. Additional, independent, evidence for a common genetic process for all the "Carpentarian Zinc belt' deposits comes from Pb isotope data which indicate that the Pb in each major deposits has model ages very similar to the depositional ages of the host sequences (Page et al., 1994). Hence, Pb mineralisation at Mount Isa is unlikely to have formed during D_2 which occurred several tens of millions of year after sedimentation.

Chemical constraints on ore genesis

Metal transport

New thermodynamic modelling indicates that several types of near surface saline hydrothermal fluids can carry sufficient base metals to form large orebodies if they were to be focussed into a suitable trap site (D. R. Cooke, pers. comm.). Hot (>>250° C) fluids can carry Fe, base metals and reduced S together in solution. Cool fluids, however, must be quite acid to carry metals and reduced S together. Oxidised, near neutral, high salinity fluids can carry large quantities of base metals, even at quite low temperatures (<<150° C), but, by definition, cannot carry reduced S.

Apart from recent work at Walford Creek (Rohrlach et al., 1996) fluid inclusion studies of these deposits do not provide direct evidence of the physico-chemical character of the hydrothermal fluids responsible for base metal transport. At Walford Creek 150° to 180° fluids precipitated sphalerite and galena in primary porosity inside syn-diagenetic pyrite mounds (Rohrlach et al., 1996).

Several lines of indirect evidence suggest that hot, reduced fluids were not responsible for base metal transport in these deposits. These include:

- the very low Cu tenor of the Zn-Pb ores (Table 1);
- although minor chalcopyrite is associated with the ores, none have well developed Cu-rich feeder zones
- no indication of boiling having occurred in deposits hosted by shallow-water sediments;
- the extremely low Au tenor of these deposits (McGoldrick et al, 1996).

Nor is it likely that acid fluids could survive transport through the carbonate-rich sedimentary substrate without being neutralised. In the basins hosting the Australian deposits cool, relatively oxidised, near neutral, saline fluids would be common connate brines, and are the favoured fluids for transporting base metals (and possible S as sulphate) to the site of mineralisation in these deposits (McGoldrick and Keays, 1990).

Sulphur source(s) and base metal sulphide precipitation

Sulphur isotopes and S/Se ratios indicate that the pyrite and base metal sulphides in these deposits contain S from a 'seawater' (or evaporitic) S source, and they do not contain magmatic S (Stanton, 1972; McGoldrick, 1986). Pyrite $\delta^{34}S$ values are heavy and variable, suggesting biogenic sulphate reduction under closed-system, or partly closed-system conditions (e.g. Lady Loretta; Carr and Smith, 1977). At temperatures over about 80°C thermochemical reduction of sulphate is a viable alternative to biogenic reduction and Painter et al. (1996) advocate this mechanism for sulphide in fine grained pyrite at Mount Isa. Base metal sulphide S isotope signatures are similar to, and overlap, the pyrite values, but, are usually more tightly clustered and suggest additional S may have been introduced with the mineralising fluid (Painter et al., 1996; Large et al. 1996). The wide range in calculated temperatures from sphalerite-galena pairs indicates isotopic disequilibrium for the mineralisation, consistent with a low temperature (<200°C) mineralising process.

CURRENT GENETIC MODEL

The general ingredients needed to form a stratiform sediment-hosted Zn-Pb-Ag deposit are a base metal transporting fluid (relatively oxidised, near neutral basinal brines), and a fluid drive which focuses this fluid into a sedimentary environment conducive to biogenic or thermochemical sulphate reduction. Base metal sulphide precipitation occurs in response to redox changes. Cooling, or mixing with less saline fluids will not promote base metal sulphide precipitation (D.R. Cooke pers. comm.).

The variety in sedimentary settings inferred from host-rock facies reflects the diversity of organic matter-rich sedimentary rocks (e.g. shallow lagoonal carbonates at Lady Loretta, deeper water clastic carbonates at HYC, open shelf marine siliciclastics for Century). The timing of introduction of metal carrying fluids into these settings can vary from syn-sedimentation (e.g. syngenetic-exhalative mineralisation at HYC and Lady Loretta), to syn-diagenesis (e.g. parts of Lady Loretta formed in the shallow sediment subsurface; Mount Isa Zn-Pb-Ag ores may have formed at quite some depth in the subsurface, after significant compaction and cementation), to syn-early basin inversion (e.g. Century mineralisation). Fluid drive and focusing mechanisms are not well understood, but the association of some deposits with major structures suggest the pre-existing structural grain is an important control on fluid movements. Seismic effects may cause intermittent high flow rates (e.g. Large et al., 1996). Deep convective circulation which would involve fluid interaction with older basement rocks is favoured by some workers (e.g. Solomon and Heinrich, 1992), but topographically driven flow in shallow aquifers may be a viable alternative (e.g. Garven, 1995).

KEY EXPLORATION TOOLS

Because of the diversity shown by these deposits, there is no single set of exploration techniques that can be used in the search for new deposits. At the basin scale understanding the structural architecture (past and present), and the distribution of organic-rich sedimentary facies can help to define areas of interest. Remote field geophysical data will elucidate basin structures and distribution of other rock types hidden beneath the sedimentary cover.

9

At the prospect scale geological mapping of structures and sedimentary facies will be important. Airborne and ground EM surveys may be used to locate pyritic and/or carbonaceous facies in the subsurface. Surface geochemical surveys and gossan studies yield useful information, but spurious anomalies and broad Zn dispersions can make interpretation difficult (e.g. Broadbent and McKnight, 1995). Detailed gravity surveys have revealed the presence of high grade Zn-Pb mineralisation at depths of several hundred metres (e.g. Duffett, 1996).

Lithogeochemical techniques applied to fresh outcrop and drill-core samples and can provide vectors to hidden mineralisation (Lambert and Scott, 1973; Large and McGoldrick, 1997)

ACKNOWLEDGMENTS

The authors acknowledge the input of all the members of the CODES sediment-hosted base metal deposit team which was formed in 1992. Research was supported by the Australian Mineral Industry Research Association and the Australian Research Council. Our interaction with many company geologists with intimate knowledge of these deposits has been enlightening and much appreciated. In particular, stimulus and encouragement has come from Mel Jones, Ken Maiden, Peter Stoker, and Dugi Wilson. PMcG would also like to acknowledge Bill Perkins' and Martin Neudert's pioneering Mount Isa work, which served to emphasise the importance of 'looking at the rocks'. Finally, we would like to thank Mike Solomon for being a sceptical sounding board for many of the ideas presented here.

REFERENCES

Aheimer, M., 1994, Geology and geochemistry of the lady Loretta SSH base metal deposit, north west Queensland [unpublished BSc (Hons) thesis]: University of Tasmania, 130pp.

Andrews, S., 1996, Stratigraphy and depositional setting of the upper McNamara Group, Lawn Hill region: MIC '96 Proceedings, p. 5-9.

Blanchard, R., and Hall, G., 1942, Rock deformation and mineralization at Mount Isa: Australasian Institute of Mining and Metallurgy Proceedings , v. 125 p. 1-60.

Broadbent, G., and McKnight, S., 1993, Microstructures of ore minerals from the Century Deposit, northern Queensland,, p. 11. Geological Society of Australia Abstracts No. 34

Broadbent, G., and McKnight, S., 1995, The Century discovery, Queensland, Australia - Is exploration ever complete?: Pacrim '95, p. 81-86.

Broadbent, G., Myers, R., and Wright, J., 1996, Geology and origin of shale-hosted Zn-Pb-Ag mineralisation at Century Mine, northwest Queensland: MIC '96 Proceedings, p. 24-27.

Bull, S.W., and Rogers, J.R., 1996, Recognition and significance of an early compressional event in the Tawallah Group, McArthur Basin, N. T.: MIC '96 Proceedings, p. 28-32.

Carr, G.R., and Smith, J.W., 1977, A comparative isotopic study of the Lady Loretta zinc-lead-silver deposit: Mineralium Deposita, v. 12, p. 105-110.

Coutts, B., 1996, Geological controls on mining at McArthur River: MIC '96 Proceedings, p. 36-39.

Crick, I.H., 1992, Petrological and maturation characteristics of organic matter from the Middle Proterozoic McArthur Basin, Australia: Australian Journal of Earth Sciences, v. 39, p. 501-519.

Croxford, N.J.W., and Jephcott, S., 1972, The McArthur lead-zinc-silver deposit, N.T., Proceedings of the Australasian Institute of Mining and Metallurgy, v. 243, p. 1-26.

Croxford, N.J.W., 1962, The mineralogy of the No. 7 lead-zinc orebody, Mount Isa, and its interpetation [unpublished Ph.D thesis]: University of New England, Armidale, N.S.W.

Dixon, G., and Davidson, G.J., 1996, Stable isotope evidence for thermochemical sulphate reduction in the Dugald River (Australia) stratabound shale-hosted zinc-lead deposit: Chemical Geology, v. 129, p. 227-246.

Duffett, M., 1996, Geophysical environment of the Lady Loretta Pb-Zn deposit: MIC '96, p. 45-46.

Dunster, J., 1996, Sedimentology of the lady Loretta Formation - a comparison of the regional setting to that of the Lady Loretta orebody: MIC '96 Proceedings, p. 47-50.

Eldridge, C.S., Williams, N., and Walshe, J.L., 1993, Sulfur isotope variability in sediment-hosted massive sulfide deposits as determined using the ion microprobe SHRIMP: II. A study of the H.Y.C. depositat McArthur River, Northern Territory, Australia: Economic Geology, v. 88, p. 1-26.

Finlow-Bates, T., and Stumpfl, E.F., 1979, The copper and lead-zinc-silver orebodies of Mount Isa mine, Queensland: products of one hydrothermal system: Annales de la Societe Geologique de Belgique, v. 102, p. 497-517.

Forrestal, P.J., 1990, Mount Isa and Hilton silver-lead-zinc deposits, *in* Hughes, F.E., ed., Geology of the Mineral Deposits of Australia and Papua New Guinea: Melbourne, The Australasian Institute of Mining and Metallurgy, p. 927-934.

Garven, G., 1995, Continental-scale groundwater flow and geological processes: Annual Reviews of Earth and Planetary Sciences, v. 23, p. 89-117.

Grondijis, H.F., and Schouten, C., 1937, A study of the Mt Isa ores: Economic Geology, v. 32, p. 407-450.

Hancock, M.C., and Purvis, A.H., 1990, Lady Loretta silver-lead-zinc deposit, *in* Hughes, F.E., ed., Geology of the mineral deposits of Australia and Papua New Guinea: , Australasian Institute of Mining and Metallurgy, p. 943-948.

Hinman, M., 1995, Base metal mineralization at McArthur River: Structure and kinematics of the HYC - Cooley zone at McArthur River, AGSO Record: 1995/5.

Hinman, M., 1996, Timing and processes of formation of the HYC Zn-Pb-Ag deposit, McArthur River: MIC '96 Proceedings, p. 56-59.

Laing, W., 1990, Evidence for a replacive origin for the Mount Isa Pb-Zn orebodies in a syntectonic hydrothermal Cu-Pb-Zn deposit: Abstracts of Mount Isa Inlier Geology Conference, Monash University, p. 64-66.

Lambert, I.B., and Scott, K.M., 1973, Implications of geochemical investigations of sedimentary rocks within and around the McArthur zinc-lead-silver deposit, Northern Territory: Journ. Geochem. Expl., v. 2, p. 307-330.

Lambert, I.B.

Large, R., Bull, S., Cooke, D., and McGoldrick, P., 1996, Review of genetic models from the HYC deposit: constraints from sedimentology, alteration halo and fluid chemical modelling: MIC '96 Proceedings, p. 72-74.

Large, R., and McGoldrick, P., 1997, Alteration halos associated with stratiform sediment-hosted ("Sedex") deposits; development of an alternative exploration approach, Geological Society of Australia Abstracts No. 44 p. 42.

Logan, R.G., 1979, The geological and mineralogical zoning of the HYC Ag-Pb-Zn deposit, McArthur River, N.T.: [unpublished M.Sc. thesis]: ANU, 187 pp.

Logan, R.G., Leung, K., and Karelse, G.J., 1993, The McArthur River Project, International Symposium – World Zinc '93: Hobart, The Australasian Institute of Mining and Metallurgy.

Logan, R.G., Murray, W.J., and Williams, N., 1990, HYC silver-lead-zinc deposit, McArthur River, *in* Hughes, F.E., ed., Geology of the Mineral Deposits of Australia and Papua-New Guinea: Melbourne, The Australasian Institute of Mining and Metallurgy, p. 907-911.

Mathias, B.V., and Clark, G.J., 1975, The Mount Isa Copper and Silver-Lead-Zinc orebodies - Isa and Hilton mines, *in* Knight, C.L., ed., Economic Geology of Australia and Papua New Guinea: , Australasian Institute of Mining and Metallurgy, p. 351-371.

Mathias, B.V., Clark, G.J., Morris, D., and Russell, R.E., 1973, The Hilton deposit — stratiform silver-lead-zinc mineralization of the Mount Isa type: BMR Bulletin 141, p. 33-58.

McClay, K.R., 1979, Folding in silver-lead-zinc orebodies, Mount Isa, Australia: Trans. (Sect. B) Inst. Min. Metal., v. 88, p. B5-B14.

McGoldrick, P.J., 1986, Volatile and precious metal geochemistry of the Mount Isa ores and their host rocks [unpublished Ph.D. thesis]: University of Melbourne, 236pp.

McGoldrick, P.J., and Keays, R.R., 1990, Mount Isa sa copper and lead-zinc-silver ores: coincidence or co-genesis?, Economic Geology, v. 85, p. 641-650.

McGoldrick, P., Dunster, J., Cooke, D., and Aheimer, M., 1996, New observations from the Lady Loretta Zn-Pb-Ag deposit: towards a new genetic model: MIC '96 Proceedings, p. 77-80.

12

McKirdy, D.M., and Powell, T.G., 1974, Metamorphic alteration of carbon isotopic composition in ancient sedimentary organic matter: new evidence from Australia and South Africa: Geology, v. 2, p. 591-595.

Muir, M.D., 1983, Depositional environments of host rocks to northern Australian lead-zinc deposits, with special reference to McArthur River: Min. Ass. Canada, Short Course Notes, v. 9, p. 141-174.

Murray, W.J., 1961, Notes on Mount Isa geology: Australasian Institute of Mining and Metallurgy Proceedings, p. 105-136.

Myers, R., Ceremuga, C., Clark, D., McSkimming, D., Price, S., Tuesley, M., and Wilkinson, D., 1996, Mount Isa lead-zinc mineralisation - what controversy?: MIC '96 Proceedings, p. 85-89.

Neudert, M., 1983, A depositional model for the Upper Mount Isa Group and implications for ore formation: [unpublished Ph.D. thesis]: ANU, 324pp.

Neudert, M., 1984, Are the Mount Isa ores really syngenetic?: Geological Society of Australia Abstracts, v. 12, p. 402-403.

Neudert, M., and McGeough, M., 1996, A new tectono-stratigraphic framework for the deposition of the upper McArthur Group, N. T.: MIC '96 Proceedings, p. 90-94.

Newbery, S.P., Carswell, J.T., Allnutt, S.L., and Mutton, A.J., 1993, The Dugald River zinc-lead-silver deposit: an example of a tectonised Proterozoic stratabound sulphide deposit: World Zinc-93 Proceedings, p. 7- 21.

Oehler, J.H., and Logan, R.G., 1977, Microfossils, cherts, and associated mineralization in the Proterozoic McArthur (H.Y.C.) lead-zinc-silver deposit: Economic Geology, v. 72, p. 1393-1409.

Page, R., Sun, S., and Carr, G., 1994, Proterozoic sediment-hosted lead-zinc-silver deposits in northern Australia — U-Pb zircon and Pb isotope studies: Geological Society of Australia Abstracts, v. 37, p. 334-335.

Painter, M., Hannon, K., and Golding, S., 1996, Sulphur isotope constraints on the formation of "fine-grained pyrite" at Mount Isa and its relationship to base metal mineralisation: MIC '96 Proceedings, p. 99-103.

Perkins, W.G., 1984, Mount Isa "silica-dolomite" and copper orebodies: the result of a syntectonic hydrothermal alteration system: Economic Geology, v. 79, p. 601-637.

Perkins, W.G., 1990, The Mount Isa Ag-Pb-Zn orebodies stratiform replacement lodes in a zoned hydrothermal system: BMR Record, v. 1990/95, p. 63-64.

Perkins, W., 1995, Features of the Mount Isa Cu-Pb-Zn deposit and comparison with Hilton, McArthur River and Mount Novit: evidence for a late syndeformational replacement origin?: Metallogeny of Proterozoic basins. MDRU Short Course Proceedings

Rohrlach, B., Fu, M., and Clarke, J., 1996, The geology and paragenesis of the Walford Creek Zn-Pb-Cu-Ag prospect: MIC '96 Proceedings, p. 99-103.

Russell, R.E., 1978, Mt Novit prospect, Mt Isa: 3rd Australian Geological Convention Abstracts, p. 31.

Solomon, M., and Heinrich, C.A., 1992, Are high-heat-producing granites essential to the origin of giant lead-zinc deposits at Mount Isa and McArthur River, Australia?: Exploration and Mining Geology, v. 1, p. 85-91.

Stanton, R.L., 1962, Elemental constitution of the Black Star orebodies, Mount Isa, Qld, and its interpretation: Trans.Inst. Min. Metall., v. 72, p. 61-144.

Stanton, R.L., 1972, Ore Petrology: McGraw-Hill, p. 713p.

Sun, S., Carr, G., and Page, R., 1996, A continued effort to improve lead-isotope model ages: AGSO Research Newsletter, n. 24, p. 19-20.

Swager, C.P., Perkins, W., and Knights, J., 1987, Strata-bound phyllosilicate zones associated with syntectonic Cu orebodies, Mount Isa, Queensland: Australian Journal of Earth Sciences, v. 34, p. 463-476.

Sweet, I.P., Hutton, L.J., Leggo, N., Pietsch, B.A., Ahmad, M., Rawlings, D.J., and Haines, P.W., 1993, The AusIMM - Northwest Queensland and Darwin Branches Carpentaria Zinc Belt Geological Excursion Gulf Region, Queensland and Northern Territory. *The Gulf Classic* – Excursion Guide: , 73pp.

Tourtelot, E.B., and Vine, J.D., 1976, Copper deposits in sedimentary and volcanogenic rocks: U.S. Geol. Survey Prof.Paper, v. 907C, p. 34.

Valenta, R., 1994, Deformation of host rocks and stratiform mineralization in the Hilton Mine area, Mt Isa: Australian Journal of Earth Science, v. 41, p. 429-443.

Walker, R.N., Logan, R.G., and Binnekamp, J.G., 1977, Recent geological advances concerning the H.Y.C. and associated deposits, McArthur River, N.T.: Journal of the Geological Society of Australia, v. 24, p. 365-380.

Waltho, A.E., Allnutt, S.L., and Radojkovic, A.M., 1993, Geology of the Century zinc deposit, northwest Queensland: World Zinc-93 Proceedings, p. 111-129.

Waltho, A.E., and Andrews, S.J., 1993, The Century zinc-lead deposit, northwest Queensland: The AusIMM Centenary Conference Proceedings, p. 41-61.

Waring, C. and ????, 1997, Proterozoic metamorphic Cu, this volume

Williams, N., 1978a, Studies of the base metal sulfide deposits at McArthur River, N.T., Australia:1. The Cooley and Ridge deposits: Economic Geology, v. 73, p. 1005-1035.

Williams, N., 1978b, Studies of the Base Metal Sulfide Deposits at McArthur River, Northern Territory. Australia: II. The Sulphide-S and Organic-C Relationships of the Concordant Deposits and their Significance: Economic Geology, v. 73, p. 1036- 1056.

Deposit	Size & grade	Mineralization	Host rocks	Age	Metamorphism /deformation	Evaporites	Oxidized sediments	Zoning	Halos	References
HYC	8 ore lenses in abt 70 m; global res. 227 Mt @ 9.2% Zn, 4.1% Pb, current project 104 Mt @ 14.1% Zn, 6.1% Pb and abt 60 g/t Ag	stratiform, f.g. py, sp, minor cpy, marcasite, ars; primary textures well preserved	Barney Creek Fmn - HYC Pyritic Shale; pyritic, organic matter-rich (up to 7% Toc), dolomitic siltstones; crs sedimentary breccias; minor tuffaceous component	1640±3 Ma	essentially unmetamorphosed; basin inversion, but no penetrative deformation	important part of sequences above and below HYC Pyritic Shale are evaporitic	W-Fold Shale (immediate f/w to mineralization) shows extensive patchy reddening; Emu FZ; various units elsewhere in McArthur and Tawallah Gps	small very Cu-rich zone in the north; general (Cu-)Pb-Zn	pyrite; Tl regionally; Fe. Mn in carbonates	Logan et al., 1990; Logan et al., 1993; & references therein; Crick, 1992
Walford Creek	no published reserve; several ore-grade intersections (Cu, Zn, Pb) of a few metres; covers an area of 6 km x 1.5 km in plan	3 stacked lenses of stratiform massive py with sp & ga as a matrix in pyritic beds; primary textures preserved	Fickling Gp - Mt Les Siltstone; dolomitic shale (regionally), highly carbonaceous, dolomitic and pyritic shales & local talus breccias	1640±7 Ma	sub-greenschist; relatively flat-lying, but bounded by a major regional structure (Fish River Fault)	pseudomorphs after gypsum in Mt Les Siltstone		Cu-rich, late stage mineralisation near FRF	pyrite	Rohrlach et al., 1996; Page et al., 1994; Sweet et al., 1981
Century	2 main ore zones in a 40 m mineralized sequence; 118 Mt @ 10.2% Zn, 1.5% Pb, 36 g/t Ag	stratiform sp, py (5-10%), ga, ±cpy (intimate association with organic matter and authigenic silica); primary textures are preserved	McNamara Gp - Lawn Hill Fmn - unit Pmh4; siliciclastic, carbonaceous (Toc 1 - 5%), sideritic, shales& siltstones; minor tuffaceous component	1595±6 Ma	sub-greenschist; open folding, faulted ore contacts; stylolitic layering is developed in ore sequence	not known	not known	highest Zn grades transgress the mineralized sequence from SE to NW	py envelope; intense siderite development in siltstones	Waltho & Andrews, 1993; Waltho et al., 1993; Broadbent et al., 1996; Page et al., 1994
Lady Loretta	single high grade lens with reserve of 8.3 Mt @ 18.4% Zn, 8.5% Pb, 125 g/t Ag; mineralized horizon is abt 50 m thick & is recognisable over several km^2	stratiform py, sp, ga, tetrahedrite, barite, silica , tr. hem; some primary textures preserved	McNamara Gp - Lady Loretta Fmn; carbonaceous, pyritic, dolomitic, sideritic siltstones & shales	1647±4 Ma	?sub-greenschist; open - tight synclinal (?D_2) structure locally, more open folding regionally	gypsum moulds from ore horizon; sulphate evaporites important in lower McNamara Group (Paradise Ck Fmn, Gunpowder Creek Fmn)	not known	Pb-Zn core to Zn-Ba flanks of main mineralization	py, siderite, Mn, Tl	Hancock & Purvis, 1990 (& references therein); McGoldrick et al., 1996
Grevillea	no published reserve; several ore-grade intersections (Zn, Pb, Ba)	stratiform massive py and barite; sp & ga in pyritic beds	McNamara Gp - Riversleigh Siltstone; siliciclastic carbonaceous mudstone & sandstone	>1636 and <1652 Ma	? sub-greenschist; relatively flat-lying, fault-bounded	pseudomorphs of mush-textured gypsum	Sandstone interbeds, and basal Shady Bore Quartzite	not known	pyrite	Coolgardie Gold Annual reports
Mount Isa	30 stacked (en echelon) ore lenses in abt 1000 m (most in upper 650 m); pre-production reserve of abt 150 Mt @7% Zn, 6% Pb, 150 g/t Ag	stratiform py, sp, ga, tetrahedrite ± po, rare mte; ores show locally intense deformation, but some primary textures are preserved	Mount Isa Gp - Urquhart Shale; carbonaceous (now graphite), pyritic, dolomitic siltstones; 'tuffaceous' component	1652±7 Ma	(?lower) greenschist facies; D_1 - D_3	pseudomorphs of dolomite after gypsum in Urq Sh; halite casts in siltstone unit above Urqt Sh	basal Mt Isa Grp; Surprise Creek Fmn (beneath and possibly lateral equivalent to Mt Isa Gp)	(Cu-) Pb - Zn	pyrite; Tl; ?Fe, Mn enrichment in carbonates	Forrestal, 1990 & references therein; McKirdy & Powell, 1974, Page et al., 1994
George Fisher	8 stacked ore lenses; approx 68 Mt @ 5.8%Pb, 12.5% Zn, 92 g/t Ag	as for Mt Isa	as for Mt Isa	as for Mt Isa	as for Mt Isa	carbonate pseudomorphs in orebodies interpreted as pseudomorphs of primary sulphates	as for Mt Isa	not known	pyrite	MIM 1995 Annual Rpt; L. Chapman, pers. comm.
Hilton	7 stacked ore lenses; approx. 120 Mt @ 10.2% Zn, 5.5% Pb, 100 g/t Ag	as for Mt Isa, but with higher grade and more Cu-rich fault-related ore	as for Mt Isa	as for Mt Isa	as for Mt Isa, but locally more structurally complex		as for Mt Isa	upper o/bs most Cu-rich; (Cu-) Pb-Zn moving up-dip	sideritic siltstones	Valenta, 1994; Mathias et al., 1973; (Forrestal, 1990)
Mount Novit	single pyrite lens up to abt 20 m thick; strike length of 5 km; no calculated resource, several intersections of >10% Zn+Pb	stratiform/stratabound (massive) coarse py, po, mte ±sp, ga	(lower) Mt Isa Gp - Moondarra Siltstone; dolomitic, pellitic schists	probably 1660 to 1650 Ma; i.e. slightly older than Urqhart Shale	greenschist/amphibolite transition; D_1 - D_3, but complexity due to faulting	not known	as for Mt Isa	not known	siderite in mineralization	Russell, 1978; MIM unpublished data
Dugald River	40 m thick lode; 38 Mt @ 13.2% Zn, 2.1% Pb, 32 g/t Ag	stratabound py, sp, po, ga, tr. cpy, pyrargyrite, ars, tetrahedrite; mostly recrystallized, but some rare primary textures	Dugald River Slates (Shear Zone) - black, f.g. carbonaceous slates; stratigraphic position is not well constrained	uncertain, but probably older than Mt Isa Group	greenschist - amphibolite transition; D_1 - D_3, re-folded isoclinal folds with mineralized sequence overturned; mineralization has mylonitic contacts	Corella Fmn in stratigraphic footwall is scapolite-rich; pseudomorphs after ?shortite from the mineralised sequence	(?post-D_3 hematitization of Corella Fmn in the stratigraphic footwall	(Cu-) Pb - Zn and S isotopes	K, Li, Rb, Tl, Pb, Se, Ag, & Sr enrichment enhancement in h/w and f/w	Newbery et al., 1993; Dixon & Davidson, 1996; Muir, 1983

Table 1 Important geological features of northern Australian Proterozoic stratiform sediment-hosted Zn-Pb deposits